Universiteit
Leiden
The Netherlands

Neuroimmune guidance cues for vascular health

Zhang, H.

Citation
Zhang, H. (2021, June 1). *Neuroimmune guidance cues for vascular health*. Retrieved from https://hdl.handle.net/1887/3176518

Version:	Publisher's Version
License:	Licence agreement concerning inclusion of doctoral thesis in the Institutional Repository of the University of Leiden
Downloaded from:	https://hdl.handle.net/1887/3176518

Note: To cite this publication please use the final published version (if applicable).

Cover Page

Universiteit Leiden

The handle http://hdl.handle.net/1887/3176518 holds various files of this Leiden University dissertation.

Author: Zhang, H.
Title: Neuroimmune guidance cues for vascular health
Issue date: 2021-06-01

Neuroimmune Guidance Cues for Vascular Health

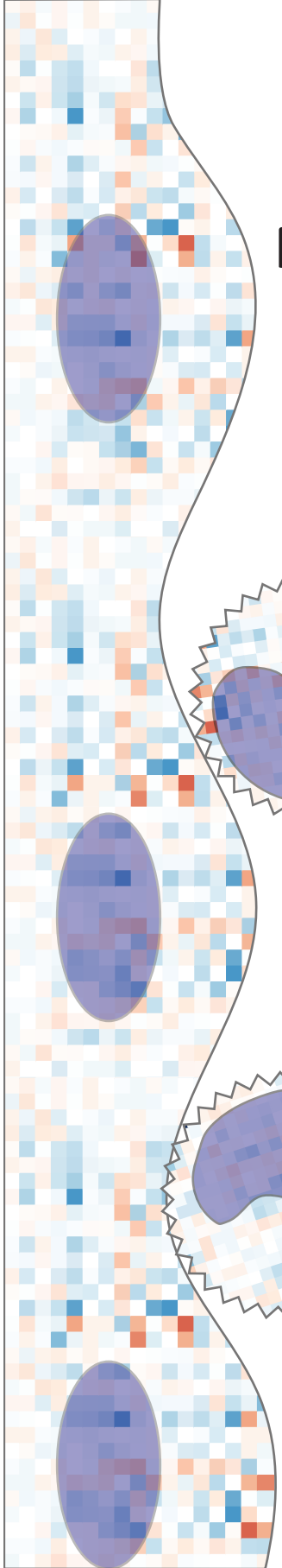

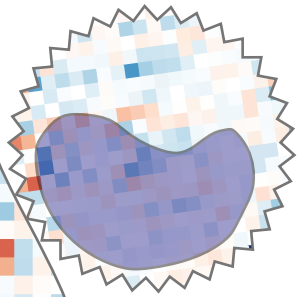

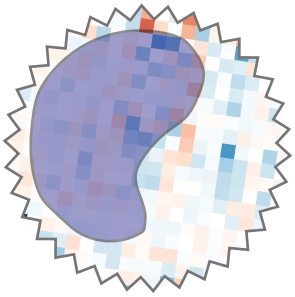

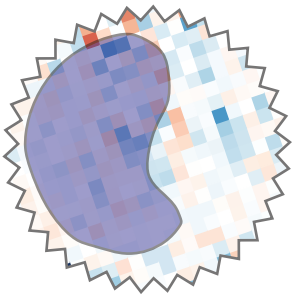

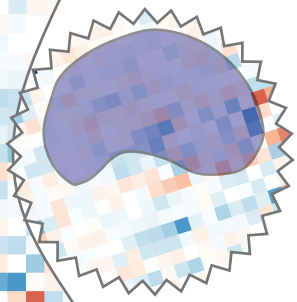

Huayu Zhang 张化宇

Neuroimmune Guidance Cues for Vascular Health

by Huayu Zhang

The studies in this thesis were carried out at the Department of Internal Medicine, Division of Nephrology, Leiden University Medical Center, the Netherlands. The research was supported by a grant from the Netherlands Heart Foundation (2013T127 to H.Z. and J.M.G.).

Neuroimmune Guidance Cues for Vascular Health
Cover design: Huayu Zhang
Printing: www.proefschriftmaken.nl
Copyright © Public Domain

Neuroimmune Guidance Cues for Vascular Health

Proefschrift

ter verkrijging van
de graad van doctor aan de Universiteit Leiden,
op gezag van rector magnificus prof.dr.ir. H. Bijl,
volgens besluit van het college voor promoties
te verdedigen op dinsdag 01 juni 2021
klokke 11.15 uur

door

Huayu Zhang
geboren te Qiqihar, China
in 1989

Promotor

Prof. Dr. A.J. van Zonneveld

Co-promotor

Dr. J.M. van Gils

Promotiecommissie

Prof. Dr. C. van Kooten	
Dr. M.R.M. Jongbloed	
Prof. Dr. Y. Wang	*First Affiliated Hospital of Xi'an Jiaotong University, China*
Prof. Dr. P. Hordijk	*Amsterdam UMC*
Prof. Dr. C. de Vries	*Amsterdam UMC*

For my parents, Xiao and Wenjun,
who have given me the best regardlessly.

Contents

Chapter 1 **General introduction and scope of the thesis** **9**

Chapter 2 **Review: Understanding Netrins and Semaphorins in Mature Endothelial Cell Biology** **15**
Pharmacol Res, 2018

Chapter 3 **Endothelial Semaphorin 3F Maintains Endothelial Barrier Function and Inhibits Monocyte Migration** **47**
Int J Mol Sci, 2020

Chapter 4 **Endothelial Netrin-4 prevents endothelial cell senescence and promotes endothelial cell survival** **75**
Int J Biochem Cell, 2021

Chapter 5 **Comprehensive analysis of neuronal guidance cue expression regulation during monocyte to macrophage differentiation reveals post-transcriptional regulatory hotspot in Semaphorin7A 3'UTR** **103**
Innate Immun, 2020

Chapter 6 **Prediction power on cardiovascular disease of neuroimmune guidance cues expression by peripheral blood monocytes determined by machine learning methods** **137**
Int J Mol Sci, 2020

Chapter 7 **Summary and General Discussion** **165**

Chapter 8 **Nederlandse Samenvatting** **175**

Chapter 9 **Appendices** **179**

Chapter 1

General introduction and scope of the thesis

1.1 Current cardiovascular disease burden and intervention strategies in brief

Despite improvements in surgical and drug treatment, cardiovascular diseases (CVD) remain the leading cause of death in modern societies. CVDs account for 3.9 million death or 45% of all death in Europe with cost of €210 billion on economy per year [1]. A major part of CVD is attributable to atherosclerosis. Correcting dyslipidemia (mostly lowering blood low density lipoprotein (LDL) cholesterol levels) and mitigating immune response are the 2 main strategies to attenuate risk for vascular mortality caused by atherosclerosis [2, 3]. The most successful and widely used intervention is inhibition of endogenous cholesterol synthesis by targeting HMGCoA (β-hydroxy β-methylglutaryl-coenzyme A) reductase using statins. Monoclonal antibody for PCSK9 can further decrease LDL levels [4]. However, there is still substantial risk after LDL levels are corrected, prompting the need for managing inflammatory response in atherosclerosis.

Comparing to LDL cholesterol lowering strategy, evidence of efficacy of interventions targeting immune response is still emerging. IL-1β antibody canakinumab was shown to reduce cardiovascular disease endpoint by 16% [5]. Nonetheless, there was the side-effect of increasing lethal infection episodes, resulted from impaired host defense. On the other hand, patients with atherosclerosis could display normal blood cholesterol levels [6]. Moreover, it is well-known that atherosclerosis lesions profoundly affect vascular bifurcations and areas with low wall shear stress, despite universal exposure to the one's blood lipid levels, suggesting an independent role of endothelial dysfunction in atherogenesis [7]. The above evidence has motivated research efforts to gain deeper insights in endothelial dysfunction and inflammatory responses in pathogenesis of atherosclerosis to further tackle the residual risk after correction of dyslipidemia. A series of recent research has identified novel functions of neuronal guidance cues in atherogenesis and related pathophysiological process (reviewed in detail in **Chapter 2**).

1.2 Pathogenesis of atherosclerosis: a brief recall

Atherosclerosis, literally meaning "artery hardening" from Greek, is the complex pathology of formation of plaques on the artery walls. The pathological process starts as early as teenage with forming of initial lesion, featured by continued exposure of the endothelium to metabolic and hemodynamic risk factors leading to a state of chronic systemic activation

of the endothelial cells [8]. Endothelial dysfunction results in enhanced macrovascular endothelial permeability, an event that augments low-density lipoprotein (LDL) accumulation in the subendothelial space. Oxidation of LDL leads to further activation of the endothelium and potentiation of pro-inflammatory responses, including upregulation of various adhesion molecules and chemokines that actively recruit inflammatory cells like monocytes [9]. Recruited monocytes can differentiate to macrophages with stimulation of various inflammatory cytokines and other regulatory factors. The monocytes and macrophages can endocytose the pro-inflammatory oxidized lipids, leading to lipid-laden cells called "foam cells" (initial lesion – fatty streak). Following the years, the lesions grow mainly by thickening of intima by deposition of lipoprotein by formation of "foam cells" and later proliferation of vascular smooth muscle cells. The foam cells in the plaques can eventually die via apoptosis or necrosis process, allowing forming of extracellular lipid core (intermediate lesion - fibroatheroma). The plaques can further growth in size, fibrosis content and histological compositions into fibrous plaques and complicated lesions. Atherosclerosis remains largely asymptotic before the size of atherosclerotic lesion causes significant stenosis, formation of atherothrombosis or plaque rapture, causing decrease or sudden loss of perfusion to the organs. Stenosis in coronary artery leads to angina due to the restrict blood supply, while occlusion of coronary artery or arteries in brain causes myocardial infarction or stroke, respectively. Essentially, pathways involved in endothelial function and dysfunction, monocyte-macrophage biology are likely to be involved in development of atherosclerosis.

1.3 What are neuronal guidance cues?

Neuronal guidance cues (NGCs) are proteins originally identified in the nervous system for their ability to directing growth of axons to the correct targets. Depending on the context, they are also called neuronal guidance proteins (to specify the molecular property), axonal guidance cues (to specify the original function) or even neuroimmune guidance cues (to emphasize on their later-found roles in immunology). It is generally accepted that NGCs consist of 4 families of ligands, namely netrin, semaphorin, slit and ephrin (Reviewed in [10]). The ligands bind to their various receptors with different specifies and affinities, exerting complex downstream signals to the target cells (See **Table 1** for a list of NGC ligands and receptors). A large part of the downstream signals results in altered activities of small-GTPases, which in turn regulates organizations of cytoskeletons: the underlying mechanism of repulsive or attractive effect of NGCs.

Class	Ligand	Receptor
Semaphorin	SEMA3A-3G SEMA4A-4G SEMA5A-5B SEMA6A-6D SEMA7A	PLXNA1-A4 PLXNB1-B3 PLXNC1 PLXND1
Netrin	NTN1 NTN3-5 NTNG1-2	UNC5A-D DCC DSCAM MCAM
Ephrin	EFNA1-A5 EFNB1-B3	EPHA1-A8 EPHA10 EPHB1-B4 EPHB6
Slit	SLIT1-3	ROBO1-3

Table 1. List of NGC ligands and receptors

1.4 Scope of this thesis

The nervous and vascular systems of vertebrates share many similarities and often overlap in anatomy. These notions led to one of the major recent insights in developmental vascular biology being that the coordinated patterning of nerves and vessels is achieved by each system separately using the same cues and signals [9]. Next to roles of NGCs during development, functions of NGCs have been described in both mature endothelium and immune cells, which is the focus in this thesis. With the knowledge in this thesis, I demonstrate the relevance of NGCs in vascular biology from bench to bedside. Previous knowledge on NGCs showed that NGCs are regulated by hemodynamic conditions and inflammations, thereby affecting endothelial cell function. In **Chapter 2**, a detailed literature review of functions of semaphorins and netrins in mature endothelial cells is given as the background of NGC research in endothelial cells. Next, in **Chapter 3** and **Chapter 4** are the studies describing the regulation and function of SEMA3F and NTN4 in mature endothelial cells, 2 of most abundantly expressed NGCs in endothelial cells. We tried to push the boundary by understanding the mechanism underlying the function of SEMA3F and NTN4. We describe a role for both SEMA3F and NTN4 in preventing endothelium dysfunction and trans-endothelial migration of monocytes, 2 critical mechanisms in development of early atherosclerotic lesions. NGCs have also been found to play a role in monocyte biology. In this regard, I move on to a comprehensive analysis of NGC gene expression and change of NGC pathway during monocyte to macrophage differentiation in **Chapter 5**. I first quantified regulation of NGC expression during monocyte to macrophage differentiation. And secondly, the role of the RNA-binding protein quaking, a regulator of monocyte-macrophage function, in regulation of NGC expression was investigated and discussed. In **Chapter 6**, I seek to prove the clinical relevance of NGCs by building predictive modeling models using NGC expression in circulating monocytes to infer the health status of CVD patients. Finally, in **Chapter 7**, I discuss the results from my studies in relevance to the current knowledge and give directions for future research.

References

1. *Timmis, A., N. Townsend, C. Gale, et al., European Society of Cardiology: Cardiovascular Disease Statistics 2017. Eur Heart J, 2018. 39(7): p. 508-579.*

2. *Bertrand, M.J. and J.C. Tardif, Inflammation and beyond: new directions and emerg-*

ing drugs for treating atherosclerosis. Expert Opin Emerg Drugs, 2017. 22(1): p. 1-26.

3. *Bruikman, C.S., R.M. Stoekenbroek, G.K. Hovingh, et al., New Drugs for Atherosclerosis. Can J Cardiol, 2017. 33(3): p. 350-357.*
4. *Robinson, J.G., M. Farnier, M. Krempf, et al., Efficacy and safety of alirocumab in reducing lipids and cardiovascular events. N Engl J Med, 2015. 372(16): p. 1489-99.*
5. *Ridker, P.M., B.M. Everett, T. Thuren, et al., Antiinflammatory Therapy with Canakinumab for Atherosclerotic Disease. N Engl J Med, 2017. 377(12): p. 1119-1131.*
6. *Fernández-Friera, L., V. Fuster, B. López-Melgar, et al., Normal LDL-Cholesterol Levels Are Associated With Subclinical Atherosclerosis in the Absence of Risk Factors. Journal of the American College of Cardiology, 2017. 70(24): p. 2979-2991.*
7. *Souilhol, C., J. Serbanovic-Canic, M. Fragiadaki, et al., Endothelial responses to shear stress in atherosclerosis: a novel role for developmental genes. Nat Rev Cardiol, 2020. 17(1): p. 52-63.*
8. *Deanfield, J.E., J.P. Halcox, and T.J. Rabelink, Endothelial function and dysfunction: testing and clinical relevance. Circulation, 2007. 115(10): p. 1285-95.*
9. *Ross, R., Atherosclerosis–an inflammatory disease. N Engl J Med, 1999. 340(2): p. 115-26.*
10. *Melani, M. and B.M. Weinstein, Common factors regulating patterning of the nervous and vascular systems. Annu Rev Cell Dev Biol, 2010. 26: p. 639-65.*

Chapter 2

Review: Understanding Netrins and Semaphorins in Mature Endothelial Cell Biology

Zhang, H., Vreeken, D., Bruikman, C. S., van Zonneveld, A. J. and van Gils, J. M. *Pharmacological research*, 2018;137.

Abstract

Netrins and semaphorins are known as neuronal guidance molecules that are important to the facilitate patterning of the nervous system in embryonic development. In recent years, their function has been broadened to guide development in other systems, including the vascular system, where netrins and semaphorins critically contribute to the development of the vascular system. Evidence is accumulating that these guidance cues are also of critical importance in the biology of the mature endothelium by regulating the maintenance of endothelial quiescence. Here we review our current insights into the roles of netrins and semaphorins in endothelial cell survival, self-renewing, barrier function, response to wall shear stress, and control of the vascular tone. We also provide suggestions for future research into the functions of netrins and semaphorins in mature endothelial cell biology.

Keywords

endothelial cells, netrin, semaphorin

2.1 Introduction

The vascular system involves an extensive network of arteries, capillaries and veins, lined by endothelial cells. While the endothelial monolayer was first thought to be an inert layer between blood and tissue, a range of discoveries has led to better understanding of the complex active homeostatic functions of the endothelium including the controlling vascular tone, blood fluidity, and vascular inflammation [1]. The observation that the anatomy and gene expression patterns of the vascular system of vertebrates often overlap with that of the nervous system has led to the growing awareness that the coordinated patterning of nerves and vessels is achieved by each system separately using the same cues and signals [2, 3]. These conserved patterning factors, together called the "neuronal guidance cues" (NGCs), were first identified in neural development and involve 4 major families of conserved ligands netrins, slits, semaphorins, and ephrins. NGCs act together through a complex interplay of short and long-range signals that can either repel or attract the cells of the developing network [4]. The effects of NGCs on the developing vascular network, especially with respect to angiogenesis, have been well characterized and received some excellent reviews [5-9]. However, next to their function in development, evidence is accumulating that a selective group of the NGCs, the netrins and semaphorins, have important homeostatic functions in the mature established endothelial monolayer. Here, we review the novel insights into the regulatory roles of netrins and semaphorins in endothelial cells in the mature endothelium.

2.2 Role of netrins and semaphorins in the survival of endothelial cells

The integrity of the vascular endothelium depends on the continued replacement of injured or senescent cells. Conditions that "stress" endothelial cells, such as an adverse hemodynamic or metabolic environment, or local and systemic inflammation, are associated with a faster turnover of endothelial cells [10, 11]. This concept of endothelial cell turnover naturally raises two questions: (1) what contributes to preservation or survival of endothelial cells, and (2) what regulates the renewal activity of endothelial cells? Recent evidence points at roles for netrins and semaphorins in both phenomena. Besides acting as a directional signal for angiogenic sprouting, vascular endothelial growth factor (VEGF) is a survival factor that plays a major role in the shaping of the vascular networks. Hypoxic tissues in need of (neo-)vascularization express VEGF that supports the generation and survival of the endothelial cells that makeup the new angiogenic network. However, this also relives the hypoxia in the tissue and, therefore, other mechanisms have to kick in to replace the pro-

survival signals previously provided by VEGF. These stabilization signals include, amongst others, angiopoietin1/TIE2 signaling, platelet-derived growth factor (receptor signaling), and signaling generated by the interaction of endothelial cells and extracellular matrix, more specifically the endothelial basement membrane, via integrins. Integrin activity has been shown to be important in stabilization and survival of mature vascular networks [12]. These stabilization signals within a functional network rely heavily on stimulation of endothelial cells by laminar shear stress. Below we discuss recent studies that demonstrate prominent roles for the netrins and semaphorins in the regulation of endothelial cell survival.

2.2.1 NTN4 promotes endothelial cell survival by activating integrin a6β1

The first vertebrate netrin was discovered in 1994 as a guidance cue for the embryonic development of commissural axons in the spinal cord [13, 14]. Up until today, expression of six different netrins has been described in mammals. Netrin-1, 3, 4, and 5 (NTN1, 3, 4, 5) are secreted proteins, while netrin-G1 and G2 (NTNG1 and G2) are membrane-bound proteins tethered by glycosyl-phosphatidylinostitol tails [15, 16]. Netrins can bind to the classical "deleted in colorectal cancer" (DCC), neogenin (NEO1) and uncoordinated-5 (UNC-5) receptors. Beside the classical ligand receptor interactions also interactions with other receptors, such as integrins [17] and adenosine A2b receptors (ADORA2B) [18], have been described (**Figure 2**). In human endothelial cells, NTN4 is the highest expressed netrin class member [19-21] (**Figure 1**) and can be upregulated by laminar shear stress [22]. Interestingly, NTN4 can serve as an activator of integrins, including endothelial integrin α6β1, a binding partner of laminin [23-25]. In human microvascular endothelial cells, NTN4 directly interacts with the integrin α6β1 complex, leading to more activated integrin β1. Functionally, a NTN4 coating indeed increases adhesion of endothelial cells in vitro to culture plate [23]. Studies from multiple groups also show that the presence of NTN4 increases activity of Akt and ERK1/2, suggesting that NTN4 is able to induce survival signaling in endothelial cells [26, 27]. In line with this, less caspase3 activity was detected when human umbilical vein endothelial cells (HUVECs) were treated with NTN4 [21, 26]. Together, these results suggest that NTN4 may provide endothelial cells with pro-survival signaling especially in stable functional vascular networks. It is important to note that NTN4 knockout mice, under normal conditions, do not have any defects in retina vascular networks [28, 29]. Therefore, to fully understand the in vivo function of NTN4, further investigation is needed. Intriguingly, NTN4 is itself a component of the basement membrane [30]; this is not

surprising as the netrin family is structurally related to the laminin superfamily which has an important role in the structure of the extracellular matrix [31]. As a component of the basement membrane, NTN4 has been shown to regulate the assembly of laminin networks, thus altering the structure of the basement membrane and thereby affecting the survival of endothelial cells [32]. A report by Reuten et al. demonstrated that NTN4 competitively binds to the laminin γ chain, causing disassembly of the laminin network and disruption of the endothelial basement membrane [32]. Adding NTN4 to capillary networks in chick embryo chorioallantoic membranes disrupted formation of stable capillary networks [32]. It was then suggested that NTN4 causes destabilization of blood vessels. This suggestion is at first glance contradictory to the pro-survival role of NTN4. However, in order to function as a laminin network disassembling agent, a concentration of 2.1 μM NTN4 was needed, which is probably hardly reached in physiological conditions. Generally, a concentration of around 1.7 pM NTN4 can be found in endothelial cell culture [21]. Therefore, the consequences of regulation of the basement membrane structure by NTN4 in the physiological concentration range are not fully elucidated yet.

2.2.2 NTN1 has an anti-apoptotic effect on endothelial cells

Next to NTN4, NTN1 was found to be expressed by various types of endothelial cells. In general, NTN1 is believed to have moderate expression in endothelial cells [19, 33, 34]. Co-localization of NTN1 with endothelium was observed in both large blood vessels and capillaries [26, 35]. There is a lack of agreement in the serum concentration NTN1. In healthy humans, several picograms to several hundred picograms per milliliter NTN1 were detected in serum using enzyme-linked immunosorbent assays, depending on the lab and reagents used. [36-41] More expression of NTN1 was found in endothelial cells cultured under shear stress and in aortic regions with higher shear stress [34]. In tumor cells and neurons, NTN1 has been shown to be a survival factor in cells expressing the netrin receptors DCC and UNC5H [42, 43]. In endothelial cells, NTN1 also acts as a survival factor as NTN1 blocked the apoptotic effect of serum starvation in HUVECs and human umbilical artery endothelial cells [44]. This anti-apoptotic effect was proven to be an antagonistic effect of NTN1 binding to UNC5B, as blocking UNC5B with siRNA also reduced apoptosis while abolishing the anti-apoptotic effect of NTN1 [44]. Further evidence also demonstrated that NTN1 promotes endothelial cell survival by blocking the UNC5B-induced inhibition of death-associated protein kinase 1 (DAPK1) [44]. Similar mechanisms were described before in DCC and UNC5B expressing

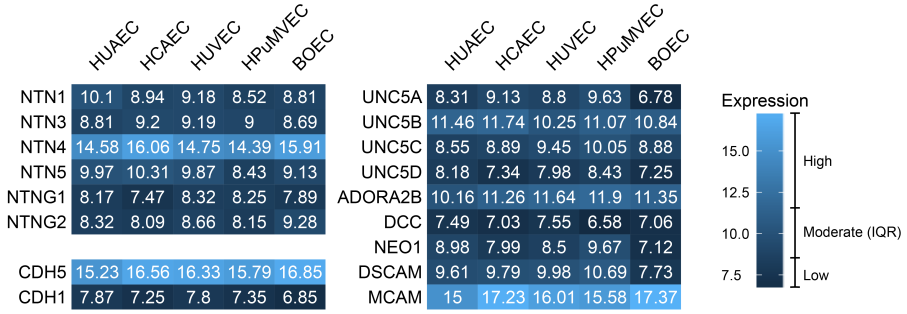

Figure 1. Expression heatmap of netrin family proteins (left) and their receptors (right) Values are the average normalized expression signals from all published data on the Affymetrix Human Genome U133 Plus 2.0 Array (HG-U133 Plus 2.0/GPL570) platform obtained using the Genevestigator software [100]. Lighter colors indicate higher expression. Expression levels within the top quantile on GPL570 platform are recognized as "high"; levels within the inter-quantile range (IQR) are recognized as "moderate"; levels within the bottom quantile are recognized as "low". These notions are used consistently throughout this article. For comparison, we include CDH5 (VE-Cadherin) as a high-expression reference and CDH1 (E-Cadherin) as a low-expression reference (bottom left).

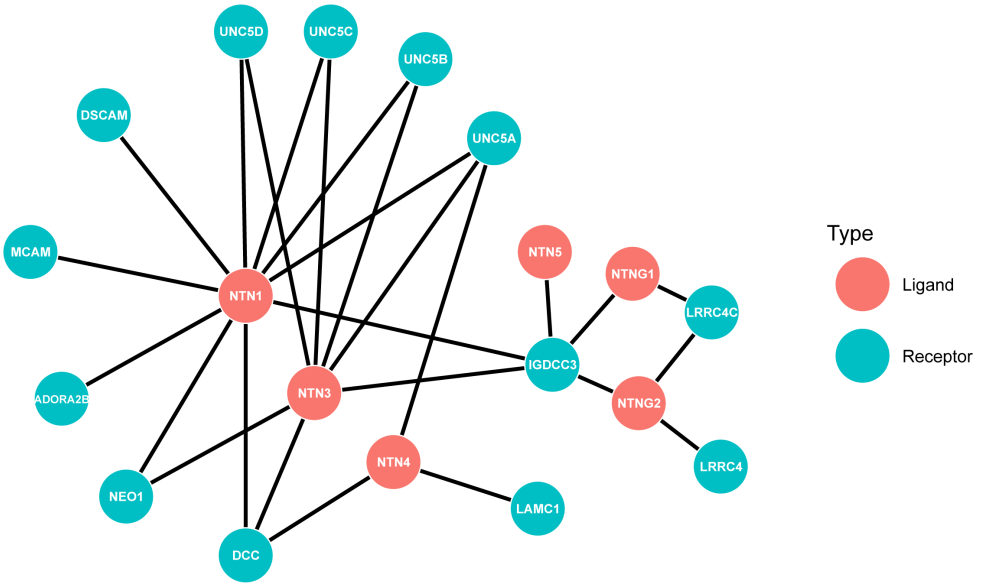

Figure 2. Ligand-receptor binding map of netrin family proteins and their receptors
Red circles represent ligands, blue circles represent receptors.

neurons, where binding of NTN1 to its receptors is essential to maintain survival of these neurons [42, 43]. Under high glucose condition, NTN1 was shown to prevent bovine aortic endothelial from high glucose induced apoptosis by activating ERK1/2 and eNOS [45]. The effect of NTN1 on increasing nitrous oxide production is discussed in Section 6.

2.2.3 Ligands of PLXND1 decrease endothelial cell survival via regulation of integrin activity

The semaphorins are a large family of secreted (Class-3 semaphorins/SEMA3s) or membrane-associated proteins (Class-4-7 semaphorins/SEMA4-7). Almost all types of endothelial cells express high levels of SEMA3F. SEMA3C and SEMA3G have varied expression levels among different endothelial cells. SEMA3A has moderate expression. Class 4-7 semaphorins generally have moderate to high expression levels (**Figure 3**). The main receptors of semaphorins comprise two groups, namely neuropilins (NRP1 and NRP2) and plexins (PLXNA1-4, PLXNB1-3, PLXNC1, and PLXND1) [46-48]. In endothelial cells, high expression levels of PLXNA1, PLXNA2, PLXNB2 and PLXND1 can be found. NRP1 and NRP2 in general also have high expression levels. PLXNA3, PLXNA4, PLXNB1 and PLXNB3

have moderate expression levels (**Figure 3**). Class-4-7 semaphorins can directly bind to plexins. Class-3 semaphorins, except SEMA3E, require neuropilins as obligate co-receptors to interact with plexins, while SEMA3E can independently bind to PLXND1 (**Figure 4**). Next to SEMA3E, SEMA3C and SEMA4A are also ligands for PLXND1 [49], and similar functional consequences have been found when endothelial cells are stimulated with these ligands [50, 51]. Looking at a more functional level, the SEMA3E-PLXND1 axis has been shown to be able to abrogate β1 integrin catch bonds, thus negatively regulating activity of the integrin. PLXND1 itself is required for the normal cluster pattern of β1 integrin on cells [52]. Since PLXND1 is widely expressed in various types of endothelial cells [50, 51, 53, 54], this observation is highly relevant also in endothelial cells. Sakurai et al. [55] have established that, in immortalized mouse endothelial cells, exogenous SEMA3E led to a decrease of β1 integrin activity and reduced focal adhesions, as demonstrated by a decrease of paxillin immunostaining. As a result, adhesion of these cells to collagen but not to poly-L-lysine reduced after SEMA3E treatment. Knockdown of PLXND1, on the other hand, almost completely abolished focal adhesion with or without SEMA3E, supporting a similar role of PLXND1 in endothelial cells on integrin patterning. Interestingly, they also found that SEMA3E induced internalization of β1 integrin, via PLXND1-dependent activation of Arf6 [55]. Together with the observations that integrins, as mentioned before, are important stabilization and survival signals, these mechanisms suggest that SEMA3E-PLXND1 interaction should reduce survival signals and induce apoptosis. Similar functional consequences were observed when endothelial cells were treated with other ligands of PLXND1 [56]: conditioning a medium with SEMA3C increased caspase3/7 activity of HUVECs possibly via inhibition of Akt activity; SEMA3C also decreased focal adhesions and the activity of focal adhesion kinase. Soluble SEMA4A, which is another direct ligand of PLXND1, similarly decreased adhesion of HUVEC to fibronectin and collagen IV. The effect could be rescued by activation of β1 integrin, indicating that binding of SEMA4A to PLXND1 also affects integrin activity. As a result of SEMA4A/PLXND1 interaction, phosphorylation of Akt was also decreased, confirming the lack of integrin activity [50]. Overall, ligands of PLXND1 are able to decrease endothelial cell survival by interfering with integrin function and downstream signaling.

2.2.4 SEMA3C promotes endothelial cell survival via integrin α5β1 and αvβ3

Using a different mechanism, an opposite function of SEMA3C on endothelial cells has also been observed. SEMA3C is found to be expressed in mouse glomerular endothelial cells, in which SEMA3C was able to directly activate integrin β1, while activity of focal adhesion kinase was not affected [51]. With exogenous SEMA3C, adhesion of mouse glomerular endothelial cells to collagen and fibronectin could be increased, but not to gelatin [51]. Indeed, blocking antibody against α5β1 and αvβ3 integrin blocked the increase of adhesion to fibronectin induced by SEMA3C [51]. This is consistent with the fact that fibronectin is a Arg-Gly-Asp-containing ligand, to which α5β1 and αvβ3 integrins can bind [57]. The difference in the extracellular matrix coating is one possible explanation why an opposite role of SEMA3C was seen here. In a similar experiment using only gelatin coating, no pro-survival function could be detected [56].

2.3 Role of netrins and semaphorins in the renewal potential of endothelial cells

The second phase in endothelial cell turnover is to replace the damaged endothelium with healthy endothelial cells, which requires endothelial renewal capability. This ability is often assessed in vitro with proliferation assays and/or wound-healing assays, mimicking the endothelial self-renewal and repairing capability, respectively. To be noted is that the mechanisms underlying the renewal potential are sometimes similar to what we have discussed in in Section 2 for endothelial survival, resulting from versatile pathways regulating both functions. In addition, interpretation of proliferative capability should be done with caution, since quiescent endothelial cells do not proliferate but make up the actual functional endothelium in stable vasculature.

2.3.1 NTN1 dose-dependently affects endothelial cell renewal

In vitro studies demonstrated that lower concentrations of NTN1 (100 ng/ml) promote proliferation of endothelial cells [58-62], while an extremely high concentration of NTN1 inhibits [60-62] or has no effect [63] on the proliferation of endothelial cells. Considering that the typical concentration of NTN1 in human plasma is only several picograms to several hundred picograms per milliliter NTN1[33], the physiological concentration in plasma is far from reaching the threshold for an inhibitory effect on proliferation. NTN1 has been found to play dual roles on the wound-healing capacity of endothelial cells. A low concentration

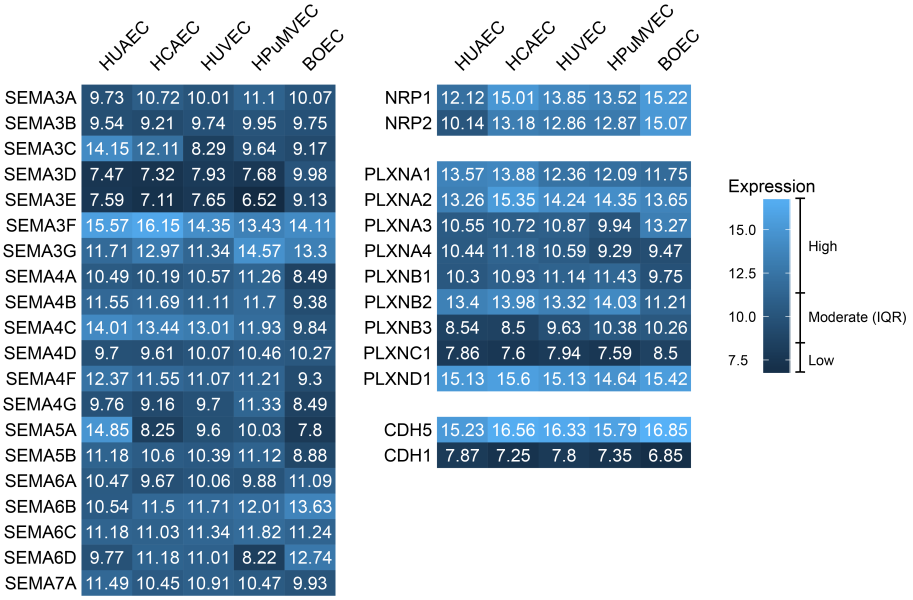

Figure 3. Expression heatmap of semaphorin family proteins (left) and their receptors (right)

Values are the average normalized expression signal from all published data on the Affymetrix Human Genome U133 Plus 2.0 Array (HG-U133 Plus 2.0/GPL570) platform obtained using the Genevestigator software [100]. Lighter colors indicate higher expression. Expression levels within the top quantile on GPL570 platform are recognized as "high"; levels within the inter-quantile range (IQR) are recognized as "moderate"; levels within the bottom quantile are recognized as "low". These notions are used consistently throughout this article. For comparison, we include CDH5 (VE-Cadherin) as a high-expression reference, and CDH1 (E-Cadherin) as a low-expression reference (bottom right).

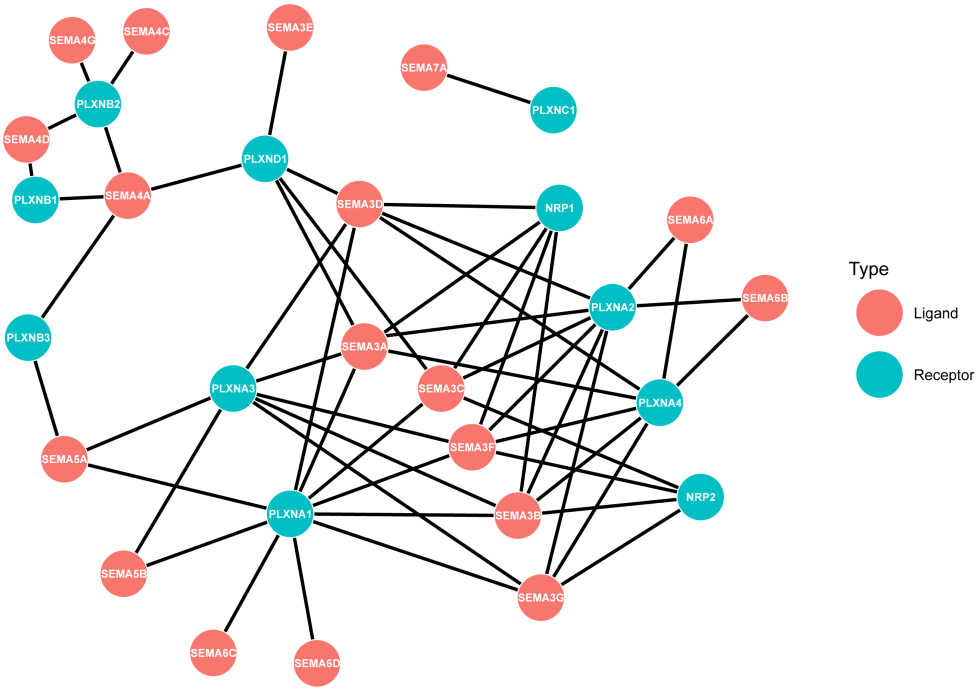

Figure 4. The ligand-receptor binding map of semaphorin family proteins and their receptors

Red circles represent ligands, blue circles represent receptors.

of NTN1 increased the rate with which the gap in a monolayer of endothelial cells was closed in culture [64-67], while a high concentration of NTN1 decreased that [65]. Multiple studies confirmed that the canonical receptor of NTN1, UNC5B, mediated the inhibitory effect of NTN1, since siRNA knockdown of UNC5B abolished this inhibitory effect [60, 62]. Interestingly, UNC5B-knockout mice displayed excessive development of blood vessels, while the same phenotype was not observed in NTN1-knockout mouse, further confirming that NTN1 in physiological concentrations does not primarily regulate the downstream signaling of UNC5B [64, 68]. In 2015, Tu et al. [62] identified the melanoma cell adhesion molecule (MCAM) or CD146 as a novel NTN1 receptor that could mediate the stimulatory effect of NTN1 on proliferation. MCAM co-immunoprecipitated with NTN1 in endothelial cells and had a better binding affinity compared to UNC5B (dissociation constant Kd = 1.33 nM vs 5.10 nM), which is consistent with the finding that MCAM is responsible for NTN1 function in lower concentration ranges. Blocking MCAM expression using siRNA indeed abolished the effect of NTN1 on the proliferation of endothelial cells [62]. Therefore, the NTN1/MCAM pathway most likely mediates the stimulatory effect of (low levels of) NTN1 on proliferation, while UNC5B mediates the NTN1-induced decrease in proliferation when high levels of NTN1 are present.

2.3.2 The effect of NTN4 on endothelial cell renewal is ambiguous

The effect of NTN4 on the endothelial cell renewal capacity is still a matter of on-going debate. Wilson et al. [59] found that NTN4, similar to NTN1, promoted proliferation of various types of endothelial cells at lower concentrations. For very high concentrations of NTN4, Nacht et al. [20] found an inhibitory effect of NTN4 on the proliferation of HMVECs. In contrast to NTN1, Dakouane-Giudicelli et al. [69] showed that a lower concentration of NTN4 also had an inhibitory effect on both proliferation and wound-healing capacity of human placenta endothelial cells. It is very likely that different mechanisms are involved in the effect of NTN4 on endothelial cells, as both structural biology analysis and kinetic binding analysis revealed that NTN4 is not able to bind to several canonical receptors of netrin family, namely DCC, Neogenin and UNC5B [32]. Instead, NTN4 could bind to laminin γ chain to regulate laminin network formation and, potentially, stiffness of the endothelial basement membrane [32]. Since stiffness of extracellular matrix also has an influence on endothelial cell function, more investigation is needed to fully understand the mechanism of NTN4 and its effect on endothelial cell proliferation [70].

2.3.3 SEMA3 family members have dual roles in endothelial cell proliferation

Multiple mechanisms have been proposed to explain the involvement of SEMA3 family members in proliferation of endothelial cells. Class-3 semaphorins except SEMA3E share neuropilins as co-receptor with the VEGF165 isoform ,although evidences showed that VEGF121 isoform can also bind NRP. Neuropillins serve to augment downstream signaling of VEGF165 in endothelial cells by forming a receptor complex with VEGFR2 [71, 72]. Survival signaling by VEGF is especially important during development but can still be of significance in a stabilized vascular network [73]. Loss of VEGF signaling after development decreases vascular integrity, causing symptoms like brain hemorrhage and heart fibrosis in endothelial conditional VEGF-knockout mice [73]. Because of the competition for NRPs between VEGF and SEMA3s, SEMA3s were found to be endogenous inhibitors of VEGF [74-76]. SEMA3A, SEMA3B, SEMA3C and SEMA3F can all reduce endothelial proliferation in the presence of VEGF, which can be blocked by NRP antibody or silencing NRP [56, 77-80]. SEMA3E, on the other hand, binds directly to PLXND1 and the binding of SEMA3E and PLXND1 could also cause upregulation of soluble VEGFR1 in endothelial cells, which serves as endogenous VEGF decoy [81]. Similar to its effect on survival of endothelial cells, SEMA3C plays dual roles on endothelial cell proliferation as well. The increase of proliferation and decrease of apoptosis was attributed to the ability of SEMA3C to induce activation of integrin β1 [51]. This effect could be blocked by NRP1 antibodies, confirming the necessity of NRP1 as a co-receptor of SEMA3C [51].

2.4 Roles of netrins and semaphorins in the response to vessel wall shear stress

Endothelial cells sense shear stress via mechanosensors and trigger a variety of downstream signals that are necessary for the survival of endothelial cells after initial angiogenic stimuli. Unidirectional laminar wall shear stress is a critical hemodynamic factor for endothelial cell maturation and quiescence. An unfavorable hemodynamic environment can disturb quiescent signaling and lead to endothelial cell activation and inflammation, often leading to the development of atherosclerotic lesions. Several studies have proposed roles for neuronal guidance cues as mediators of effects of shear stress.

2.4.1 NTN1 and SEMA3A repel leukocytes in response to laminar shear stress

Expression of both netrins and semaphorins is regulated by wall shear stress. In LDL receptor knockout mice, lower expression of NTN1 could be detected in the inner curvature of the aorta compared to the outer curvature [34]. Given that the endothelium in the inner curvature of mouse aorta experiences lower wall shear stress than in the outer curvature, NTN1 is positively regulated by shear stress. This regulation was confirmed in vitro using human coronary artery endothelial cells cultured under unidirectional laminar flow [34]. In addition, NTN1 was shown to have a repellent role on both migration and adhesion of leukocytes [18, 34, 35, 82]. Neutralizing NTN1 using a blocking antibody abolished the inhibitory effect of NTN1 on leukocyte adhesion to endothelial cells both in vitro and in cremaster capillaries in mice [34]. UNC5B, the receptor of NTN1 involved in its inhibitory proliferative effects, is expressed in peripheral blood leukocytes [35]. Blocking UNC5B using an inhibitory antibody abolished the effect of NTN1 on monocyte migration, confirming the canonical NTN1-UNC5B pathway as the underlying mechanism for the inhibition of leukocyte adhesion and migration [34]. As we discussed above, NTN1 also has a pro-survival function for endothelial cells under physiological concentrations. These observations suggest that NTN1 is one of the mediators for the adaptation of endothelial cells to their hemodynamic environment, to promote survival of endothelial cells, and to inhibit leukocyte adhesion to quiescent endothelium under laminar shear stress. Similar regulation of expression by wall shear stress applies to SEMA3A. Higher expression of SEMA3A was found both in the outer curvature of the aorta of LDL receptor knockout mice and in human coronary artery endothelial cells cultured under laminar flow. SEMA3A also inhibits adhesion of RAW264.7 cells (a macrophage-like cell line) and transwell migration of THP-1 cells (a monocyte-like cell line) in vitro. In addition, a blocking peptide of SEMA3A increases leukocyte adhesion to endothelium in cremaster capillaries [34]. These observations implicate SEMA3A as another mediator for the adaptation of endothelial cells to their hemodynamic environment. However, the mechanism how SEMA3A has this effect needs to be further elucidated.

2.4.2 SEMA7A enhances atherosclerosis in response to disturbed blood flow

In contrast to NTN1 and SEMA3A, SEMA7A is upregulated in the left carotid artery of ApoE -/- mice upon disturbed flow induced by a partial carotid artery ligation procedure [83]. This positive regulation was confirmed by the elevated expression of SEMA7A in HUVECs

cultured under oscillatory shear stress. The upregulation was mediated by downregulation of CREB phosphorylation, while CREB is known as a downstream effector of laminar shear stress. The disturbed flow in the left carotid artery of ApoE -/- mice with partial ligation promoted atherogenesis in this region, but much less atherosclerotic lesions could be seen in the same region in ApoE -/- SEMA7A -/- double knockout mice. Further studies found that SEMA7A overexpressing HUVECs also expressed more ICAM and VCAM, and allowed more monocyte adhesion [83]. The reason for such changes is yet to be determined, but these observations make SEMA7A a possible mediator of the effects of adverse hemodynamic environment on endothelial cells and even renders it a potential therapeutic target.

2.4.3 Downregulation of SEMA6A/6D by shear stress induced miR-27b promote pericyte recruitment

In the case of SEMA6A and SEMA6D, shear stress regulates their expression indirectly via upregulation of microRNA miR-27b. Downregulation of SEMA6A and SEMA6D by such mechanism in HUVECs was found to increase adhesion of human brain vascular pericytes to HUVECs. Inhibition of miR-27b in mice by intraperitoneally injection of locked nucleic acid (LNA) reduce pericyte to endothelial ratio in the uterus. Since pericyte recruitment is a key step in vascular maturation, these experiments provide one of the mechanisms how semaphorins are regulated downstream of shear stress via microRNA to allow endothelium-pericytes interaction [84].

2.5 Roles of netrins and semaphorins in the endothelial barrier function

Vascular endothelium provides a crucial selective barrier for molecule exchange between blood and tissue fluid and for controlled blood cell infiltration. A well-maintained endothelial barrier function relies on correct cytoskeleton arrangements and formation of endothelial cell-cell junctions. Quiescent endothelial cells have abundant cortical filamentous actin (F-actin) network and few stress fibers. Such a cytoskeletal structure limits centripetal tension in endothelial cells and keeps them in a spread morphology. The intercellular connections of endothelial cells are made possible by the formation of both tight junctions and adherens junctions. On the molecular level, tight junctions and adherens junctions 'seal' adjacent endothelial cells by a hemophilic interaction of claudin and occludin proteins, and vascular endothelial cadherin (VE-cadherin or CDH5) proteins, respectively. The cytoplasmic tails of CDH5 interact with several intracellular components resulting in actin filament binding.

Factors that have influence on either cytoskeletal networks or directly on endothelial cell-cell junctions can alter the endothelial barrier function. Through these mechanisms, netrins and semaphorins are identified as regulators of the barrier function of the endothelium.

2.5.1 NTN1 is necessary for tight junctions in the blood-brain barrier

Intact tight junctions are critical in the blood-brain barrier to ensure more selective exchange of molecules between cerebrospinal fluid and blood. Neonatal mice with a NTN1 knockout genotype displayed impaired function of the blood-brain barrier, as the permeability for macromolecules increased [19]. The effect was due to disrupted tight junctions, as evidenced by a decrease of occludin and JAM-A (tight junction proteins) expression that was observed in the endothelium of brain blood vessels of NTN1 knockout mice [19]. It is possible that NTN1 in wild type conditions is presented to endothelial cells by astrocytes in the brain, since conditioned medium from astrocytes, similar to recombinant NTN1, up-regulates several tight junction components including ZO-1, p120 and α-catenin in human brain-derived endothelial cells [19, 85]. The therapeutic potential of NTN1 has been examined in experimental autoimmune encephalomyelitis and middle cerebral artery occlusion models [19, 86]. In both cases, mice treated with NTN1 showed improved barrier function of the blood-brain barrier [19, 86]. However, the exact mechanism on how NTN1 contributes to formation or maintenance of the tight junctions is not known yet. It is interesting to note that MCAM is part of the endothelial cell-cell junction alongside tight junctions and adherent junctions [87]. Previously, we discussed the involvement of MCAM as a receptor for NTN1 in endothelial cell survival. Whether the NTN1/MCAM signaling pathway can play a role in endothelial junction formation remains an interesting topic for future research.

2.5.2 SEMA3A induces endothelial permeability

Multiple studies demonstrated SEMA3A as a factor inducing permeability [88-91]. Injection of SEMA3A led to increased vessel permeability in mouse retro-orbital venous sinus [88], mouse ear vessels [89], mouse retina [90], and mouse subcutaneous capillaries [91]. This effect was confirmed in vitro with human brain endothelial cells [88], rat brain capillary endothelial cells [89], and HUVECs [90, 91]. Increase in phosphorylation of CDH5 was observed in endothelial cells after SEMA3A treatment, resulting in internalization of CDH5 and destabilization of adherent junctions [88, 90, 91]. The effects were dependent on NRP1 expressed by endothelial cells [90, 91]. As one of the underlying mechanisms, Le Guelte et

al. [88] suggested that SEMA3A/NRP1/PLXNA2 signaling leads to phosphorylation of Src kinase, which causes dissociation of PP2A from CDH5, thereby exposing a phosphorylation site on CDH5. SEMA3A has also been found to increase association of VEGFR1 to Mical2, with Mical2 being an enhancer of F-actin depolymerization [89]. Indeed, SEMA3A was found to induce a collapse in F-actin fibers [54, 80]. In addition, in SEMA3A-knockout mice ischemia-reperfusion in the brain caused less leakage from brain blood vessels compared to wild-type mice [89]. Altogether this implies that SEMA3A increase endothelial permeability by disrupting adherens junction and collapsing cytoskeleton. However, controversy remains on the source of SEMA3A as endothelial cells express significant but low levels of SEMA3A and endothelial cell-specific knockout of SEMA3A did not cause a change in permeability of skin vessels [92].

2.6 Role of netrin-1 in controlling of the vascular tone

One of the important functions of endothelial cells is to control vascular tone. This function is realized by production of both vasodilators and vasoconstrictors by endothelial cells. Nitric oxide (NO), a soluble gas, is an important endogenous vasodilator. Besides vasodilation, NO also serves as an anti-inflammatory and anti-oxidative factor for endothelial cells (see the review by Tousoulis et al. [93]). Limited data is available to elucidate the role of NGCs in the regulation of vascular tone. To our knowledge, no role for semaphorins in controlling vascular tone has been described. For the netrins however, an interesting role for NTN1 in this process is described in several studies.

2.6.1 NTN1 controls vascular tone by stimulating release of nitric oxide via DCC receptors

In 2006, Nguyen and Cai [67] found that NTN1 increased activity of endothelial nitric oxide synthase (eNOS) via phosphorylation of extracellular signal-regulated kinase (ERK1/2). Phosphorylation of ERK1/2 led to an increased activity of eNOS, which then catalyzed the oxidation of L-arginine to produce NO [67, 94]. This effect could be blocked by a DCC antibody, suggesting involvement of DCC as the responsible receptor [45, 67, 95-97]. Despite low expression of DCC on endothelial cells, it was shown that NO itself preserves DCC from degradation in endothelial cells via inhibition of the E3 ubiquitin ligase “seven in absentia homolog” (SIAH) [98]. The ability of NTN1 to activate NO production gives it a protective function in organ ischemia reperfusion. Infusion of NTN1 following ischemia reperfusion of

mouse hearts decreases infarct size and improves mitochondrial dysfunction, resulting from the increased bio-availability of NO [96, 97, 99]. Very recently, induction of NO production by NTN1 was confirmed in vivo in NTN1 transgenic mice. Compared to WT mice, NTN1 transgenic mice showed increased level of NO in aortic ring assessed by 4,5-diaminofluorescein (DAF-2) staining. Under normal condition, response of aortas to acetylcholine (relaxation), nitroprusside (relaxation) and phenylephrine (contraction) did not change by NTN1 transgene. In diabetic condition, NTN1 overexpression transgene could protect the mice from dampened response to relaxation agents and exaggerated response to contraction agent. [45]

2.7 Concluding remarks

In this review, we summarized relevant studies about the involvement of netrins (**Figure 5**) and semaphorins (**Figure 6**) in the function of mature endothelial cells. Netrins and semaphorins were originally identified to have axonal guidance function in the nervous system. Given the striking similarity in anatomy of the peripheral nervous and vascular systems, it is not surprising that the vascular system uses the same group of molecules in development. A lesson learned in recent years is that the function of mature and quiescent endothelial cells is of great importance and requires active regulation. Besides other well-known mechanisms, evidence accumulates suggesting that netrins and semaphorins continue to serve as intercellular and extracellular cues for endothelial cells to maintain their quiescent state and related functions as described in this review. These functions also give both netrins and semaphorins implications in the development of several diseases. Despite the fact that more and more attention is being paid to the regulation of endothelial cell function by NGCs, most research has been performed in vitro. More in vivo evidence is required to fully confirm the necessity of semaphorins and netrins. As research into this aspect is ongoing, we expect new insights in the near future. For example, it has already been shown that NTN1 promotes endothelial tight junctions in the blood-brain barrier in a model of experimental autoimmune encephalomyelitis (which is a mouse model for brain inflammation caused by loss of blood-brain barrier function) and middle cerebral artery occlusion models (mouse models for stroke). Moreover, SEMA7A can elevate monocyte adhesion in regions with disturbed flow and thereby promote atherosclerosis. Taken together, NGCs are intrinsically involved in endothelial pathophysiology and there is no doubt that further investigations of NGCs will reveal novel insights in and disease targets towards sustaining vascular health and integrity.

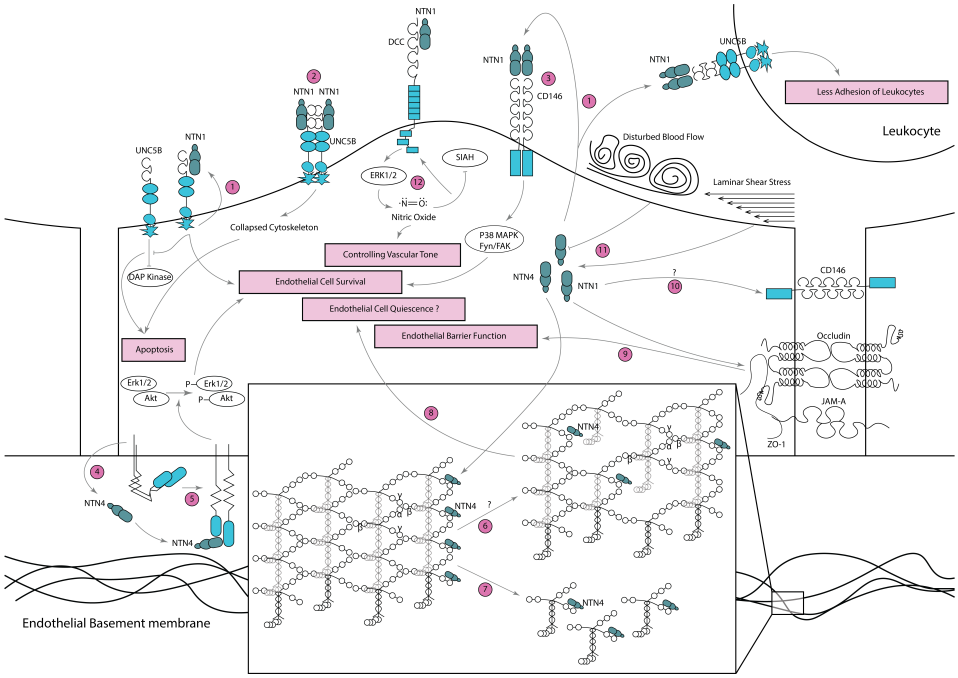

Figure 5. Schematic representation of mature endothelial cell biology, indicating the roles of netrin family proteins

(1) Moderate secretion of NTN1. (2) Saturated concentration of NTN1. (3) High affinity binding. (4) Basolateral secretion. (5) Activation of integrin $\alpha 6\beta 1$. (6) Physiological concentration of NTN4 possibly changes the stiffness of the laminin matrix. (7) Saturating concentration of NTN4 dissociates the laminin network. (8) Low stiffness of extracellular matrix promotes endothelial cell quiescence. (9) NTN1 is necessary for tight junction stability in the blood-brain barrier. (10) NTN1 binds to MCAM; this could have an influence on endothelial barrier. (11) Laminar shear stress increases the expression of NTN1, while disturbed flow decreases it. (12) NTN1 increases NO production via DCC receptors and ERK1/2. In addition, NO protects DCC from degradation through inhibition of E3 ubiquitin ligase SIAH.

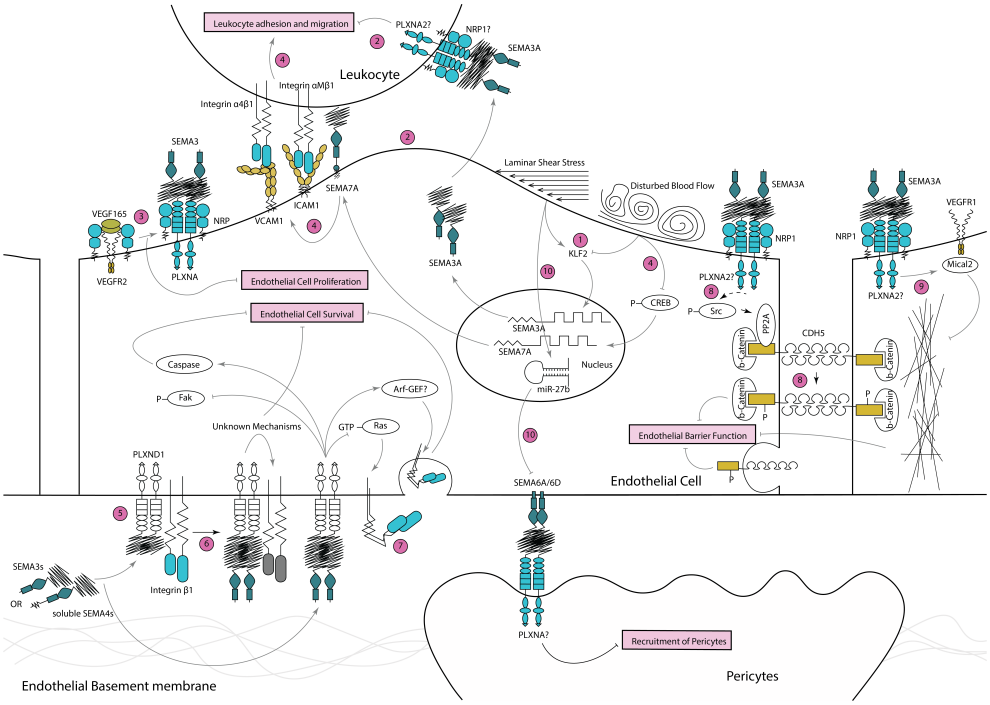

Figure 6. Schematic representation of mature endothelial cell biology, indicating the roles of semaphorin family proteins

(1) Laminar shear stress upregulates the flow-dependent transcription factor KLF2. Translocation of KLF2 into the nucleus increases the expression of its target gene SEMA3A. (2) SEMA3A secreted by endothelial cells reduce adhesion of leukocytes and repel leukocyte migration. (3) Competition on co-receptor neuropillin between Class-3 semaphorin and VEGF decreases VEGF signaling, thus decreasing endothelial cell proliferation. (4) SEMA7A, upregulated by turbulent flow on endothelial cells, increases expression of adhesion molecules ICAM-1 and VCAM-1, thereby increasing monocyte adhesion to endothelial cells. (5) PLXND1 itself patterns integrin β1 on the endothelial cell surface. (6) Binding of ligands to PLXND1 causes loss of integrin catch bond, thus decreasing integrin activity. (7) Binding of ligands to PLXND1 inactivate integrin activity and induce integrin internalization. (8) Binding of SEMA3A to its receptor complex increases phosphorylation of Src kinase, which causes dissociation of PP2A from CDH5, resulting in phosphorylation of CDH5 and thereby its internalization. This disturbs the adherent junction between endothelial cells. (9) Binding of SEMA3A to its receptor complex induces association of Mical2 to VEGFR1, which leads to depolymerization of cortical F-actin. Loss of cortical actin filaments undermines the ability of endothelial cells to counteract centripetal tension, thus destabilizing the endothelial barrier. (10) Laminar shear stress increases expression of miR-27b, which represses expression of SEMA6A and SEMA6B. Repression of these 2 semaphorins increases recruitment of pericytes to endothelium.

Acknowledgements

This research was supported by a grant from the Netherlands Heart Foundation (2013T127 to H.Z. and J.M.G.).

Conflict of interest

The authors declare no conflicts of interest.

References

1. *Cines, D.B., E.S. Pollak, C.A. Buck, J. Loscalzo, G.A. Zimmerman, R.P. McEver, J.S. Pober, T.M. Wick, B.A. Konkle, B.S. Schwartz, E.S. Barnathan, K.R. McCrae, B.A. Hug, A.M. Schmidt, and D.M. Stern, Endothelial cells in physiology and in the pathophysiology of vascular disorders. Blood, 1998. 91(10): p. 3527-61.*
2. *Carmeliet, P., Blood vessels and nerves: common signals, pathways and diseases. Nat Rev Genet, 2003. 4(9): p. 710-20.*
3. *Carmeliet, P. and M. Tessier-Lavigne, Common mechanisms of nerve and blood vessel wiring. Nature, 2005. 436(7048): p. 193-200.*
4. *Melani, M. and B.M. Weinstein, Common factors regulating patterning of the nervous and vascular systems. Annu Rev Cell Dev Biol, 2010. 26: p. 639-65.*
5. *Arese, M., G. Serini, and F. Bussolino, Nervous vascular parallels: axon guidance and beyond. Int J Dev Biol, 2011. 55(4-5): p. 439-45.*
6. *Adams, R.H. and A. Eichmann, Axon guidance molecules in vascular patterning. Cold Spring Harb Perspect Biol, 2010. 2(5): p. a001875.*
7. *Wang, B., N. Zhang, K.X. Qian, and J.G. Geng, Conserved molecular players for axon guidance and angiogenesis. Curr Protein Pept Sci, 2005. 6(5): p. 473-8.*
8. *Klagsbrun, M. and A. Eichmann, A role for axon guidance receptors and ligands in blood vessel development and tumor angiogenesis. Cytokine Growth Factor Rev, 2005. 16(4-5): p. 535-48.*
9. *Serini, G. and F. Bussolino, Common cues in vascular and axon guidance. Physiology (Bethesda), 2004. 19: p. 348-54.*
10. *Foteinos, G., Y. Hu, Q. Xiao, B. Metzler, and Q. Xu, Rapid endothelial turnover in atherosclerosis-prone areas coincides with stem cell repair in apolipoprotein E-deficient mice. Circulation, 2008. 117(14): p. 1856-63.*

11. *Tricot, O., Z. Mallat, C. Heymes, J. Belmin, G. Leseche, and A. Tedgui, Relation between endothelial cell apoptosis and blood flow direction in human atherosclerotic plaques. Circulation, 2000. 101(21): p. 2450-3.*

12. *Yamamoto, H., M. Ehling, K. Kato, K. Kanai, M. van Lessen, M. Frye, D. Zeuschner, M. Nakayama, D. Vestweber, and R.H. Adams, Integrin beta1 controls VE-cadherin localization and blood vessel stability. Nat Commun, 2015. 6: p. 6429.*

13. *Serafini, T., T.E. Kennedy, M.J. Galko, C. Mirzayan, T.M. Jessell, and M. Tessier-Lavigne, The netrins define a family of axon outgrowth-promoting proteins homologous to C. elegans UNC-6. Cell, 1994. 78(3): p. 409-24.*

14. *Kennedy, T.E., T. Serafini, J.R. de la Torre, and M. Tessier-Lavigne, Netrins are diffusible chemotropic factors for commissural axons in the embryonic spinal cord. Cell, 1994. 78(3): p. 425-35.*

15. *Nakashiba, T., T. Ikeda, S. Nishimura, K. Tashiro, T. Honjo, J.G. Culotti, and S. Itohara, Netrin-G1: a novel glycosyl phosphatidylinositol-linked mammalian netrin that is functionally divergent from classical netrins. J Neurosci, 2000. 20(17): p. 6540-50.*

16. *Nakashiba, T., S. Nishimura, T. Ikeda, and S. Itohara, Complementary expression and neurite outgrowth activity of netrin-G subfamily members. Mech Dev, 2002. 111(1-2): p. 47-60.*

17. *Cirulli, V. and M. Yebra, Netrins: beyond the brain. Nat Rev Mol Cell Biol, 2007. 8(4): p. 296-306.*

18. *Rosenberger, P., J.M. Schwab, V. Mirakaj, E. Masekowsky, A. Mager, J.C. Morote-Garcia, K. Unertl, and H.K. Eltzschig, Hypoxia-inducible factor-dependent induction of netrin-1 dampens inflammation caused by hypoxia. Nat Immunol, 2009. 10(2): p. 195-202.*

19. *Podjaski, C., J.I. Alvarez, L. Bourbonniere, S. Larouche, S. Terouz, J.M. Bin, M.A. Lecuyer, O. Saint-Laurent, C. Larochelle, P.J. Darlington, N. Arbour, J.P. Antel, T.E. Kennedy, and A. Prat, Netrin 1 regulates blood-brain barrier function and neuroinflammation. Brain, 2015. 138(Pt 6): p. 1598-612.*

20. *Nacht, M., T.B. St Martin, A. Byrne, K.W. Klinger, B.A. Teicher, S.L. Madden, and Y. Jiang, Netrin-4 regulates angiogenic responses and tumor cell growth. Exp Cell Res, 2009. 315(5): p. 784-94.*

21. *Han, Y., Y. Shao, T. Liu, Y.L. Qu, W. Li, and Z. Liu, Therapeutic effects of topical netrin-4 inhibits corneal neovascularization in alkali-burn rats. PLoS One, 2015. 10(4): p. e0122951.*

22. *Conway, D.E., M.R. Williams, S.G. Eskin, and L.V. McIntire, Endothelial cell responses to atheroprone flow are driven by two separate flow components: low time-average shear stress and fluid flow reversal. Am J Physiol Heart Circ Physiol, 2010. 298(2): p. H367-74.*

23. *Larrieu-Lahargue, F., A.L. Welm, K.R. Thomas, and D.Y. Li, Netrin-4 activates endothelial integrin alpha6beta1. Circ Res, 2011. 109(7): p. 770-4.*

24. *Yebra, M., G.R. Diaferia, A.M. Montgomery, T. Kaido, W.J. Brunken, M. Koch, G. Hardiman, L. Crisa, and V. Cirulli, Endothelium-derived Netrin-4 supports pancreatic epithelial cell adhesion and differentiation through integrins alpha2beta1 and alpha3beta1. PLoS One, 2011. 6(7): p. e22750.*

25. *Li, L., Y. Hu, I. Ylivinkka, H. Li, P. Chen, J. Keski-Oja, and M. Hyytiainen, NETRIN-4 protects glioblastoma cells FROM temozolomide induced senescence. PLoS One, 2013. 8(11): p. e80363.*

26. *Lambert, E., M.M. Coissieux, V. Laudet, and P. Mehlen, Netrin-4 acts as a pro-angiogenic factor during zebrafish development. J Biol Chem, 2012. 287(6): p. 3987-99.*

27. *Lange, J., Y. Yafai, A. Noack, X.M. Yang, A.B. Munk, S. Krohn, I. Iandiev, P. Wiedemann, A. Reichenbach, and W. Eichler, The axon guidance molecule Netrin-4 is expressed by Muller cells and contributes to angiogenesis in the retina. Glia, 2012. 60(10): p. 1567-78.*

28. *Li, Y.N., G. Pinzon-Duarte, M. Dattilo, T. Claudepierre, M. Koch, and W.J. Brunken, The expression and function of netrin-4 in murine ocular tissues. Exp Eye Res, 2012. 96(1): p. 24-35.*

29. *Kociok, N., S. Crespo-Garcia, Y. Liang, S.V. Klein, C. Nurnberg, N. Reichhart, S. Skosyrski, E. Moritz, A.K. Maier, W.J. Brunken, O. Strauss, M. Koch, and A.M. Joussen, Lack of netrin-4 modulates pathologic neovascularization in the eye. Sci Rep, 2016. 6: p. 18828.*

30. *Kabosova, A., D.T. Azar, G.A. Bannikov, K.P. Campbell, M. Durbeej, R.F. Ghohestani, J.C. Jones, M.C. Kenney, M. Koch, Y. Ninomiya, B.L. Patton, M. Paulsson,*

Y. Sado, E.H. Sage, T. Sasaki, L.M. Sorokin, M.F. Steiner-Champliaud, T.T. Sun, N. Sundarraj, R. Timpl, I. Virtanen, and A.V. Ljubimov, Compositional differences between infant and adult human corneal basement membranes. Invest Ophthalmol Vis Sci, 2007. 48(11): p. 4989-99.

31. *Rajasekharan, S. and T.E. Kennedy, The netrin protein family. Genome Biol, 2009. 10(9): p. 239.*
32. *Reuten, R., T.R. Patel, M. McDougall, N. Rama, D. Nikodemus, B. Gibert, J.G. Delcros, C. Prein, M. Meier, S. Metzger, Z. Zhou, J. Kaltenberg, K.K. McKee, T. Bald, T. Tuting, P. Zigrino, V. Djonov, W. Bloch, H. Clausen-Schaumann, E. Poschl, P.D. Yurchenco, M. Ehrbar, P. Mehlen, J. Stetefeld, and M. Koch, Structural decoding of netrin-4 reveals a regulatory function towards mature basement membranes. Nat Commun, 2016. 7: p. 13515.*
33. *Xing, Y., J. Lai, X. Liu, N. Zhang, J. Ming, H. Liu, and X. Zhang, Netrin-1 restores cell injury and impaired angiogenesis in vascular endothelial cells upon high glucose by PI3K/AKT-eNOS. J Mol Endocrinol, 2017. 58(4): p. 167-177.*
34. *van Gils, J.M., B. Ramkhelawon, L. Fernandes, M.C. Stewart, L. Guo, T. Seibert, G.B. Menezes, D.C. Cara, C. Chow, T.B. Kinane, E.A. Fisher, M. Balcells, J. Alvarez-Leite, A. Lacy-Hulbert, and K.J. Moore, Endothelial expression of guidance cues in vessel wall homeostasis dysregulation under proatherosclerotic conditions. Arterioscler Thromb Vasc Biol, 2013. 33(5): p. 911-9.*
35. *Ly, N.P., K. Komatsuzaki, I.P. Fraser, A.A. Tseng, P. Prodhan, K.J. Moore, and T.B. Kinane, Netrin-1 inhibits leukocyte migration in vitro and in vivo. Proc Natl Acad Sci U S A, 2005. 102(41): p. 14729-34.*
36. *Kizmaz, M., K. Marakoglu, A. Kiyici, and E. Ay, Plasma netrin-1 levels significantly increase in smokers. Clin Biochem, 2016. 49(10-11): p. 832-4.*
37. *Layne, K., T. Goodman, A. Ferro, and G. Passacquale, The effect of aspirin on circulating netrin-1 levels in humans is dependent on the inflammatory status of the vascular endothelium. Oncotarget, 2017. 8(49): p. 86548-86555.*
38. *Ay, E., K. Marakoglu, M. Kizmaz, and A. Unlu, Evaluation of Netrin-1 Levels and Albuminuria in Patients With Diabetes. J Clin Lab Anal, 2016. 30(6): p. 972-977.*
39. *Kefeli, U., M.E. Yildirim, D. Aydin, O.C. Madenci, N. Yasar, N. Sener, A.G. Mert, S. Yuksel, O.B. Ercelep, T. Korkmaz, R. Yildiz, and M. Gumus, Netrin-1 concentrations*

in patients with advanced gastric cancer and its relation with treatment. Biomarkers, 2012. 17(7): p. 663-7.

40. Ramesh, G., A. Berg, and C. Jayakumar, Plasma netrin-1 is a diagnostic biomarker of human cancers. Biomarkers, 2011. 16(2): p. 172-80.

41. Liu, C., X. Ke, Y. Wang, X. Feng, Q. Li, Y. Zhang, J. Zhu, and Q. Li, The level of netrin-1 is decreased in newly diagnosed type 2 diabetes mellitus patients. BMC Endocr Disord, 2016. 16(1): p. 33.

42. Mehlen, P., S. Rabizadeh, S.J. Snipas, N. Assa-Munt, G.S. Salvesen, and D.E. Bredesen, The DCC gene product induces apoptosis by a mechanism requiring receptor proteolysis. Nature, 1998. 395(6704): p. 801-4.

43. Llambi, F., F. Causeret, E. Bloch-Gallego, and P. Mehlen, Netrin-1 acts as a survival factor via its receptors UNC5H and DCC. EMBO J, 2001. 20(11): p. 2715-22.

44. Castets, M., M.M. Coissieux, C. Delloye-Bourgeois, L. Bernard, J.G. Delcros, A. Bernet, V. Laudet, and P. Mehlen, Inhibition of endothelial cell apoptosis by netrin-1 during angiogenesis. Dev Cell, 2009. 16(4): p. 614-20.

45. Toque, H.A., A. Fernandez-Flores, R. Mohamed, R.B. Caldwell, G. Ramesh, and R.W. Caldwell, Netrin-1 is a novel regulator of vascular endothelial function in diabetes. PLoS One, 2017. 12(10): p. e0186734.

46. Pasterkamp, R.J., Getting neural circuits into shape with semaphorins. Nat Rev Neurosci, 2012. 13(9): p. 605-18.

47. Takamatsu, H. and A. Kumanogoh, Diverse roles for semaphorin-plexin signaling in the immune system. Trends Immunol, 2012. 33(3): p. 127-35.

48. Tamagnone, L., Emerging role of semaphorins as major regulatory signals and potential therapeutic targets in cancer. Cancer Cell, 2012. 22(2): p. 145-52.

49. Sharma, A., J. Verhaagen, and A.R. Harvey, Receptor complexes for each of the Class 3 Semaphorins. Front Cell Neurosci, 2012. 6: p. 28.

50. Toyofuku, T., M. Yabuki, J. Kamei, M. Kamei, N. Makino, A. Kumanogoh, and M. Hori, Semaphorin-4A, an activator for T-cell-mediated immunity, suppresses angiogenesis via Plexin-D1. Embo j, 2007. 26(5): p. 1373-84.

51. *Banu, N., J. Teichman, M. Dunlap-Brown, G. Villegas, and A. Tufro, Semaphorin 3C regulates endothelial cell function by increasing integrin activity. Faseb j, 2006. 20(12): p. 2150-2.*

52. *Choi, Y.I., J.S. Duke-Cohan, W. Chen, B. Liu, J. Rossy, T. Tabarin, L. Ju, J. Gui, K. Gaus, C. Zhu, and E.L. Reinherz, Dynamic control of beta1 integrin adhesion by the plexinD1-sema3E axis. Proc Natl Acad Sci U S A, 2014. 111(1): p. 379-84.*

53. *van der Zwaag, B., A.J. Hellemons, W.P. Leenders, J.P. Burbach, H.G. Brunner, G.W. Padberg, and H. Van Bokhoven, PLEXIN-D1, a novel plexin family member, is expressed in vascular endothelium and the central nervous system during mouse embryogenesis. Dev Dyn, 2002. 225(3): p. 336-43.*

54. *Torres-Vazquez, J., A.D. Gitler, S.D. Fraser, J.D. Berk, N.P. Van, M.C. Fishman, S. Childs, J.A. Epstein, and B.M. Weinstein, Semaphorin-plexin signaling guides patterning of the developing vasculature. Dev Cell, 2004. 7(1): p. 117-23.*

55. *Sakurai, A., J. Gavard, Y. Annas-Linhares, J.R. Basile, P. Amornphimoltham, T.R. Palmby, H. Yagi, F. Zhang, P.A. Randazzo, X. Li, R. Weigert, and J.S. Gutkind, Semaphorin 3E initiates antiangiogenic signaling through plexin D1 by regulating Arf6 and R-Ras. Mol Cell Biol, 2010. 30(12): p. 3086-98.*

56. *Yang, W.J., J. Hu, A. Uemura, F. Tetzlaff, H.G. Augustin, and A. Fischer, Semaphorin-3C signals through Neuropilin-1 and PlexinD1 receptors to inhibit pathological angiogenesis. EMBO Mol Med, 2015. 7(10): p. 1267-84.*

57. *Margadant, C., H.N. Monsuur, J.C. Norman, and A. Sonnenberg, Mechanisms of integrin activation and trafficking. Curr Opin Cell Biol, 2011. 23(5): p. 607-14.*

58. *Park, K.W., D. Crouse, M. Lee, S.K. Karnik, L.K. Sorensen, K.J. Murphy, C.J. Kuo, and D.Y. Li, The axonal attractant Netrin-1 is an angiogenic factor. Proc Natl Acad Sci U S A, 2004. 101(46): p. 16210-5.*

59. *Wilson, B.D., M. Ii, K.W. Park, A. Suli, L.K. Sorensen, F. Larrieu-Lahargue, L.D. Urness, W. Suh, J. Asai, G.A. Kock, T. Thorne, M. Silver, K.R. Thomas, C.B. Chien, D.W. Losordo, and D.Y. Li, Netrins promote developmental and therapeutic angiogenesis. Science, 2006. 313(5787): p. 640-4.*

60. *Yang, Y., L. Zou, Y. Wang, K.S. Xu, J.X. Zhang, and J.H. Zhang, Axon guidance cue Netrin-1 has dual function in angiogenesis. Cancer Biol Ther, 2007. 6(5): p. 743-8.*

61. *Xie, H., L. Zou, J. Zhu, and Y. Yang, Effects of netrin-1 and netrin-1 knockdown on human umbilical vein endothelial cells and angiogenesis of rat placenta. Placenta, 2011. 32(8): p. 546-53.*

62. *Tu, T., C. Zhang, H. Yan, Y. Luo, R. Kong, P. Wen, Z. Ye, J. Chen, J. Feng, F. Liu, J.Y. Wu, and X. Yan, CD146 acts as a novel receptor for netrin-1 in promoting angiogenesis and vascular development. Cell Res, 2015. 25(3): p. 275-87.*

63. *Yang, X., S. Li, J. Zhong, W. Zhang, X. Hua, B. Li, and H. Sun, CD151 mediates netrin-1-induced angiogenesis through the Src-FAK-Paxillin pathway. J Cell Mol Med, 2017. 21(1): p. 72-80.*

64. *Lu, X., F. Le Noble, L. Yuan, Q. Jiang, B. De Lafarge, D. Sugiyama, C. Breant, F. Claes, F. De Smet, J.L. Thomas, M. Autiero, P. Carmeliet, M. Tessier-Lavigne, and A. Eichmann, The netrin receptor UNC5B mediates guidance events controlling morphogenesis of the vascular system. Nature, 2004. 432(7014): p. 179-86.*

65. *Yu, Y., J. Zou, Y. Han, L. Quyang, H. He, P. Hu, Y. Shao, and P. Tu, Effects of intravitreal injection of netrin-1 in retinal neovascularization of streptozotocin-induced diabetic rats. Drug Des Devel Ther, 2015. 9: p. 6363-77.*

66. *Prieto, C.P., M.C. Ortiz, A. Villanueva, C. Villarroel, S.S. Edwards, M. Elliott, J. Lattus, S. Aedo, D. Meza, P. Lois, and V. Palma, Netrin-1 acts as a non-canonical angiogenic factor produced by human Wharton's jelly mesenchymal stem cells (WJ-MSC). Stem Cell Res Ther, 2017. 8(1): p. 43.*

67. *Nguyen, A. and H. Cai, Netrin-1 induces angiogenesis via a DCC-dependent ERK1/2-eNOS feed-forward mechanism. Proc Natl Acad Sci U S A, 2006. 103(17): p. 6530-5.*

68. *Yung, A.R., A.M. Nishitani, and L.V. Goodrich, Phenotypic analysis of mice completely lacking netrin 1. Development, 2015. 142(21): p. 3686-91.*

69. *Dakouane-Giudicelli, M., S. Brouillet, W. Traboulsi, A. Torre, G. Vallat, S. Si Nacer, M. Vallee, J.J. Feige, N. Alfaidy, and P. de Mazancourt, Inhibition of human placental endothelial cell proliferation and angiogenesis by netrin-4. Placenta, 2015. 36(11): p. 1260-5.*

70. *Sack, K.D., M. Teran, and M.A. Nugent, Extracellular Matrix Stiffness Controls VEGF Signaling and Processing in Endothelial Cells. J Cell Physiol, 2016. 231(9): p. 2026-39.*

71. *Herzog, B., C. Pellet-Many, G. Britton, B. Hartzoulakis, and I.C. Zachary, VEGF binding to NRP1 is essential for VEGF stimulation of endothelial cell migration, complex formation between NRP1 and VEGFR2, and signaling via FAK Tyr407 phosphorylation. Mol Biol Cell, 2011. 22(15): p. 2766-76.*

72. *Whitaker, G.B., B.J. Limberg, and J.S. Rosenbaum, Vascular endothelial growth factor receptor-2 and neuropilin-1 form a receptor complex that is responsible for the differential signaling potency of VEGF(165) and VEGF(121). J Biol Chem, 2001. 276(27): p. 25520-31.*

73. *Domigan, C.K., C.M. Warren, V. Antanesian, K. Happel, S. Ziyad, S. Lee, A. Krall, L. Duan, A.X. Torres-Collado, L.W. Castellani, D. Elashoff, H.R. Christofk, A.M. van der Bliek, M. Potente, and M.L. Iruela-Arispe, Autocrine VEGF maintains endothelial survival through regulation of metabolism and autophagy. J Cell Sci, 2015. 128(12): p. 2236-48.*

74. *Parker, M.W., A.D. Linkugel, and C.W. Vander Kooi, Effect of C-terminal sequence on competitive semaphorin binding to neuropilin-1. J Mol Biol, 2013. 425(22): p. 4405-14.*

75. *Parker, M.W., L.M. Hellman, P. Xu, M.G. Fried, and C.W. Vander Kooi, Furin processing of semaphorin 3F determines its anti-angiogenic activity by regulating direct binding and competition for neuropilin. Biochemistry, 2010. 49(19): p. 4068-75.*

76. *Guo, H.F., X. Li, M.W. Parker, J. Waltenberger, P.M. Becker, and C.W. Vander Kooi, Mechanistic basis for the potent anti-angiogenic activity of semaphorin 3F. Biochemistry, 2013. 52(43): p. 7551-8.*

77. *Yu, W., Y. Bai, N. Han, F. Wang, M. Zhao, L. Huang, and X. Li, Inhibition of pathological retinal neovascularization by semaphorin 3A. Mol Vis, 2013. 19: p. 1397-405.*

78. *Vacca, A., C. Scavelli, G. Serini, G. Di Pietro, T. Cirulli, F. Merchionne, D. Ribatti, F. Bussolino, D. Guidolin, G. Piaggio, A. Bacigalupo, and F. Dammacco, Loss of inhibitory semaphorin 3A (SEMA3A) autocrine loops in bone marrow endothelial cells of patients with multiple myeloma. Blood, 2006. 108(5): p. 1661-7.*

79. *Narazaki, M. and G. Tosato, Ligand-induced internalization selects use of common receptor neuropilin-1 by VEGF165 and semaphorin3A. Blood, 2006. 107(10): p. 3892-901.*

80. *Guttmann-Raviv, N., N. Shraga-Heled, A. Varshavsky, C. Guimaraes-Sternberg, O. Kessler, and G. Neufeld, Semaphorin-3A and semaphorin-3F work together to repel endothelial cells and to inhibit their survival by induction of apoptosis. J Biol Chem, 2007. 282(36): p. 26294-305.*

81. *Zygmunt, T., C.M. Gay, J. Blondelle, M.K. Singh, K.M. Flaherty, P.C. Means, L. Herwig, A. Krudewig, H.G. Belting, M. Affolter, J.A. Epstein, and J. Torres-Vazquez, Semaphorin-PlexinD1 signaling limits angiogenic potential via the VEGF decoy receptor sFlt1. Dev Cell, 2011. 21(2): p. 301-14.*

82. *van Gils, J.M., M.C. Derby, L.R. Fernandes, B. Ramkhelawon, T.D. Ray, K.J. Rayner, S. Parathath, E. Distel, J.L. Feig, J.I. Alvarez-Leite, A.J. Rayner, T.O. McDonald, K.D. O'Brien, L.M. Stuart, E.A. Fisher, A. Lacy-Hulbert, and K.J. Moore, The neuroimmune guidance cue netrin-1 promotes atherosclerosis by inhibiting the emigration of macrophages from plaques. Nat Immunol, 2012. 13(2): p. 136-43.*

83. *Hu, S., Y. Liu, T. You, J. Heath, L. Xu, X. Zheng, A. Wang, Y. Wang, F. Li, F. Yang, Y. Cao, H. Zhang, J.M. van Gils, A.J. van Zonneveld, H. Jo, Q. Wu, Y. Zhang, C. Tang, and L. Zhu, Vascular Semaphorin 7A Upregulation by Disturbed Flow Promotes Atherosclerosis Through Endothelial beta1 Integrin. Arterioscler Thromb Vasc Biol, 2017.*

84. *Demolli, S., A. Doddaballapur, K. Devraj, K. Stark, Y. Manavski, A. Eckart, C.M. Zehendner, T. Lucas, T. Korff, M. Hecker, S. Massberg, S. Liebner, D. Kaluza, R.A. Boon, and S. Dimmeler, Shear stress-regulated miR-27b controls pericyte recruitment by repressing SEMA6A and SEMA6D. Cardiovasc Res, 2017. 113(6): p. 681-691.*

85. *Wen, J., S. Qian, Q. Yang, L. Deng, Y. Mo, and Y. Yu, Overexpression of netrin-1 increases the expression of tight junction-associated proteins, claudin-5, occludin, and ZO-1, following traumatic brain injury in rats. Exp Ther Med, 2014. 8(3): p. 881-886.*

86. *Yu, J., C. Li, Q. Ding, J. Que, K. Liu, H. Wang, and S. Liao, Netrin-1 Ameliorates Blood-Brain Barrier Impairment Secondary to Ischemic Stroke via the Activation of PI3K Pathway. Frontiers in Neuroscience, 2017. 11: p. 700.*

87. *Bardin, N., F. Anfosso, J.M. Masse, E. Cramer, F. Sabatier, A. Le Bivic, J. Sampol, and F. Dignat-George, Identification of CD146 as a component of the endothelial junction involved in the control of cell-cell cohesion. Blood, 2001. 98(13): p. 3677-84.*

88. *Le Guelte, A., E.M. Galan-Moya, J. Dwyer, L. Treps, G. Kettler, J.K. Hebda, S. Dubois, C. Auffray, H. Chneiweiss, N. Bidere, and J. Gavard, Semaphorin 3A elevates endothelial cell permeability through PP2A inactivation. J Cell Sci, 2012. 125(Pt 17): p. 4137-46.*

89. *Hou, S.T., L. Nilchi, X. Li, S. Gangaraju, S.X. Jiang, A. Aylsworth, R. Monette, and J. Slinn, Semaphorin3A elevates vascular permeability and contributes to cerebral ischemia-induced brain damage. Sci Rep, 2015. 5: p. 7890.*

90. *Cerani, A., N. Tetreault, C. Menard, E. Lapalme, C. Patel, N. Sitaras, F. Beaudoin, D. Leboeuf, V. De Guire, F. Binet, A. Dejda, F.A. Rezende, K. Miloudi, and P. Sapieha, Neuron-derived semaphorin 3A is an early inducer of vascular permeability in diabetic retinopathy via neuropilin-1. Cell Metab, 2013. 18(4): p. 505-18.*

91. *Acevedo, L.M., S. Barillas, S.M. Weis, J.R. Gothert, and D.A. Cheresh, Semaphorin 3A suppresses VEGF-mediated angiogenesis yet acts as a vascular permeability factor. Blood, 2008. 111(5): p. 2674-80.*

92. *Ochsenbein, A.M., S. Karaman, S.T. Proulx, M. Berchtold, G. Jurisic, E.T. Stoeckli, and M. Detmar, Endothelial cell-derived semaphorin 3A inhibits filopodia formation by blood vascular tip cells. Development, 2016. 143(4): p. 589-94.*

93. *Tousoulis, D., A.M. Kampoli, C. Tentolouris, N. Papageorgiou, and C. Stefanadis, The role of nitric oxide on endothelial function. Curr Vasc Pharmacol, 2012. 10(1): p. 4-18.*

94. *Salerno, J.C., D.K. Ghosh, R. Razdan, K.A. Helms, C.C. Brown, J.L. McMurry, E.A. Rye, and C.A. Chrestensen, Endothelial nitric oxide synthase is regulated by ERK phosphorylation at Ser602. Biosci Rep, 2014. 34(5).*

95. *Siu, K.L., C. Lotz, P. Ping, and H. Cai, Netrin-1 abrogates ischemia/reperfusion-induced cardiac mitochondrial dysfunction via nitric oxide-dependent attenuation of NOX4 activation and recoupling of NOS. J Mol Cell Cardiol, 2015. 78: p. 174-85.*

96. *Bouhidel, J.O., P. Wang, K.L. Siu, H. Li, J.Y. Youn, and H. Cai, Netrin-1 improves post-injury cardiac function in vivo via DCC/NO-dependent preservation of mitochondrial integrity, while attenuating autophagy. Biochim Biophys Acta, 2015. 1852(2): p. 277-89.*

97. *Zhang, J. and H. Cai, Netrin-1 prevents ischemia/reperfusion-induced myocardial infarction via a DCC/ERK1/2/eNOS s1177/NO/DCC feed-forward mechanism. J Mol Cell Cardiol, 2010. 48(6): p. 1060-70.*

98. *Li, Q., P. Wang, K. Ye, and H. Cai, Central role of SIAH inhibition in DCC-dependent cardioprotection provoked by netrin-1/NO. Proc Natl Acad Sci U S A, 2015. 112(3): p. 899-904.*

99. *Li, Q. and H. Cai, Induction of cardioprotection by small netrin-1-derived peptides. Am J Physiol Cell Physiol, 2015. 309(2): p. C100-6.*

100. *Hruz, T., O. Laule, G. Szabo, F. Wessendorp, S. Bleuler, L. Oertle, P. Widmayer, W. Gruissem, and P. Zimmermann, Genevestigator v3: a reference expression database for the meta-analysis of transcriptomes. Adv Bioinformatics, 2008. 2008: p. 420747.*

Chapter 3

Endothelial Semaphorin 3F Maintains Endothelial Barrier Function and Inhibits Monocyte Migration

Zhang, H., Vreeken, D., Junaid, A., Wang, G., Sol, W., de Bruin, R. G., van Zonneveld, A. J. and van Gils, J. M.

International Journal of Molecular Sciences, 2020;21.

Abstract

In normal physiology, endothelial cells (ECs) form a vital barrier between the blood and underlying tissue controlling leukocyte diapedesis and vascular inflammation. Emerging data suggest that neuronal guidance cues, typically expressed during development, have roles outside the nervous system in vascular biology and immune responses. In particular, Class III semaphorins have been reported to affect EC migration and angiogenesis. While ECs express high levels of semaphorin 3F (SEMA3F), little is known about its function in mature ECs. Here we show that SEMA3F expression is reduced by inflammatory stimuli and increased by laminar flow. Endothelial cells exposed to laminar flow secrete SEMA3F, which subsequently binds to heparan sulfates on the surface of ECs. However, under pro-inflammatory conditions, reduced levels of SEMA3F make ECs more prone to monocyte diapedesis and display impaired barrier function as measured with an electric cell–substrate impedance sensing system and a microfluidic system. In addition, we demonstrate that SEMA3F can directly inhibit the migration of activated monocytes. Taken together, our data suggest an important homeostatic function for EC-expressed SEMA3F, serving as a mediator of endothelial quiescence.

Keywords

semaphorin; endothelial cells; monocytes

3.1 Introduction

Endothelial cells (ECs) form a vital barrier between the blood and underlying tissue, and are crucial for maintaining vessel homeostasis by controlling vascular tone, blood fluidity, endothelial permeability and the regulation of plasma constituents and leukocyte transendothelial migration [1]. The observation that the anatomy and the cellular transcriptomes of the vascular systems of vertebrates often overlap with that of their nervous systems has led to one of the major recent insights in developmental vascular biology, i.e., that the coordinated patterning of nerves and vessels is achieved by each system separately using the same cues and signals [2, 3]. These conserved patterning factors, together called the neuronal guidance cues, were first identified in neural development and involve four major families of conserved ligands being the semaphorins (SEMAs), netrins, ephrins and slits. Neuronal guidance cues act together through a complex interplay of short and long-range signals that can either repel or attract the cells of the developing network [4]. More recently, their critical roles in physiological and pathological regulation of vascular biology and immune responses have been increasingly recognized. In particular, members of the Class III SEMA family have been reported to affect endothelial biology [5-7]. Class III SEMAs are secreted proteins typically composed of a signal peptide for cellular secretion, a SEMA domain (involved in dimerization and receptor binding to plexins/neuropilins), an Immunoglobulin (Ig) domain, a PSI domain (domain found in Plexins, Semaphorins and Integrins necessary for receptor binding to neuropilins) and a basic tail [8]. Class III SEMA protein molecules form homodimers by disulfide bonds and bind to its canonical receptors Plexin (PLXN) A1-4 or D1 with the help of neuropilin (NRP) 1 or 2, which increases ligand binding affinity [9]. The intracellular regions of these PLXN receptors have a Rho-GTPase binding domains and an R-Ras GTPase activating protein domain, allowing the interaction with small GTPases [10, 11]. Of the Class III SEMAs the function of SEMA3A has been investigated the most in endothelial biology. Less is known about the necessity of SEMA3F in EC biology, though SEMA3A has only moderate expression and almost all types of ECs express high levels of SEMA3F [6]. In this article, we confirmed the high expression of SEMA3F in ECs and demonstrated its modulation by shear stress and inflammatory factors. We further investigated the functional importance of SEMA3F and propose the involvement of SEMA3F in endothelial barrier function and monocyte migration.

3.2 Materials and Methods

3.2.1 Access of Gene Expression Omnibus Data

Curated gene expression data of all human cell types that were profiled on Affymetrix Human Genome U133 Plus 2.0 Array platform (Accession: GPL570/HG-U133_Plus_2) were obtained using Genevestigator software [12]. For each cell type, average expression value and the standard deviation were calculated. Graphs were created with R package ggplot2 [13].

3.2.2 Cell Culture

HEK293T cells (ATCC, CRL-3216) were cultured in DMEM (Gibco) supplemented with 10% FCS (v/v) and antibiotics. THP-1 cells (ATCC, TIB-202) were cultured in RPMI 1640 (Gibco, Paisley, UK) supplemented with 10% FCS (v/v), antibiotics and 0.05 mM 2-mercaptoethanol. Primary HUVECs were isolated from in house human umbilical cords and were cultured in EGM2 medium (Lonza, Walkersville, MD, USA) supplemented with antibiotics. Gelatin (0.5% w/v in water) coated plates or flasks were used for HUVECs. All experiments using HUVECs were repeated at least 3 times using cells from different donors. All cells were maintained in a 37 °C incubator with 5% CO2.

3.2.3 Laminar or Oscillatory Shear Stress Culture Conditions

Culturing cells under laminar or oscillatory flow was performed using an iBiDi flow system according to the manufacture's instruction. Briefly, HUVECs were seeded into closed perfusion chambers (IbidiTreat 0.4 µ-Slide I, Luer, Ibidi, Martinsried, Germany) and allowed to adhere for 15 minutes. The 2 inlets of the slide were then connected to 2 syringes, which acts as the reservoir for medium. The tops of the 2 syringes were connected to an iBiDi pump, which introduces pressure on one of the syringes in alternate manner. A central valve was placed on the tube, which allowed alternation of the flow direction. For the laminar flow condition, the alternation of pressure introduction was synchronized with the valve-controlled alternation of flow direction, resulting in unidirectional flow over the cells with constant shear stress. For oscillatory flow, the pump still alternated similar to laminar flow, while the valve alternated every 1 second, creating oscillatory flow over the cells. The pump setup allowed perfusion of culture medium over the monolayer of ECs at a shear stress of 10 dyn/cm^2, both laminar and oscillatory. The chamber and reservoirs containing the medium

were kept in an incubator at 37 °C and 5% CO2. Medium was refreshed after 1 and 4 days of culture. After 1 day or 7 days of flow, tubing connections were removed. Trizol (Invitrogen, 15596026, Carlsbad, CA, USA) or RIPA (Cell Signaling Technology, #9806, Danvers, MA, USA) buffer were added for RNA analysis or protein analysis, respectively.

3.2.4 Lentiviral Vector for KLF2 Overexpression or SEMA3F or KLF2 Knockdown

Second generation lentiviral system was used for delivery of a plasmid containing the KLF2 gene or a plasmid containing short hairpin RNA (shRNA) construct targeting SEMA3F mRNA (SEMA3F KD) or KLF2 mRNA (KLF2 KD). Plasmids without the KLF2 gene (mock) or with a scrambled shRNA (scrambled) were used as controls. Briefly, packaging plasmids (pPAX), envelope plasmids (pVSVG) and plasmids containing shRNA constructs were transfected into HEK293T cells using the polyethylenimine transfection method. The culture medium containing lentivirus particles was harvested 2 days and 3 days after transfection and was filtered with 0.45 μM filters to exclude cell remnants. The lentiviral particle containing medium was then used to transduce HUVECs with dilution ratio of 1:10 in EGM2 medium. The inoculum was removed after 1 day. Puromycin (2 μg/mL, Thermo Fisher, Grand Island, NY, USA) selection was done 2 days after the lentiviral transduction. Cells that were resistant to puromycin for 24 hours were subcultured and used in subsequent experiments.

3.2.5 Quantitative Polymerase Chain Reaction

For quantification of mRNA expression, cells were lysed in Trizol (Invitrogen, 15596026, Carlsbad, CA, USA) and total RNA was isolated using RNeasy miniKit (Qiagen, 74106, Hilden, Germany) according to the manufacturer's instructions. First strand complementary DNA synthesis was done using M-MLV reverse transcriptase kit (Promega, M1701, Madison, WI, USA) with oligodT as primer. Quantitative polymerase chain reactions (qPCR) were done using SYBR green/polymerase mix (Applied Biosystems, 4472903, Vilnius, Lithuania) on a Biorad CFX384 system. GAPDH served as the reference gene. List of primers used in qPCR is provided in **Table 1**.

3.2.6 Western Blot Analysis

For Western blot analysis, cells were lysed with the ice cold RIPA buffer (Cell Signaling Technology, #9806, Danvers, MA, USA) supplemented with a Complete Protease Inhibitor Cocktail (Roche, 11836153001, Mannheim, Germany). The cell debris was precipitated by

Gene	Forward Sequence	Reverse Sequence
GAPDH	CCTGCACCACCAACTGCTTA	GGCCATCCACAGTCTTCTGAG
SEMA3A	CTTGCATTCATCTCTTCTGGTGT	GTGCCAAGGCTGAAATTATCCT
SEMA3B	ACATTGGTACTGAGTGCATGAAC	GCCATCCTCTATCCTTCCTGG
SEMA3C	GTATGTCTGTGGGAGTGGCG	ACGTTGGGGTTGAAAGAGCA
SEMA3D	TCAGAGCACTACTGGCTCAAT	ATCGGAGGTACTGCCTTCTTG
SEMA3E	TGTCCTTTTGACCCCAGCTC	CGTCATGCTCAGTGCGGATA
SEMA3F	CCACAGCGCATCGAGGAAT	CATGGGGTTGTAGGCACCTG
SEMA3G	TGGCTCGAACCATGTCACTG	CATTTGTTCACCAGCACCCG
KLF2	CTACACCAAGAGTTCGCATCTG	CCGTGTGCTTTCGGTAGTG
NOS3	TGATGGCGAAGCGAGTGAAG	ACTCATCCATACACAGGACCC
NRP2	GCTGGCTATATCACCTCTCCC	TCTCGATTTCAAAGTGAGGGTTG
PLXNA1	CGTGCTGTTCACTGTGTTCG	ACTGGATGCGCTCCTTAATCT
PLXNA3	CGGACATGTTCAGTCTCGTGTA	CGCTGACGAAGCCGTAGAT

Table 1. List of primers

centrifuging at 14,000 rpm for 20 min and supernatant was harvested. Protein concentration in samples was measured using Pierce BCA Protein Assay Kit (ThermoFisher Scientific, 23225, Rockford, IL, USA). For electrophoresis, 10 μg samples in 20 μL were prepared with loading buffer (Cell Signaling Technology, #7722, Danvers, MA, USA) with or without DTT, depending on whether the reductive environment was needed. After electrophoresis separation on a 4%–15% polyacrylamide gel (BioRad, 4561084, Temse, Belgium), proteins on gels were transferred onto PVDF membranes (BioRad, 1704156, Temse, Belgium) using BioRad turbo transfer system (BioRad, 1704150). The membranes were blocked using 5% BSA solution (w/v in TBST). The primary antibodies were prepared in 5% BSA solution: rabbit anti-human SEMA3F (Abcam, ab135880 1:500, Cambridge, UK) and rabbit anti-human GAPDH (Cell Signaling Technology, #2118, 1:5000, Danvers, MA, USA). After overnight incubation of primary antibody at 4 °C, secondary antibody (Dako, P044801-2, 1:5000, Glostrup, Denmark) was added and incubated for 1 hour. HPR signal was detected with a Pierce™ ECL Western Blotting Substrate (ThermoFisher Scientific, 34095, Rockford, IL, USA) and captured by the Chemidoc system (BioRad, 17001401). The images were analyzed in ImageJ software.

3.2.7 Immunofluorescence Staining

For immunofluorescence staining, HUVECs were cultured on μ-Slide 8 well (Ibidi, C80826, Martinsried, Germandy) and fixated with 4% formaldehyde (v/v in HBSS supplemented with calcium and magnesium (HBSS+), Gibco, Paisley, UK) for 10 minutes. Cells were then permeabilized with 0.1% triton-X100 for 2 minutes for F-actin and blocked by 5% BSA (w/w in HBSS) for 30 minutes. Except when staining for heparan sulfate and SEMA3F, then cells were not permeabilized and directly incubated with blocking solution. The primary antibody was prepared in 0.5% BSA (w/v in HBSS+): CDH5 mouse anti-human antibody (BD Biosciences, 555661, 1:200, San Jose, CA, USA), SEMA3F rabbit anti-human antibody (Abcam, ab77760, 1:50, Cambridge, UK) and heparan sulfate (JM403; 1.1 mg/mL, gift from Dr. van der Vlag and Dr. Kuppevelt (Nijmegen Center for Molecular Life Sciences, Radboud University Medical Center, Nijmegen, The Netherlands), 1:110). Overnight incubation of the primary antibody was done at 4 °C. The secondary antibody was also prepared in 0.5% BSA (goat anti-mouse IgG alexa 488, goat anti-rabbit IgG alexa 568 or goat anti-mouse alexa 488, Invitrogen, 1:250, Eugene, OR, USA), together with Rhodamine Phalloidin (Invitrogen, 1:200, Eugene, OR, USA) and Hoechst (Invitrogen, 1:2000, Eugene, OR, USA) to stain F-actin and cell nuclei. Fluorescence images were captured by the Leica sp5 confocal microscopic system and analyzed using ImageJ software.

3.2.8 Electric Cell–Substrate Impedance Sensing

Electric cell–substrate impedance sensing (ECIS) assays were done using the ECIS Ztheta (Applied BioPhysics, Troy, NY, USA) device with the standard 8 well arrays (Applied BioPhysics, 8W10E) or 96 wells array (Applied BioPhysics, 96W20idf), which measures the change in the EC monolayer barrier function in real time [14]. The plate was treated with 10 mM L-cysteine for 10 minutes to prepare the surface of gold electrodes and washed twice with water. We then coated the plate with 0.5% gelatin solution for 30 minutes at 37 °C. After the coating, the gelatin solution was washed away with the EGM2 medium and 400 μL medium was added to each well. Thereafter, cell-free baseline measurements were taken. After approximately 30 minutes, measurements were paused and 1 × 105 HUVECs in suspension (200 μL) were added to the wells by mixing the cell suspension with medium in the wells. The measuring was then resumed for at least 30 hours. For both baseline and experiment timepoints, impedance was measured at multiple frequencies every 5 minutes. Measurements at 4000 Hz were used for data analysis, because impendence is contributed

mainly from cell junction resistance at this frequency.

3.2.9 Permeability of 3D Endothelial Culture

HUVECs with or without SEMA3F knockdown were seeded in gelatin coated microvascular channels of custom-made gradient design OrganoPlate® (Mimetas, Leiden, the Netherlands) with 4 mg/mL type 1 collagen (Trevigen; Gaithersburg, United States) in the extracellular matrix channel. After allowing the cells to adhere for 1 hour, culture medium was replace by a mix of Endothelial Cell Growth Medium MV2 (PromoCell, Heidelberg, Germany) and Pericyte Growth Medium (Angio-Proteomie, Boston, MA, USA) in a ratio of 1:1. The device was placed on a rocker platform with 7° angle of motion and eight minutes timed operation to allow continuous flow of medium in the microvessels. After 24 hours, the medium was refreshed and the HUVECs were cultured for 3-4 more days. To measure vessel permeability, the culture medium in the extracellular matrix (ECM) channels was replaced by HBSS+ buffers and the culture medium of the microvascular channels were replaced with HBSS+ buffer containing 125 µg/mL Albumin-Alexa 555 (Life Technologies, Eugene, OR, USA). Following this, the OrganoPlate® was placed in the environmental chamber (37 °C; 5% CO2) of a fluorescent microscope system (Nikon Eclipse Ti) and time-lapse images were captured. The permeability coefficient was calculated by determining the fluorescent intensities in the microvascular channel and in the ECM channel of the capture images. The fluorescent intensity of the ECM channel was normalized with the fluorescent intensities in the microvascular channel of each measured time point. This showed the change in intensity ratio inside the gel channel as a function of time. The scatter plot was fitted with a linear trend line to determine the slope. Finally, using Fick's First Law the apparent permeability was determined as:

$$P_{app}(\cdot 10^{-6} cm/s) = \frac{d\left(\frac{I_g}{I_p}\right)}{dt} \cdot \frac{A_g}{l_w} \tag{3.1}$$

where I_p is the intensity in the microvascular channel, I_g is the intensity in the ECM channel, $A_g(480 \cdot 10^{-6} cm^2)$ is the area of the ECM channel and is the length of the vessel wall that separates between ECM and microvascular region. All data analysis was done with ImageJ (http://rsbweb.nih.gov/ij/, NIH, United States) and Matlab (MathWorks).

3.2.10 Transwell Migration

Chemotaxis of THP-1 monocytes was measured using 24-well Transwell culture inserts with a 5 μm pore size filter (Corning, 734-1573, Kennebunk, ME, USA), either coated with 10 μg/mL Fibronectin (Sigma, F4759, St. Louis, MO, USA) or containing an endothelial monolayer. For transendothelial migration experiments, ECs were seeded at density of 4 × 104 cells/cm^2 on the Transwell insert one day before the experiments and then kept in EGM2 (100 μL in the top chamber and 500 μL in the bottom chamber). Two hours before migration, EGM2 was replaced by migration medium (RPMI 1640 with 0.25% BSA) to let ECs adapt to the new medium. When indicated, 15 h before the experiment, THP-1 cells were treated with 2 ng/mL TNFα. Before the experiment, THP-1 cells were washed with migration medium and resuspended to a concentration of 1 × 107 per mL. Calcein AM (ThermoFisher, C3100MP, 1:1000, Eugene, OR, USA) was added so that THP-1 cells would carry green fluorescence. After labeling, THP-1 cells were washed twice in migration medium and resuspended to a concentration of 1 × 106/mL. For SEMA3F pretreatment, 500 ng/mL SEMA3F (gift from Dr. Nakayama and Prof. Briscoe, Boston Children's Hospital and Harvard Medical School, Boston, MA, USA) was added to the suspension and cells were incubated for 30 minutes. After 30 minutes, THP-1 cells were added to Transwell inserts and the inserts were placed on wells with 500 μL migration medium supplemented with 10 nM MCP1 (R&D Systems, 279-MC, Minneapolis, MN, USA) with or without 500 ng/mL SEMA3F. The cells were allowed to migration for 2 hours. Thereafter, the cells in the bottom chambers (containing migrated THP-1 cells) were pelleted and lysed by 1% TritonX-100. Fluorescent signal of Calcein AM was measured by a colorimetric analyzer (excitation: 480 nm; emission: 525 nm), representing the number of THP-1 cells migrated.

3.3 Results

3.3.1 Semaphorin 3F Is the Highest Expressed Class III Semaphorin in Endothelial Cells

We set off by studying the expression of Class III SEMAs in ECs using available transcriptomics data on GPL570 platform, a commonly used human transcriptome microarray platform. Of the Class III SEMAs, SEMA3A, SEMA3C and SEMA3G are abundantly expressed by some of the ECs (**Figure 1A**). High abundance of SEMA3F transcripts was detected in all types of ECs profiled to date. The SEMA3F levels were in several types of

ECs comparable to that of vascular endothelial cadherin (VE-cadherin, CDH5), the main component of adherent junctions. Epithelial cadherin (E-cadherin, CDH1) was taken along as negative control. Endothelial cells from larger arteries, such as aortic ECs, coronary artery ECs, iliac artery ECs and umbilical artery ECs, showed higher expression of SEMA3F, compared to microvascular ECs. In order to compare SEMA3F expression level of the ECs to other cell types, all 369 cell types that were profiled on GPL570 platforms were ranked by expression of SEMA3F. The top 10 cell types consist of five EC types and five epithelial-related cell types (**Figure 1B**).

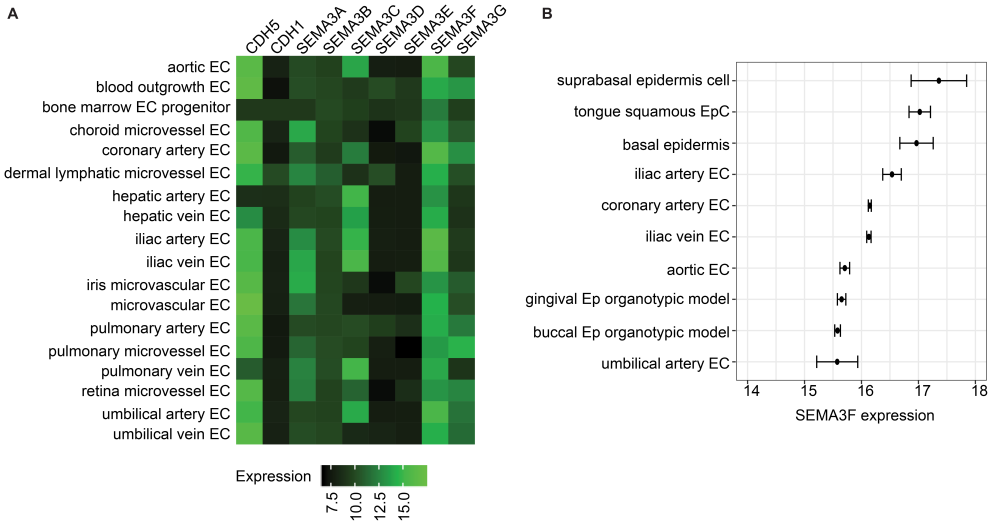

Figure 1. High expression of SEMA3F in various types of endothelial cells

(A) Heatmap of Class III semaphorin expression of all types of human endothelial cells profiled on Affymetrix Human Genome U133 Plus 2.0 Array platform (GEO accession: GPL570). Numbers indicate normalized microarray signals on log2 scale. Black color: lower expression and green color: higher expression. Expression signals of CDH5 and CDH1 were included as references. (B) SEMA3F expression in 10 human cell types with highest SEMA3F expression. Data is presented as Mean ± SEM; n = 3.

3.3.2 Expression of SEMA3F Is Regulated by Inflammatory Cytokines and Shear Stress

Given the high expression of SEMA3F in ECs, we next assessed if inflammatory and hemodynamic conditions affected the expression of SEMA3F. For this we used human umbil-

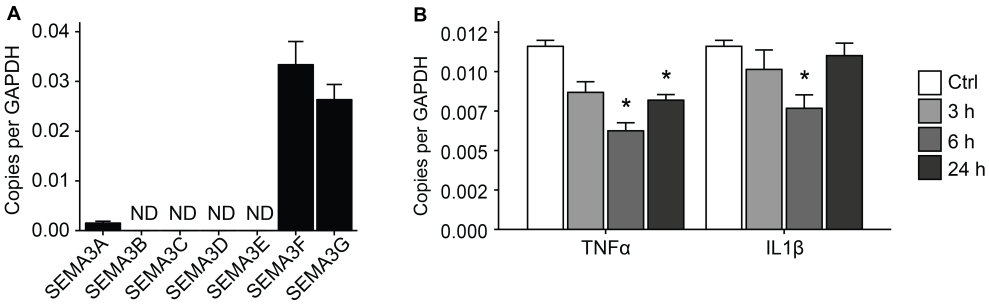

Figure 2. Confirmation of SEMA3F expression in human umbilical vein endothelial cells (HUVECs) and its response to inflammatory factors

(A) Quantification of expression of Class III semaphorins with qPCR in HUVECs. Results are presented as copy numbers per GAPDH, Mean ± SEM, n = 3. (B) SEMA3F expression in HUVECs stimulated with the inflammatory factors, TNFα (10 ng/mL) or IL1β (20 ng/mL). RNA was harvested 3, 6 and 24 h after stimulation started. Results are presented as copy numbers per GAPDH, Mean ± SEM, n = 3, * $p < 0.05$.

ical vein endothelial cells (HUVECs), in which we confirmed the expression of Class III SEMAs by qPCR (**Figure 2A**). Treatment with inflammatory cytokines decreased the expression of SEMA3F (**Figure 2B**). HUVECs treated with tumor necrosis factor alpha (TNFα) had a decrease in expression by 50% after 6 hours and the effect persist until at least 24 hours. Similar observations were made for treatment with interleukin 1 beta (IL1β) after 6 hours, while the expression of SEMA3F was restored after 24 hours of IL1β treatment. The expression of SEMA3A and SEMA3G were changed upon inflammatory cytokine stimulation, however only IL1β reduced SEMA3A expression, while IL1β increased SEMA3G levels, as did TNFα for SEMA3A expression upon 24 h stimulation (**Figure S1A**). To study the regulation of SEMA3F expression by shear stress, ECs were cultured under laminar flow or oscillatory flow (10 dyn/cm^2) for 1 day or 7 days and gene expression to static cultured ECs was compared. As expected, laminar shear stress induced the expression of shear-dependent transcription factor Kruppel Like Factor 2 (KLF2) after 1 day and further after 7 days, while oscillatory shear stress failed to do so (**Figure 3A**). Quantitative PCR revealed that mRNA expression of SEMA3F was also augmented by a shear dependent mechanism, for SEMA3A and SEMA3G this was not observed (**Figure S1B**). The expression of SEMA3F followed a similar pattern as KLF2 with a significant 2.4-fold increased expression after 7 days (**Figure 3B**). Moreover, immunoblot analysis of control (static) and 7 days sheared ECs revealed an

evident increase in SEMA3F protein expression, as well as known shear responsive NOS3 (**Figure 3C**). Interestingly, presence of SEMA3F dimers could only be detected in the conditioned medium from ECs cultured under laminar flow, but not in the static condition (**Figure 3C**). This implied that shear stress not only increased the transcription and translation of SEMA3F, but also the secretion of SEMA3F protein. Immunofluorescence staining of SEMA3F revealed colocalization with heparan sulfate on the surface of the cells (**Figure 3D–F**). Treatment with heparanase reduced the presence of SEMA3F on the flow cultured ECs (**Figure 3D–F**), indicating binding of SEMA3F to the endothelial glycocalyx, a network of membrane-bound proteoglycans and glycoproteins. To assess if SEMA3F expression can be mediated by the shear induced transcription factor KLF2, we overexpressed KLF2 in ECs (**Figure 4A**). Overexpression of KLF2 resulted in increased expression of SEMA3F mRNA and protein in static cultured cells (**Figure 4B,C**). To confirm the KLF2-dependent regulation of SEMA3F under laminar shear stress we silenced KLF2 in ECs using shRNA vectors, and cultured these cells for 7 days under flow (**Figure 4D**). Knockdown of KLF2 in endothelial cells suppressed the induction of SEMA3F by laminar flow (**Figure 4E**). NOS3 detection was used to validate functional overexpression or knock down of KLF2 (**Figure 4C,F**).

3.3.3 Loss of SEMA3F Impairs Endothelial Barrier Function

In order to study the functional importance of SEMA3F for ECs, SEMA3F expression in ECs was silenced using lentiviral shRNA vectors targeting the SEMA3F mRNA. A non-SEMA3F targeting scrambled shRNA was used as a control. Repression of SEMA3F (SEMA3F KD) was validated using qPCR (**Figure 5A**). Endothelial cells with reduced levels of SEMA3F showed a more spindle-like and elongated morphology compared to scrambled shRNA transduced cells (**Figure 5B,C**). Immunostaining of CDH5 revealed striped discontinuous adherens junctions (**Figure 5C,D**), which is often caused by excessive pulling force from cytoskeleton to the junction [15]. Indeed, staining for filamented actin (F-actin) showed a surfeit of stress fiber (**Figure 5C,E**). The morphological change strongly indicates the possibility of impaired endothelial barrier function after reduction of SEMA3F expression. To test this postulation we assessed the effect of SEMA3F KD on endothelial barrier function through the use of electric cell–substrate impedance sensing (ECIS) [16] and the more physiological 3D-endothelial tube in a microfluidics platform [17]. With each method we found that targeted reduction of SEMA3F in ECs resulted in impaired barrier function

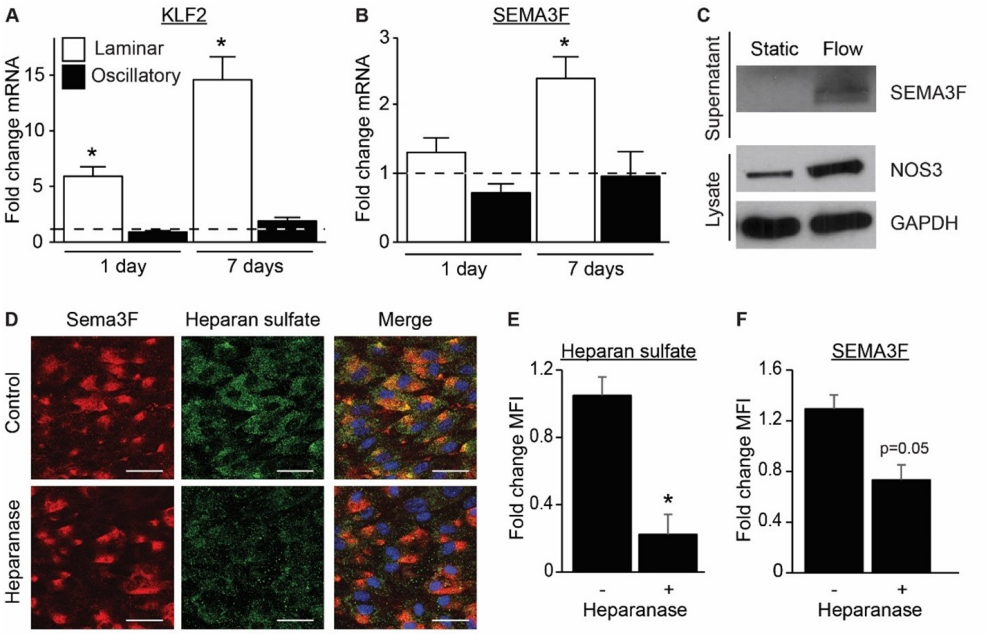

Figure 3. Regulation of SEMA3F expression and secretion by shear stress

(A-B) Quantitative qPCR analysis of KLF2 (A) and SEMA3F (B) mRNA isolated from HUVECs cultured under laminar or oscillatory flow conditions (10 dyn/cm^2) for 1 or 7 days compared to static culture conditions. Results are presented relative to static cultured cells, set as 1, dotted line. Mean ± SEM of n = 3, * $p < 0.05$. (C) Immunoblot analysis of SEMA3F protein dimer in the supernatant and NOS3 or GAPDH in cell lysates. Representative of n = 2–3. (D–F) Immunofluorescence staining of SEMA3F (red), Heparan sulfate (green) and nuclei (blue) in HUVECs cultured under laminar flow conditions for 7 days and treated with or without heparanase (1.5 µg/mL) for 2 hours at the end of the 7 days culture. Scale bar = 40 µm. Quantification of mean fluorescence intensity of heparan sulfate (E) and SEMA3F (F) of 3 independent experiments. Mean ± SEM, * $p < 0.05$.

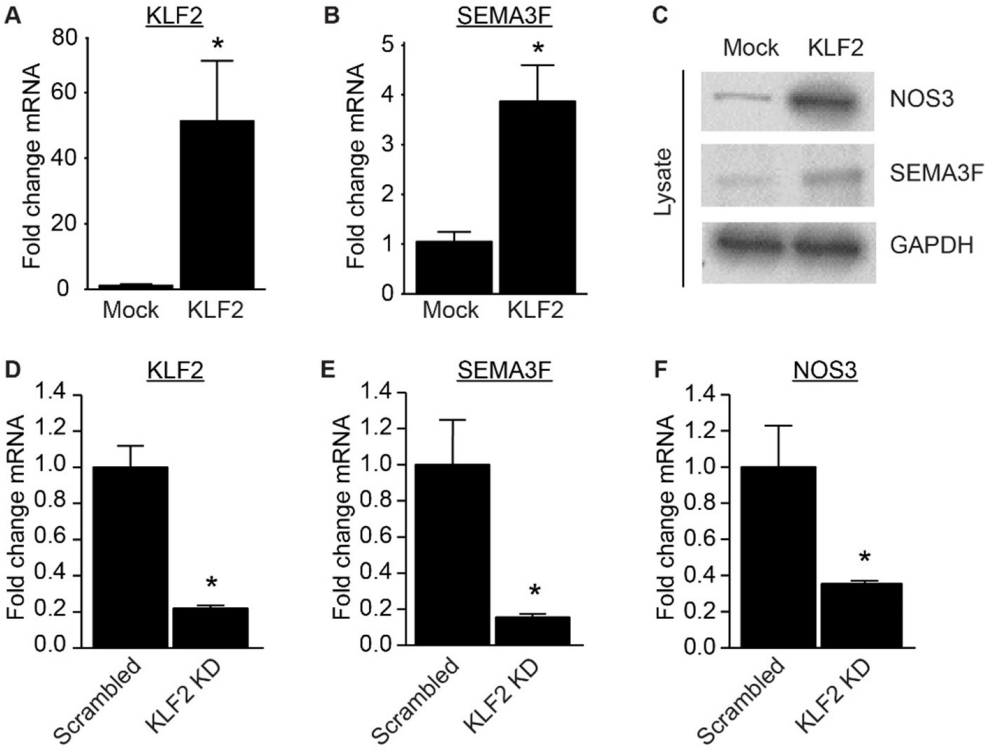

Figure 4. SEMA3F is induced by KLF2

(A-B) Quantitative qPCR analysis of KLF2 (A) and SEMA3F (B) mRNA isolated from HUVECs transduced with mock or KLF2 overexpressing lentivirus. Results are presented relative to cells transduced with mock virus, set as 1. Mean ± SEM of n = 3; * $p < 0.05$. (C) Representative immunoblot analysis of NOS3, SEMA3F or GAPDH in protein lysates of HUVEC transduced with mock or KLF2 overexpressing lentivirus. (D-F) KLF2 (D), SEMA3F (E) and NOS3 (F) mRNA expression in HUVECs after transduction with lentiviral anti-KLF2 shRNA (KLF2 KD) or scrambled shRNA (scrambled) and cultured under laminar flow conditions (10 dyn/cm^2) for 7 days compared to static culture conditions. Results are presented relative to scrambled, set as 1. Mean ± SEM of n = 3, * $p < 0.05$.

(**Figure 6A–C**). The impaired barrier function of cells with SEMA3F KD could be improved by treating the endothelial cells with supernatant of non-transduced endothelial cells cultured under laminar flow, indicated by more localization of CDH5 at cell–cell contacts and increased impedance measurement (**Figure 6D,E**). Next, we assessed whether loss of barrier function upon SEMA3F knock down alters monocyte transendothelial migration with monocyte chemotaxis over Transwell filters containing endothelial monolayers with SEMA3F knock down or control cells. Consistent with the reduced barrier function, we found that loss of SEMA3F led to increased monocyte transendothelial migration (**Figure 6F**).

3.3.4 SEMA3F Itself Works as an Inhibitor of Migration for Activated Monocytes

Since SEMA3A can inhibit directional migration of monocytes [18], we investigated whether SEMA3F could also affect monocyte migration by directly acting on monocytes. For this, we started by looking at the expression of SEMA3F receptors, namely PLXNA1 and PLXNA3, and the co-receptor NRP2, by naïve monocytes and inflammatory stimulated monocytes. We found that monocytes express all these receptors, and their expression levels are induced upon stimulation with TNFα (**Figure 7A**). Next, SEMA3F was either used to pretreat the monocytes or it was added to the Transwell migration system, either in the bottom or in both compartments. Consistent with our receptor expression data, we observed that the migration of TNFα-stimulated monocytes was inhibited by either pretreatment of SEMA3F or addition of SEMA3F to the monocytes during the migration experiment. Having SEMA3F only in the bottom compartment of the Transwell system did not affect migration (**Figure 7B,C**). Together these observations have demonstrated that SEMA3F does have an inhibitory effect on migration inflammatory stimulated monocyte, but not a repellent effect.

3.4 Discussion

In this study, we confirmed the high expression of SEMA3F in ECs found with gene expression meta-analysis of omni datasets. We revealed a KLF2-dependent regulation of SEMA3F under laminar shear stress. Using an shRNA knock down model, we pinpointed an essential role for SEMA3F in maintaining the endothelial barrier function and inhibiting the mobility of monocytes. Collectively, these results support that SEMA3F expressed by ECs can serve as a mediator of quiescent ECs. The function of Class III SEMAs in EC biology has received a good amount of attention with SEMA3A being the most thoroughly

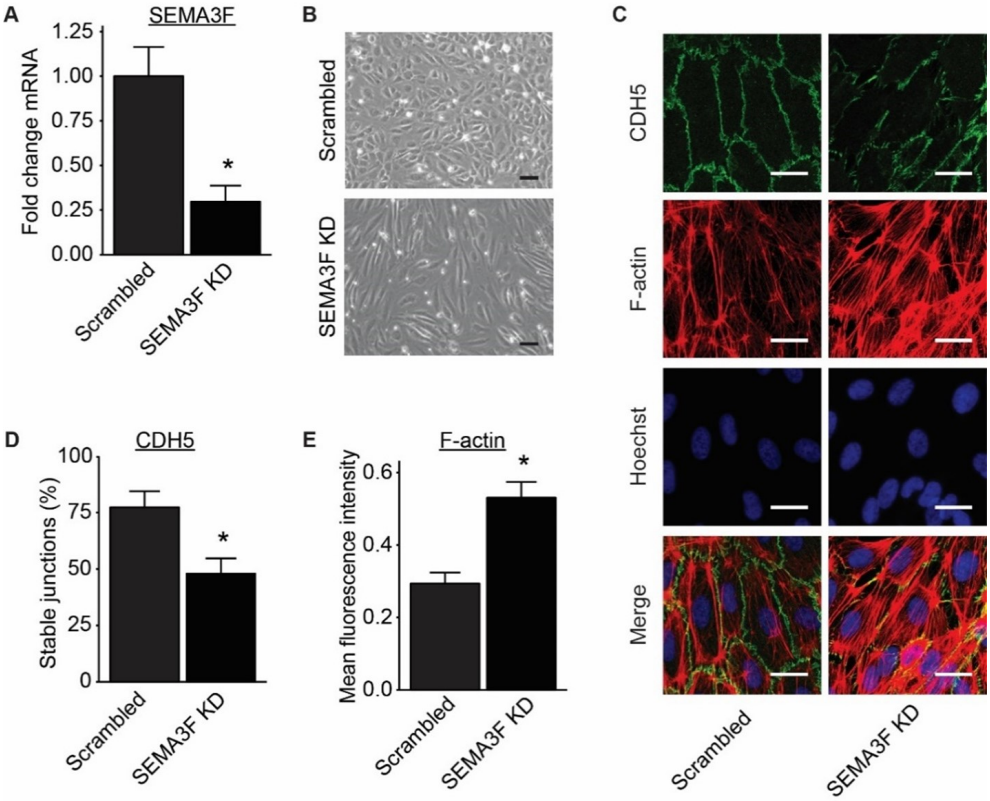

Figure 5. Reduction of SEMA3F expression in endothelial cells leads to disrupted endothelial adherens junctions

(A) SEMA3F mRNA expression after transduction with lentiviral anti-SEMA3F shRNA (SEMA3F KD) or scrambled shRNA (Scrambled). Mean ± SEM of n = 3, * $p < 0.05$. (B) Bright field microscope images from HUVECs transduced with anti-SEMA3F shRNA (SEMA3F KD) or scrambled shRNA (scrambled). Scale bar = 40 µm. (C–E) Immunofluorescence staining of CDH5 (green), F-actin (red) and nuclei (blue) in SEMA3F KD or scrambled HUVECs. Scale bar = 10 µm (D,E) Bar graphs show the quantification of percentage of stable adherens junctions (D) and F-actin staining (E). Mean ± SEM of n = 3, * $p < 0.05$.

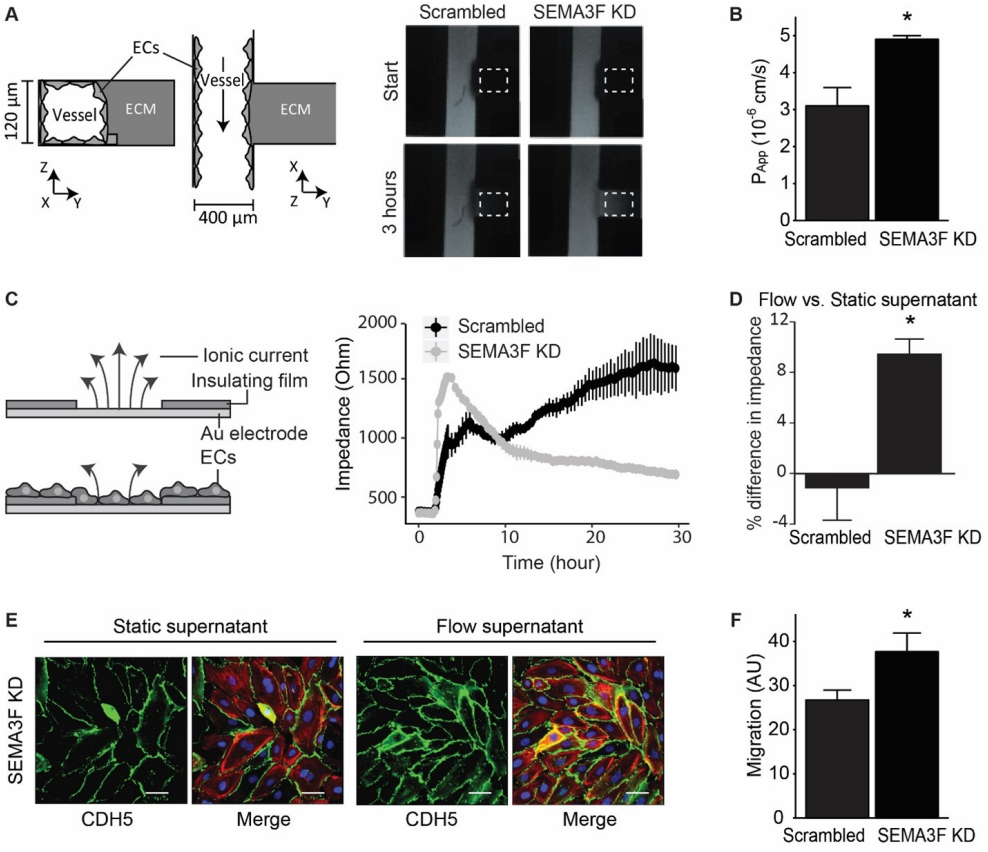

Figure 6. Reduction of SEMA3F expression impairs barrier function of the endothelial monolayer

(A-B) HUVECs transduced with anti-SEMA3F shRNA (SEMA3F KD) or scrambled shRNA (scrambled) were seeded in the vertical channel of a microfluidic device with collagen in the horizontal channel. At the start of the measurement the fluorescently labeled albumin were infused in the vessel lumen and after 30 minutes albumin leakage outside the vessel channel was visualized and quantified. Dotted box indicates region of quantification. Bar graph (B) shows quantification of permeability presented as Mean ± SEM of n = 3, * $p < 0.05$. (C) Transendothelial electrical resistance of HUVECs transduced with anti-SEMA3F shRNA (SEMA3F KD) or scrambled shRNA (scrambled) and seeded on electric cell–substrate impedance sensing (ECIS) electrodes. Data are from one experiment representative of five independent experiments (Mean ± SD of triplicate samples). (D) HUVECs transduced with anti-SEMA3F shRNA (SEMA3F KD) or scrambled shRNA (scrambled) were seeded and cultured on ECIS electrodes in the presence of supernatant of non-transduced endothelial cells cultured under static or laminar flow (7 days, 10 dyn/cm^2). Results are presented as percentage difference in impedance of the cells treated for 42 hours with supernatant from flow compared with static endothelial cultures. Data are Mean ± SD of n = 2–3, * $p < 0.05$. (E) Immunofluorescence staining of CDH5 (green), F-actin (red) and nuclei (blue) in SEMA3F KD HUVECs cultured in the presence of supernatant of non-transduced endothelial cells cultured under static or laminar flow (7 days, 10 dyn/cm^2) for 24 h. Scale bar = 50 µm. (F) Migration of THP-1 cells across SEMA3F KD or scrambled HUVEC-coated filters towards MCP1 (10 µM). Data are Mean ± SEM of n = 3, * $p < 0.05$.

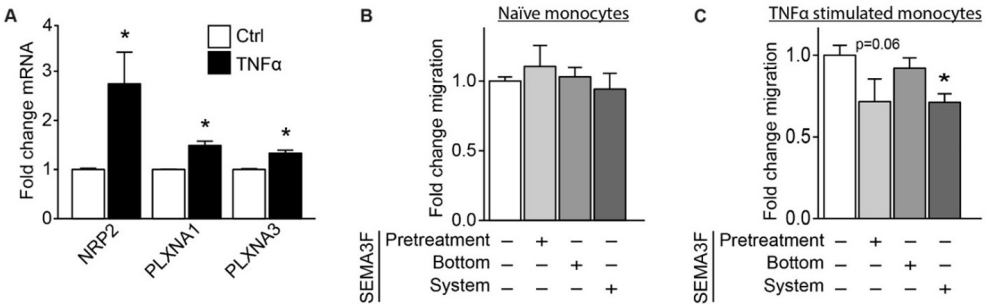

Figure 7. SEMA3F inhibits migration of TNFα stimulated monocytes

(A) Quantitative qPCR analysis of NRP2, PLXNA1 and PLXNA3 mRNA in THP-1 cells stimulated for 15 h with TNFα (2 ng/mL), presented relative to mRNA in unstimulated cells (control), set as 1. Mean ± SEM of n = 3, * $p < 0.05$. (B,C) Migration of THP1 cells unstimulated (B) or stimulated for 15 h with TNFα (2 ng/mL, C) and with or without pretreatment with SEMA3F (500 ng/mL) or exposure to SEMA3F (500 ng/mL) in the bottom or in the whole Transwell system towards MCP1 (10 μM). Results are presented relative to cells not exposed to SEMA3F, set as 1. Mean ± SEM of n = 3, * $p < 0.05$.

investigated. SEMA3A binds to PLXNA2 (instead of PLXNA1 and PLXNA3 in the case of SEMA3F), which activates the Rho-family small GTPase Rnd1 and induces a collapse of the cytoskeleton [11, 19]. The ligand–receptor interaction was shown to inhibit stress fiber formation and collapse of the ECs cell membrane [20]. SEMA3A was also shown to cause internalization of CDH5, thus affecting the integrity of adherens junctions [21]. Via these mechanisms, SEMA3A increased permeability of the endothelium in several situations [21-24]. Compared to the effect of SEMA3A on endothelium permeability, available evidences for a role of SEMA3F are rather ambiguous. High doses of exogenous SEMA3F were shown to collapse the EC membrane and cytoskeleton, but it did not affect EC permeability [20]. Peritoneal injection of SEMA3F in mice caused elevation of leukocyte numbers in the peritoneal cavity, which may be explained by the disturbance of the endothelial or epithelial cell function by SEMA3F [25]. Instead of using exogenous SEMA3F, we studied the effect of reduced level of SEMA3F on EC barrier function, which should be more physiologically relevant. In line with SEMA3F being shown to inhibit stress fiber formation [26, 27], after the knockdown of SEMA3F, we observed excessive amounts of F-actin, especially at the cortical regions of HUVECs. The end of stress fibers connects components of adherens junctions. Excessive amounts of stress fibers can apply a pulling force on endothelial adherens

junctions, resulting in disrupted integrity of these junctions and increased permeability [28, 29]. Indeed, our results show the disruption of adherens junctions with CDH5 immunofluorescence staining. The fact that SEMA3F is a shear inducible protein, it is possible that SEMA3F works as a shear-dependent auto- or paracrine regulator of endothelial cortical F-actin via PLXN-small GTPase signaling, thus stabilizing the adherens junctions. Knowledge on the exact small GTPase governing the downstream signaling is still lacking and requires further research. One of the most common reasons for endothelial dysfunction is an adverse hemodynamic environment, evidenced by the fact that more atherosclerotic plaques can be found at bifurcations of vessels and regions with low vessel wall shear stress [30, 31]. The underlying mechanism is that high (and laminar) shear stress provokes quiescence of ECs via mechano-sensing proteins and downstream shear-dependent transcription factors, including KLF2 and KLF4. Quiescent ECs have a good bioavailability of nitric oxide, better barrier function and little inflammatory responses. Low shear stress or disturbed flow (also called turbulence) stimulates EC proliferation, apoptosis and inflammation [32]. Adaption and alteration of EC function under adverse hemodynamic environments involves and induces changes in gene expression and is consequently the driver of functionalities changes [33]. For SEMA3A it has been shown, in vitro and in vivo, that its expression is decreased by ECs at regions of disturbed flow and upon inflammatory stimulations [18]. For SEMA3F, in line with the findings in our prolonged flow culture and KLF2 overexpression experiments, upregulation has been reported in a microarray of ECs overexpressing the flow-responsive transcription factor KLF2 [34]. Next to an increased SEMA3F expression upon laminar flow we observed a decrease in expression upon inflammatory stimulations in the ECs. In tumor cells it has been shown that the transcription repressors zinc finger E-box binding homeobox (ZEB)-1 and inhibitors of DNA binding/differentiation 2 (Id2) proteins can decrease the expression of SEMA3F [35, 36]. In tumor cells these transcription factors can be activated by inflammation [37, 38], and similar pathways might be at play in ECs in regulating SEMA3F expression. Interestingly, we could not detect the SEMA3F protein in the medium of ECs cultured under static conditions, whereas the SEMA3F protein could be detected in the conditioned medium of ECs cultured under prolonged laminar flow. These observations indicated that shear stress not only coordinated induction of SEMA3F gene expression, but also stimulated secretion of SEMA3F, confirming the concept that induction of SEMA3F expression is at least a concomitant event in endothelial maturation and quiescence. One key aspect of endothelial function is the ability to synthesize and maintain

a network of membrane-bound proteoglycans and glycoproteins at the endothelium lumen, called the glycocalyx [39]. This glycocalyx contains heparan sulfate proteoglycans providing binding for endothelium- and plasma-derived soluble molecules facilitating protein–receptor interactions and the formation of surface gradients of chemokines and growth factors [40]. While heparan sulfates are shown to be essential for the development of the nervous system and specifically can affect several neuronal guidance cues [41], a role for these heparan sulfate in SEMA-mediated function is barely described. A role for heparan sulfate proteoglycans in SEMA function is suggested from the phenotypic similarities between central nervous system development in mice defective in secreted SEMA signaling and mice lacking the heparan sulfate elongation gene 1 (Ext1) [41]. For SEMA5A, an interaction with axonally expressed heparan sulfate proteoglycans has been shown [42]. In addition, De Wit et al. have shown that heparan sulfates can effectively compete SEMA3A from neuronal cells [43]. We have found that treatment with heparanase reduces the presence of SEMA3F on ECs, proving an interaction of SEMA3F with the endothelial glycocalyx probably mediated by heparan sulfate. In this way, SEMA3F might be presented to leukocytes in the circulation and/or be beneficial for a tight endothelial barrier by competing for VEGF on the glycocalyx. In regard to leukocyte guidance, several members of the Class III SEMAs have been studied in the context of inflammation and leukocyte recruitment. Studies have revealed that these Class III SEMAs can dampen inflammation or mediate resolution of inflammation [44-48]. SEMA3A has been shown to inhibit migration of monocytes [18, 47] and for SEMA3E it has been shown that it can inhibit the migration of macrophages [49] and neutrophils [48]. Only for mature dendritic cells there have been reports that SEMA3A, -C and -F can promote their migration [50]. For SEMA3F the functional effect on leukocyte migration had not been fully studied. In our experiments, we showed that SEMA3F could affect monocyte migration via both modulating EC adherens junction stability and acting directly on monocytes. Intriguingly, in a recent study, Reichert et al. showed that SEMA3F promotes transmigration of peripheral blood mononuclear cells via increasing PECAM1 at cellular junctions [25]. Similarly, we observed reduction of PECAM1 with reduction of SEMA3F (unpublished data). In both cases, the presence of PECAM1 in endothelial adherens junction was positively correlated with SEMA3F expression. PECAM1 is essential in maintaining endothelial barrier function and promoting monocyte diapedesis through junctions of ECs [51-53]. When endothelial junctions are intact, PECAM1 concentrates at the junctions, binds homophilically to leukocyte expressed PECAM1 and facilitates transmigration of these cells [54]. When

endothelial junctions are disrupted, junctional PECAM1 disappears and transmigration of leukocytes is then independent of PECAM1. The above mechanism could explain why an increase of monocyte migration through the EC monolayer is observed both with the SEMA3F treatment or SEMA3F KD [25]. We also investigated whether SEMA3F could directly act on monocyte migration. To our surprise, SEMA3F did not regulate the migration of resting THP-1 cells. However, we saw that monocyte expression of SEMA3F receptors, namely NRP2, PLXNA1 and PLXNA3, were induced by stimulation with TNFα. Similar observations have been made in DCs and natural killer cells (NKs), in which SEMA receptors were upregulated upon cell activation [44, 50]. We next demonstrated that migration of TNFα-stimulated monocytes was reduced by pretreatment with SEMA3F, or by having SEMA3F in the migration system, but not by having SEMA3F only in the bottom chamber of the Transwell system. Therefore, we concluded from our studies that SEMA3F acts as a general inhibitor of monocyte migration, as observed before for SEMA3A [18]. Moreover, we revealed that TNFα could sensitize monocytes by inducing the expression of SEMA3F receptors. In conclusion, we demonstrated a novel function of SEMA3F in endothelial quiescence. As a shear-inducible secretory factor, SEMA3F is essential for the endothelial barrier function and is able to regulate monocyte migration. Together these studies provide novel insight into the role of endothelial expressed SEMA3F as a mediator of endothelial homeostasis contributing to vascular health.

Acknowledgement

This research was funded by Dutch Heart Foundation, grant number 2013T127 and RECONNECT CVON, European Research Area Network on Cardiovascular Diseases, grant number 038 MISsCVD, and ZonMW MKMD, grant number 114022501.

Conflicts of Interest

The authors declare no conflict of interest.

References

1. *Cines, D.B., E.S. Pollak, C.A. Buck, et al., Endothelial cells in physiology and in the pathophysiology of vascular disorders. Blood, 1998. 91(10): p. 3527-61.*

2. *Carmeliet, P., Blood vessels and nerves: common signals, pathways and diseases. Nat Rev Genet, 2003. 4(9): p. 710-20.*

3. *Carmeliet, P. and M. Tessier-Lavigne, Common mechanisms of nerve and blood vessel wiring. Nature, 2005. 436(7048): p. 193-200.*

4. *Melani, M. and B.M. Weinstein, Common factors regulating patterning of the nervous and vascular systems. Annu Rev Cell Dev Biol, 2010. 26: p. 639-65.*

5. *Treps, L., A. Le Guelte, and J. Gavard, Emerging roles of Semaphorins in the regulation of epithelial and endothelial junctions. Tissue Barriers, 2013. 1(1): p. e23272.*

6. *Zhang, H., D. Vreeken, C.S. Bruikman, et al., Understanding netrins and semaphorins in mature endothelial cell biology. Pharmacol Res, 2018. 137: p. 1-10.*

7. *Cora, D., E. Astanina, E. Giraudo, et al., Semaphorins in cardiovascular medicine. Trends Mol Med, 2014. 20(10): p. 589-98.*

8. *Worzfeld, T. and S. Offermanns, Semaphorins and plexins as therapeutic targets. Nat Rev Drug Discov, 2014. 13(8): p. 603-21.*

9. *Janssen, B.J., T. Malinauskas, G.A. Weir, et al., Neuropilins lock secreted semaphorins onto plexins in a ternary signaling complex. Nat Struct Mol Biol, 2012. 19(12): p. 1293-9.*

10. *Zanata, S.M., I. Hovatta, B. Rohm, et al., Antagonistic effects of Rnd1 and RhoD GTPases regulate receptor activity in Semaphorin 3A-induced cytoskeletal collapse. J Neurosci, 2002. 22(2): p. 471-7.*

11. *Wang, H., P.K. Hota, Y. Tong, et al., Structural basis of Rnd1 binding to plexin Rho GTPase binding domains (RBDs). J Biol Chem, 2011. 286(29): p. 26093-106.*

12. *Hruz, T., O. Laule, G. Szabo, et al., Genevestigator v3: a reference expression database for the meta-analysis of transcriptomes. Adv Bioinformatics, 2008. 2008: p. 420747.*

13. *Wickham, H., ggplot2: Elegant Graphics for Data Analysis. Springer-verlag New York, (ISBN 978-3-319-24277-4).*

14. *Hong, J., K. Kandasamy, M. Marimuthu, et al., Electrical cell-substrate impedance sensing as a non-invasive tool for cancer cell study. Analyst, 2011. 136(2): p. 237-45.*

15. *Millan, J., R.J. Cain, N. Reglero-Real, et al., Adherens junctions connect stress fibres between adjacent endothelial cells. BMC Biol, 2010. 8: p. 11.*

16. *Tiruppathi, C., A.B. Malik, P.J. Del Vecchio, et al., Electrical method for detection of endothelial cell shape change in real time: assessment of endothelial barrier function. Proc.Natl.Acad.Sci.U.S.A, 1992. 89(17): p. 7919-7923.*

17. *Junaid, A., H. Tang, A. van Reeuwijk, et al., Ebola Hemorrhagic Shock Syndrome-on-a-Chip. iScience, 2019. 23(1): p. 100765.*

18. *van Gils, J.M., B. Ramkhelawon, L. Fernandes, et al., Endothelial expression of guidance cues in vessel wall homeostasis dysregulation under proatherosclerotic conditions. Arterioscler Thromb Vasc Biol, 2013. 33(5): p. 911-9.*

19. *Nobes, C.D., I. Lauritzen, M.G. Mattei, et al., A new member of the Rho family, Rnd1, promotes disassembly of actin filament structures and loss of cell adhesion. J Cell Biol, 1998. 141(1): p. 187-97.*

20. *Bielenberg, D.R., A. Shimizu, and M. Klagsbrun, Semaphorin-induced cytoskeletal collapse and repulsion of endothelial cells. Methods Enzymol, 2008. 443: p. 299-314.*

21. *Le Guelte, A., E.M. Galan-Moya, J. Dwyer, et al., Semaphorin 3A elevates endothelial cell permeability through PP2A inactivation. J Cell Sci, 2012. 125(Pt 17): p. 4137-46.*

22. *Hou, S.T., L. Nilchi, X. Li, et al., Semaphorin3A elevates vascular permeability and contributes to cerebral ischemia-induced brain damage. Sci Rep, 2015. 5: p. 7890.*

23. *Cerani, A., N. Tetreault, C. Menard, et al., Neuron-derived semaphorin 3A is an early inducer of vascular permeability in diabetic retinopathy via neuropilin-1. Cell Metab, 2013. 18(4): p. 505-18.*

24. *Acevedo, L.M., S. Barillas, S.M. Weis, et al., Semaphorin 3A suppresses VEGF-mediated angiogenesis yet acts as a vascular permeability factor. Blood, 2008. 111(5): p. 2674-80.*

25. *Reichert, S., S. Scheid, T. Roth, et al., Semaphorin 3F Promotes Transendothelial Migration of Leukocytes in the Inflammatory Response After Survived Cardiac Arrest. Inflammation, 2019. 42(4): p. 1252-1264.*

26. *Shimizu, A., H. Nakayama, P. Wang, et al., Netrin-1 promotes glioblastoma cell invasiveness and angiogenesis by multiple pathways including activation of RhoA, cathepsin B, and cAMP-response element-binding protein. J Biol Chem, 2013. 288(4): p. 2210-22.*

27. *Shimizu, A., A. Mammoto, J.E. Italiano, Jr., et al., ABL2/ARG tyrosine kinase mediates SEMA3F-induced RhoA inactivation and cytoskeleton collapse in human glioma cells. J Biol Chem, 2008. 283(40): p. 27230-8.*

28. *Bogatcheva, N.V. and A.D. Verin, The role of cytoskeleton in the regulation of vascular endothelial barrier function. Microvasc Res, 2008. 76(3): p. 202-7.*

29. *Millán, J., R.J. Cain, N. Reglero-Real, et al., Adherens junctions connect stress fibres between adjacent endothelial cells. BMC Biol, 2010. 8: p. 11.*

30. *Tomita, H., J. Hagaman, M.H. Friedman, et al., Relationship between hemodynamics and atherosclerosis in aortic arches of apolipoprotein E-null mice on 129S6/SvEvTac and C57BL/6J genetic backgrounds. Atherosclerosis, 2012. 220(1): p. 78-85.*

31. *Chiu, J.J. and S. Chien, Effects of disturbed flow on vascular endothelium: pathophysiological basis and clinical perspectives. Physiol Rev, 2011. 91(1): p. 327-87.*

32. *Chistiakov, D.A., A.N. Orekhov, and Y.V. Bobryshev, Effects of shear stress on endothelial cells: go with the flow. Acta Physiol (Oxf), 2017. 219(2): p. 382-408.*

33. *Qiao, C., F. Meng, I. Jang, et al., Deep transcriptomic profiling reveals the similarity between endothelial cells cultured under static and oscillatory shear stress conditions. Physiol Genomics, 2016. 48(9): p. 660-6.*

34. *Dekker, R.J., R.A. Boon, M.G. Rondaij, et al., KLF2 provokes a gene expression pattern that establishes functional quiescent differentiation of the endothelium. Blood, 2006. 107(11): p. 4354-63.*

35. *Clarhaut, J., R.M. Gemmill, V.A. Potiron, et al., ZEB-1, a repressor of the semaphorin 3F tumor suppressor gene in lung cancer cells. Neoplasia, 2009. 11(2): p. 157-66.*

36. *Coma, S., D.N. Amin, A. Shimizu, et al., Id2 promotes tumor cell migration and invasion through transcriptional repression of semaphorin 3F. Cancer Res, 2010. 70(9): p. 3823-32.*

37. *Li, Y., L. Wang, L. Pappan, et al., IL-1beta promotes stemness and invasiveness of colon cancer cells through Zeb1 activation. Mol Cancer, 2012. 11: p. 87.*

38. *Zhu, X., Y. Lin, M. Bacanamwo, et al., Interleukin-1 beta-induced Id2 gene expression is mediated by Egr-1 in vascular smooth muscle cells. Cardiovasc Res, 2007. 76(1): p. 141-8.*

39. *Reitsma, S., D.W. Slaaf, H. Vink, et al., The endothelial glycocalyx: composition, functions, and visualization. Pflugers Arch, 2007. 454(3): p. 345-59.*

40. *Rabelink, T.J., B.M. van den Berg, M. Garsen, et al., Heparanase: roles in cell survival, extracellular matrix remodelling and the development of kidney disease. Nat Rev Nephrol, 2017. 13(4): p. 201-212.*

41. *de Wit, J. and J. Verhaagen, Proteoglycans as modulators of axon guidance cue function. Adv Exp Med Biol, 2007. 600: p. 73-89.*

42. *Kantor, D.B., O. Chivatakarn, K.L. Peer, et al., Semaphorin 5A is a bifunctional axon guidance cue regulated by heparan and chondroitin sulfate proteoglycans. Neuron, 2004. 44(6): p. 961-75.*

43. *De Wit, J., F. De Winter, J. Klooster, et al., Semaphorin 3A displays a punctate distribution on the surface of neuronal cells and interacts with proteoglycans in the extracellular matrix. Mol Cell Neurosci, 2005. 29(1): p. 40-55.*

44. *Alamri, A., R. Rahman, M. Zhang, et al., Semaphorin-3E Produced by Immature Dendritic Cells Regulates Activated Natural Killer Cells Migration. Front Immunol, 2018. 9: p. 1005.*

45. *Teng, Y., Z. Yin, J. Li, et al., Adenovirus-mediated delivery of Sema3A alleviates rheumatoid arthritis in a serum-transfer induced mouse model. Oncotarget, 2017. 8(39): p. 66270-66280.*

46. *Movassagh, H., L. Shan, J.S. Duke-Cohan, et al., Semaphorin 3E Alleviates Hallmarks of House Dust Mite-Induced Allergic Airway Disease. Am J Pathol, 2017. 187(7): p. 1566-1576.*

47. *Rienks, M., P. Carai, N. Bitsch, et al., Sema3A promotes the resolution of cardiac inflammation after myocardial infarction. Basic Res Cardiol, 2017. 112(4): p. 42.*

48. *Movassagh, H., A. Saati, S. Nandagopal, et al., Chemorepellent Semaphorin 3E Negatively Regulates Neutrophil Migration In Vitro and In Vivo. J Immunol, 2017. 198(3): p. 1023-1033.*

49. *Wanschel, A., T. Seibert, B. Hewing, et al., Neuroimmune guidance cue Semaphorin 3E is expressed in atherosclerotic plaques and regulates macrophage retention. Arterioscler Thromb Vasc Biol, 2013. 33(5): p. 886-93.*

50. *Curreli, S., B.S. Wong, O. Latinovic, et al., Class 3 semaphorins induce F-actin reorganization in human dendritic cells: Role in cell migration. J Leukoc Biol, 2016. 100(6): p. 1323-1334.*

51. *Duncan, G.S., D.P. Andrew, H. Takimoto, et al., Genetic evidence for functional redundancy of Platelet/Endothelial cell adhesion molecule-1 (PECAM-1): CD31-deficient mice reveal PECAM-1-dependent and PECAM-1-independent functions. J Immunol, 1999. 162(5): p. 3022-30.*

52. *Liao, F., H.K. Huynh, A. Eiroa, et al., Migration of monocytes across endothelium and passage through extracellular matrix involve separate molecular domains of PECAM-1. J Exp Med, 1995. 182(5): p. 1337-43.*

53. *Ferrero, E., M.E. Ferrero, R. Pardi, et al., The platelet endothelial cell adhesion molecule-1 (PECAM1) contributes to endothelial barrier function. FEBS Lett, 1995. 374(3): p. 323-6.*

54. *Dangerfield, J., K.Y. Larbi, M.T. Huang, et al., PECAM-1 (CD31) homophilic interaction up-regulates alpha6beta1 on transmigrated neutrophils in vivo and plays a functional role in the ability of alpha6 integrins to mediate leukocyte migration through the perivascular basement membrane. J Exp Med, 2002. 196(9): p. 1201-11.*

Supplemental figure 1

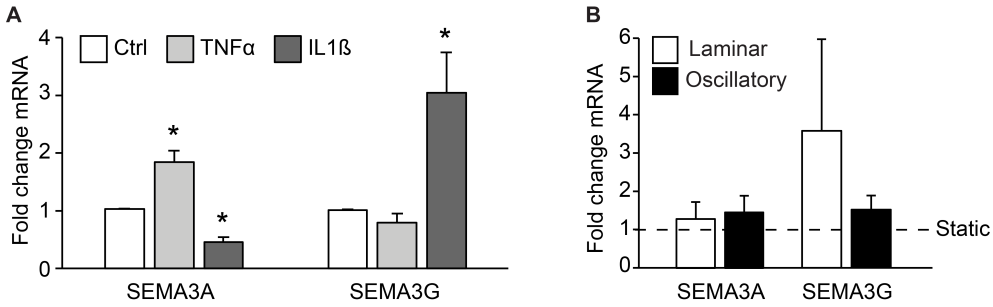

Figure S1. Regulation of SEMA3A and SEMA3G by inflammatory factors and shear stress in HUVECs

Chapter 4

Endothelial Netrin-4 prevents endothelial cell senescence and promotes endothelial cell survival

Zhang, H., Vreeken, D., Leuning, D. G., Bruikman, C. S., Junaid, A., Stem, W., deBruin, R. G., Sol, W. M. P. J., Rabelink, T. J., van den Berg, B. M., van Zonneveld, A. J. and van Gils, J. M.

International Journal of Biochemistry and Cell Biology, 2021;134.

Abstract

Netrin-4, recognized in neural and vascular development, is highly expressed by mature endothelial cells. The function of this netrin-4 in vascular biology after development has remained unclear. We found that the expression of netrin-4 is highly regulated in endothelial cells and is important for quiescent healthy endothelium. Netrin-4 expression is upregulated in endothelial cells cultured under laminar flow conditions, while endothelial cells stimulated with tumor necrosis factor alpha resulted in decreased netrin-4 expression. Targeted reduction of netrin-4 in endothelial cells resulted in increased expression of vascular cell adhesion molecule 1 and intercellular adhesion molecule 1. Besides, these endothelial cells were more prone to monocyte adhesion and showed impaired barrier function, measured in electric cell-substrate impedance sensing system, as well as in an 'organ-on-a-chip' microfluidic system. Importantly, endothelial cells with reduced levels of netrin-4 showed increased expression of the senescence-associated markers cyclin-dependent kinase inhibitor-1 and -2A, an increased cell size and decreased ability to proliferate. Consistent with the gene expression profile, netrin-4 reduction was accompanied with more senescent associated β-galactosidase activity, which could be rescued by adding netrin-4 protein. Finally, using human decellularized kidney extracellular matrix scaffolds, we found that pre-treatment of the scaffolds with netrin-4 increased numbers of endothelial cells adhering to the matrix, showing a pro-survival effect of netrin-4. Taken together, netrin-4 acts as an anti-senescence and anti-inflammation factor in endothelial cell function and our results provide insights as to maintain endothelial homeostasis and supporting vascular health.

Keywords

endothelial cells, netrin-4, senescence, inflammation, barrier function

4.1 Introduction

Endothelium is the interior surface lining of blood vessels. It is involved in physiological regulation of vascular barrier function, hemostasis and controlling of vascular tone. In disease conditions, the endothelium can undergo functional adaptions and plays a role in inflammatory response. Recent studies have identified novel roles of netrin class proteins in these processes[1-4]. Netrin class proteins belong to the broader families of neuronal guidance cues, which were originally identified in the nervous system for their role in directing axon growth, but were later found to have expression and functions in many other tissues [5]. Among netrin family proteins, we and others found netrin-4 (NTN4) to be the most abundantly expressed in endothelial cells[6-8]. NTN4 is a special member of the netrin family in several ways. Firstly, N-terminal domains of NTN4 are homologous to laminin β chain, whereas those of other secreted netrins are homologous to laminin γ chain [5]. Secondly, NTN4 has low binding affinity to the canonical netrin receptors, UNC5B, NEO1 and DCC [9]. Instead, NTN4 has the property to bind to laminin γ chain in a way that could disassemble the laminin network [9, 10]. Through this mechanism, high levels of exogenous NTN4 were shown to disrupt branching of the epithelium in submandibular gland explants and to decrease capillary development in a chick chorioallantoic membrane assay[9, 10]. The involvement of NTN4 in endothelial cell biology is most studied in the context of angiogenesis, though consistency of evidence is still lacking. NTN4 was found to either increase[11, 12] or inhibit[7, 13, 14] endothelial cell migration and tube formation. However, the role of endothelial NTN4 in physiology remains unclear. In this study, we confirmed the high expression of NTN4 in endothelial cells and demonstrated its modulation by inflammation and hemodynamic factors. State-of-art assays were used to further investigate the functional importance of NTN4. We observed a premature cellular senescent phenotype with inflammation and barrier loss upon reduced expression levels of NTN4 by endothelial cells. Furthermore, we found that addition of NTN4 to extracellular matrix favored the survival of endothelial cells.

4.2 Materials and Methods

4.2.1 Access to curated online gene expression datasets

Curated online gene expression datasets from all anatomical types on the microarray platform “Affymetrix Human Genome U133 Plus 2.0 Array” (abbreviation: HG-U133_Plus_2;

accession: GPL570) were obtained using Genevestigator software [15]. Average expression of selected genes from endothelial types of cells and the standard deviation was extracted. A heatmap illustrating the expression values was created with R package ggplot2[16].

4.2.2 Cell culture

Human umbilical vein endothelial cells (HUVECs) were isolated in house from human umbilical cords as described previously [17] and cultured in endothelial growth medium-2 (EGM2, Lonza, CC-3162) supplemented with antibiotics, unless indicated otherwise. Human pulmonary microvascular endothelial cells (MVECs) were a kind gift from Prof. M.J.T.H. Goumans, Leiden University Medical Center, Leiden, the Netherlands. MVECs were culture in microvascular endothelial cell medium-2 (EGM-2-MV, Lonza). Primary human peripheral blood monocytes were isolated as described previously [18] and cultured in RPMI1640 medium (Gibco, 21875034) supplemented with 10% FBS (v/v) and antibiotics. HEK293T cells were purchased from ATCC and cultured in DMEM medium (Gibco, 41965039) supplemented with 10% FBS and antibiotics. All cells were kept at 37 °C with 5% CO2.

4.2.3 Human tissue

Human transplant grade kidneys that were discarded for surgical reasons were used after research consent was given. Procedures of kidney biopsies and decellularization were adapted from Ott et al.[19] and were previously described by Leuning et al. [20]. In brief, the renal artery was cannulated with a Luer-lock connector (Cole-Parmer, Barendrecht, the Netherlands) and the kidney was perfused with 1% SDS in PBS containing antibiotics, antimycotics, and DNAse, under a constant pressure of maximal 75 mm Hg for 5 days. Afterwards the kidneys were perfused with dH2O with antibiotics, antimycotics, and DNAse overnight. Then the kidneys were flushed with 1% (v/v) Triton-X 100 (Sigma) for one day and afterwards flushed with PBS with antibiotics and antimycotics for at least 5 days, all under a constant pressure of max. 75 mm Hg. Kidneys were stored at 4 °C in PBS until further use. Biopsies of ≈ 1 cm^3 were taken and either snap frozen in liquid nitrogen or fixed overnight in 4% formaldehyde (Klinipath, Duiven, the Netherlands), stored in 70% ethanol, embedded in paraffin and cut in 4 µm thick sections. Coronary atherosclerotic plaques were retrieved from the archives of the Department of Pathology, Academic Medical Center, the Netherlands. Materials were obtained after research consent and paraffin embedding.

4.2.4 Quantitative PCR analysis for gene expression

For gene expression analysis, cells were lysed in Trizol (Invitrogen, 15596026). Total RNA was extracted using RNeasy Mini Kit (Qiagen, 74106) according to the manufacture's manual. Genomic DNA was removed using RNase-Free DNase Set (Qiagen, 79254). First strand complementary DNA was synthesized with equal amount of RNA input using M-MLV Reverse Transcriptase (Promega, M1701) with OligodT primers (Promega, C1101). Quantitative PCR (qPCR) analysis was performed with SYBR Green Master Mix (Applied Biosystems, A25777). List of primers used can be found in **Supplemental table 1**.

4.2.5 Immunohistochemistry or immunofluorescence staining

For immunofluorescence staining of snap frozen human (decellularized) kidney sections, sections were fixed in 4% paraformaldehyde (w/w in PBS) for 10 min at room temperature. The samples were then washed three times with PBS and blocked with Serum-Free Protein Block (Dako, X090930-2) for 30 minutes at room temperature. Primary antibodies were prepared in 1% BSA (w/w in PBS). Incubation of primary antibodies was set at 4 °C overnight. After the incubation, samples were washed three times with PBS again and incubated with Alexa fluorochrome conjugated secondary antibody mix prepared in 1% BSA (w/w in PBS supplemented with Hoechst (1:1000, Invitrogen, 11534886). Sections were then washed three times with PBS and mounted with Prolong Gold (Invitrogen, P36930). For immunohistochemistry staining of human coronary arteries, slides were deparaffinized in 100% xylene and rehydrated in ethanol. Heat-induced epitope retrieval was performed in tris-EDTA buffer (pH 9.0) for 20 minutes at 98°C. Next, nonspecific antigens were blocked with 1% BSA in TBS for 30 minutes, followed by incubation with primary antibody overnight. After washing in TBS slides were incubated with HRP-labeled secondary antibody for one hour and counterstained with Bright DAB substrate kit (BS04-110, Vector laboratories, Burlingame, CA, USA). Slides were covered with glycergel (C0563, Agilent, Glostrup, Denmark) and a glass coverslip. For immunofluorescence staining of HUVECs, cells were washed with Hank's Balanced Salt Solution with calcium and magnesium (HBSS+, Gibco, 14025092) and fixed with 4% formaldehyde (v/v in HBSS+) for 10 minutes at room temperature. The cells were then permeabilized with 0.1% Triton X-100 (w/w in HBSS) for two minutes, washed with HBSS and incubated with 5% BSA (w/w in HBSS+) to reduce non-specific antibody binding. Primary antibody prepared in 0.5% BSA (w/w in HBSS+) was used to incubate the cells overnight at 4 °C: The cells were washed three times. Alexa fluorochrome conjugated

secondary antibody mix was prepared in 0.5% BSA (w/w in HBSS+) supplemented with Hoechst 33528 (1:1000, Invitrogen, 11534886). After incubation with the mix for one hour at room temperature, cells were washed again three times with HBSS+. Fluorescent images were captured using Leica TCS SP5 confocal microscopy system (pinhole 1 airy; imaged 7-8 µm z-distance with step size of about 0.5 µm) and analyzed using ImageJ software. List of antibodies used can be found in **Supplemental table 2**.

4.2.6 Lentiviral vectors, lentiviral particle production and transduction

Four different shRNA constructs targeting human QKI, and four different shRNA constructs targeting human NTN4 were obtained from the Mission Library (Sigma Aldrich), and tested for their efficiency to knockdown QKI or NTN4, respectively. The best shRNAs for targeting QKI or NTN4 were selected to perform all experiments. As a control, a non-targeting shRNA (scramble) was used. Lentiviral particles were produced as described by the Sigma Library protocol using HEK293T cells. Selection of transduced cells was achieved using puromycin (2 µg/mL).

4.2.7 RNA immunoprecipitation

RNA-immunoprecipitation was performed with MVECs using Millipore's validated RIPAb+ QKI-5 kit according to manufacture instructions.

4.2.8 Immunoblot analysis

Endothelial cells were washed with cold PBS and lysed in cold RIPA buffer (Cell signaling, 9806). After centrifugation of the samples at 14000rpm for 10 minutes at 4 °C, protein concentration in the supernatant was measured using the Pierce BCA Protein Assay Kit (Thermo Scientific, 23255). Equal amounts of protein sample were denatured using DTT and heating at 95 °C for 10 minutes followed by size separation on a 10% Mini-PROTEAN gel (Biorad, 4561033). Proteins were transferred to PVDF membranes (Biorad, 1704156) using the Trans-Blot Turbo system (Biorad), after which membranes were blocked in either TBST-5% BSA (Sigma, A2058) for phosphorylated proteins or TBST-5% milk. Overnight incubation was performed with primary antibodies. Incubation with HRP-conjugated secondary antibodies (1:5000, Dako) and Western lightning ECL (PerkinElmer, NEL103001EA) or SuperSignal Western Blot Enhancer (ThermoFisher, 46640) enabled us to visualize protein bands with the ChemiDoc Touch Imaging System (Biorad). Expression was quantified using ImageLab software (Biorad) and ImageJ software (http://rsbweb.nih.gov/ij/). List of

antibodies used can be found in **Supplemental table 2**.

4.2.9 Proliferation assay

MTT (3-(4,5-dimethylthiazol-2-yl)-2,5-diphenyltetrazolium bromide), a yellow tetrazole, can be reduced to purple formazan by living cells. Thus, the number of viable cells can be quantified in colorimetric manner. HUVECs were seeded in 24-well plates in subconfluent density to allow space to proliferate (10,000 cells per well). At day one, three and five after seeding, 3-(4,5-dimethylthiazol-2-yl)-2,5-diphenyltetrazolium bromide (MTT) solution (0.5 µg/mL in PBS) was added to designated wells after a wash with PBS. The cells were incubated for 30 minutes at 37 °C. After the incubation, MTT solution was removed and 150 µL acidified isopropanol (0.04 M hydrochloride acid in isopropanol) solution was added to lyse the cells. The lysate was transferred to a 96-well plate. Colorimetric reading was done at 562 nm.

4.2.10 Senescence associated β-galactosidase staining

Senescence associated β-galactosidase staining was done using Senescence Cell Histochemical Staining Kit (Sigma, CS0030) according to the manufacturer's protocol. Briefly, HUVECs were seeded in subconfluent density (10,000 per cm^2) in µ8 slides (IBIDI, 80826). After overnight culture, cells were washed twice with PBS and fixed with 1x Fixation Buffer for six minutes. After fixation, cells were washed three times with PBS. The staining mixture (200 µL) was added to each well and allowed to incubate overnight at 37 °C. After staining, the number of positively stained cells (blue) and total cells were counted per field of view. Percentage of positively stained cells was calculated for each condition.

4.2.11 Adhesion assay of primary monocytes to endothelial cell monolayer

HUVECs were seeded at confluent density (40,000 per cm^2) one day before the experiment in 96-well plates. Peripheral blood was obtained after informed consent (Ethical Approval Number BTL 10.090) and peripheral mononuclear cells were isolated by density gradient separation using Ficoll. CD14 Microbeads (Miltenyi Biotec, 130-050-201) and LS columns (Miltenyi Biotec, 130-042-401) were used for magnetic separation of CD14 positive monocytes. Freshly isolated monocytes were labelled with 5 µg/mL Calcein AM (Molecular Probes Life Technologies, C3100MP) and incubated on top of a monolayer of HUVECs for 30 minutes at 37 °C. Non-adhering cells were washed away by multiple washing steps with PBS, after which images were made. Cells were then lysed in Triton-X 1% for 10 minutes.

Fluorescence was measured at λex 485 nm and λem 514 nm.

4.2.12 Electric cell-substrate impedance sensing

Electric Cell-substrate Impedance Sensing (ECIS) assays were done using the ECIS Ztheta device (Applied BioPhysics) with standard 8-well arrays (Applied BioPhysics, 8W10E). The 8-well arrays had gold electrodes fixed onto the bottom of the wells, enabling real time measurement of impedance, which represents endothelial barrier function. Prior to the experiment, electrodes were pretreated using 10 mM L-cysteine for 10 minutes. The wells were washed twice using water and coated with 0.5% gelatin (w/w in water) for 10 minutes. Gelatin solution was then replaced by 400 uL EGM2 medium and cell free baseline measurements were taken for approximately 30 minutes. Meanwhile, HUVECs were trypsinized and resuspended at a concentration of 1e6 per 200 µL. The measurements were paused, 1e6 HUVECs were added to each well in the volume of 200 µL. The measurements were then resumed for at least 24 hours. Measurements were taken at multiple frequencies every five minutes. Readings at 4000 Hz were used for data analysis and illustration, because at this frequency the impendence measurement is mainly contributed by cell-cell junction resistance.

4.2.13 Permeability of 3D endothelial culture

HUVECs with or without NTN4 knockdown were seeded in gelatin coated microvascular channels of custom-made gradient design OrganoPlate® (Mimetas) with 4 mg/mL type 1 collagen (Trevigen) in the extracellular matrix channel. After allowing the cells to adhere for one hour, culture medium was replaced by a mix of Endothelial Cell Growth Medium MV2 (PromoCell) and Pericyte Growth Medium (Angio-Proteomie) in a ratio of 1:1. The device was placed on a rocker platform with 7° angle of motion and eight minutes timed operation to allow continuous flow of medium in the microvessels. After 24 hours, the medium was refreshed and the HUVECs were cultured for 3-4 more days. To measure vessel permeability, the culture medium in the microvascular channels was replaced with culture medium containing 125 µg/mL Albumin-Alexa 555 (Life Technologies). Following this, the OrganoPlate® was placed in the environmental chamber (37 °C; 5% CO2) of a fluorescent microscope system (Nikon Eclipse Ti) and time-lapse images were captured. The permeability coefficient was calculated by determining the fluorescent intensities in the microvascular channel and in the extracellular matrix channel. The fluorescent intensity of the extracellular matrix channel was normalized with the fluorescent intensities in the

microvascular channel of each measured time point. This showed the change in intensity ratio inside the gel channel as a function of time. The scatter plot was fitted with a linear trend line to determine the slope. Finally, using Fick's First Law, the apparent permeability was determined as:

$$P_{app}(\cdot 10^{-6} cm/s) = \frac{d\left(\frac{I_g}{I_p}\right)}{dt} \cdot \frac{A_g}{l_w} \tag{4.1}$$

where I_p is the intensity in the microvascular channel, I_g is the intensity in the ECM channel, $A_g(480 \cdot 10^{-6} cm^2)$ is the area of the ECM channel and is the length of the vessel wall that separates between ECM and microvascular region. All data analysis was done with ImageJ (http://rsbweb.nih.gov/ij/, NIH, United States) and Matlab (MathWorks).

4.2.14 Decellularized human kidneys

For pretreatment of NTN4 on decellularized kidney sections, the snap frozen sections of decellularized kidneys were prepared on coverslips, placed in 24 wells plate and incubated with recombinant human NTN4 (1 µg/mL in 200 uL PBS, R&D systems, 1254-N4-025) overnight at 4 °C. Incubation using only PBS served as a control. The next day, NTN4 solution was removed and, when indicated, 5e4 HUVECs were seeded into the wells to allow the interaction between HUVECs and the kidney extracellular matrix. The cells were cultured for 24 hours at 37 °C, before being fixed with 4% paraformaldehyde (w/w in PBS) for one hour at room temperature. Immunofluorescent staining of laminin, NTN4 and CD31 was performed as described in the immunofluorescent staining section.

4.2.15 Statistical analyses

The difference between two group means was analyzed by Student's t-test. Comparison of three group means was analyzed by one-way ANOVA with Dunnett's post hoc analysis for the paired comparison to the control group. Mix effects of two conditions were analyzed by two-way ANOVA with the interaction term. P values of less than 0.05 were considered significant for all types of statistical analyses.

4.3 Results

4.3.1 NTN4 is the highest expressed Netrin in endothelial cells

We set off by studying the expression of NTN4 in various kinds of endothelial cells using available transcriptomics data on the GPL570 platform, a commonly used human transcriptome microarray platform. The average expression values of netrin family genes are

presented in a heatmap, and expression of cadherin 5 (CDH5, vascular endothelial cadherin) and cadherin 1 (CDH1, epithelial cadherin) were taken along as references of genes with high or low expression (**Figure 1A**). NTN4 is the highest expressed netrin family gene in all endothelial cell types, except for bone marrow endothelial progenitor cells. In some endothelial cell types, NTN4 expression is comparable to that of CDH5, which encodes one of the main components of endothelial adherens junctions. We also compared the NTN4 expression of endothelial cell types to that of other cell types by ranking all cell types by NTN4 expression. The ranking resulted in seven endothelial cells types and the capillary-rich structure of glomerulus in the top-10 list, confirming higher expression of NTN4 in endothelial cells relative to other cell types (**Figure 1B**). The high expression of NTN4 in HUVECs was confirmed by qPCR (**Figure 2A**). In accordance to the gene expression data, protein expression of NTN4 was observed in the endothelium of human coronary artery (**Figure 2B**), and in the glomeruli and peritubular micro-vessels of human kidney (**Figure 2C**). Consistent with the fact that NTN4 is secreted to endothelial basement membrane, staining of NTN4 co-localized with laminin signal at areas of vascular structures (**Figure 2C**).

4.3.2 Inflammation reduces and laminar shear stress induces NTN4 expression in endothelial cells

Given the high expression of NTN4 in endothelial cells, we next assessed if inflammatory and hemodynamic conditions could affect the expression of NTN4. Stimulation of HUVECs with the inflammatory cytokines tumor necrosis factor (TNFα) and interleukin 1β (IL1β) decreased the expression of NTN4 (**Figure 3A**), while culturing the cells under prolonged laminar flow conditions upregulated expression of NTN4 (**Figure 3B, C, Supplementary Figure 1**). Using confocal microscopy, NTN4 staining was found to be apparent in vesicles, consistent with NTN4 being a secreted protein (**Figure 3C and Supplementary Figure 1**). In addition, we observed no clear NTN4 staining at the extracellular basement membrane itself (**Supplementary Figure 1**). As the RNA-binding protein Quaking (QKI), discovered as post-transcriptional regulator and important for the development of central nervous system[21, 22], is also regulated in the same manner by flow conditions [17] (**Figure 3D**), we investigated the role of QKI in regulating NTN4 expression. Knockdown of QKI (**Supplementary Figure 2A**) suppressed the expression of NTN4 in endothelial cells (**Figure 3E**). We next sought to determine whether QKI can directly bind to mRNA

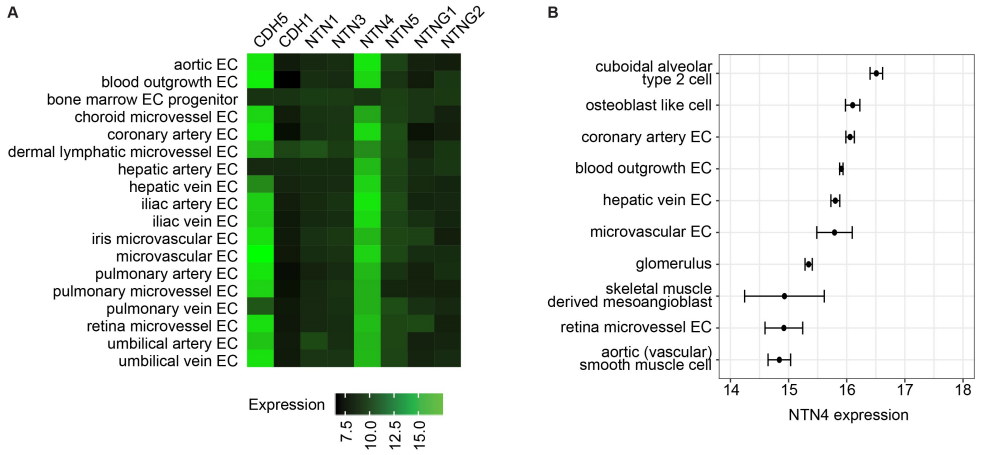

Figure 1. High expression of NTN4 in various types of endothelial cells

(A) Heatmap of netrin family expression in all types of human endothelial cells profiled on Affymetrix Human Genome U133 Plus 2.0 Array platform (GEO accession: GPL570). Numbers indicate normalized microarray signals on log2 scale. Black color: lower expression and green color: higher expression. Expression signals of CDH5 and CDH1 were included as references. (B) NTN4 expression in 10 human cell types with highest NTN4 expression. Data is presented as Mean ± SEM; n ≥ 3.

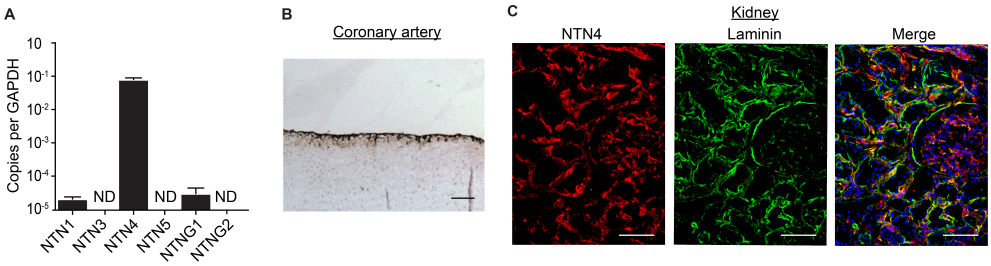

Figure 2. Confirmation of NTN4 expression in endothelial cells

(A) Quantification of expression of the netrin family with qPCR in HUVECs. Results are presented as copy numbers per GAPDH, Mean ± SEM, n = 5. (B) Immunohistochemistry of NTN4 (brown) in human coronary artery. Scale bar = 50 µm. (C) Immunofluorescent staining of NTN4 (red), laminin (green) and DNA (blue) in human kidney sections. Scale bars: 100 µm

of NTN4 using an RNA-immunoprecipitation experiment. Indeed, mRNA of NTN4 was highly enriched in the QKI-antibody precipitated RNA fraction (**Figure 3F, G**), indicating binding of QKI to NTN4 mRNA.

4.3.3 Reducing NTN4 promotes an inflammatory phenotype in endothelial cells

In order to study the functional importance of NTN4 for endothelial cells, NTN4 expression in endothelial cells was silenced using lentiviral shRNA vectors targeting NTN4 mRNA. A non-NTN4 targeting scrambled shRNA was used as a control. Repression of NTN4 was validated using qPCR and immunofluorescence staining (**Supplementary Figure 2B, C**). Staining of endothelial cells with reduced levels of NTN4 compared to endothelial cells transduced with scrambled shRNA showed less aligned adherens junctions, made visible by Cadherin 5 staining. Using antibodies binding to an epitope of the integrin β1 that is exposed constitutively or only exposed upon activation, respectively[23, 24],we showed that endothelial cells with reduced levels of NTN4 have more total and activated integrin β1 (**Figure 4A, B, Supplementary Figure 3**). As increased integrin activity levels can be induced by inhibition of protein kinase B (PKB, also known as Akt)[25, 26], we investigated Akt phosphorylation levels using western blot. Reducing NTN4 in endothelial cells resulted in less P-Akt (**Figure 4C**).

In addition, we investigated whether loss of NTN4 induces vascular leakage, since the morphological change with less aligned adherens junctions strongly indicates the possibility of reduced endothelial barrier function. In both electric cell–substrate impedance sensing (ECIS) system [27] and the more physiological 3D-endothelial tube in a microfluidics platform [28], we found that targeted reduction of NTN4 in endothelial cells resulted in impaired barrier function (**Figure 5A, B**). Since reduction in endothelial barrier function is often caused by an inflammatory phenotype, we examined whether the NTN4 knockdown endothelial cells are more inflammatory-like. Endothelial cells with NTN4 KD indeed showed more adhesion of primary monocytes (**Figure 5C**) and exhibited elevated expression of ICAM1 and VCAM1 both at mRNA and protein levels (**Figure 5D, E**).

4.3.4 Reducing NTN4 induces endothelial cell senescence

Next to the inflammatory phenotype, we observed enlarged cell bodies at the same seeding density (**Figure 6A**) and reduced capacity to proliferate (**Figure 6B**) in endothelial cells with reduced expression of NTN4. These observations prompted us to assess cell senes-

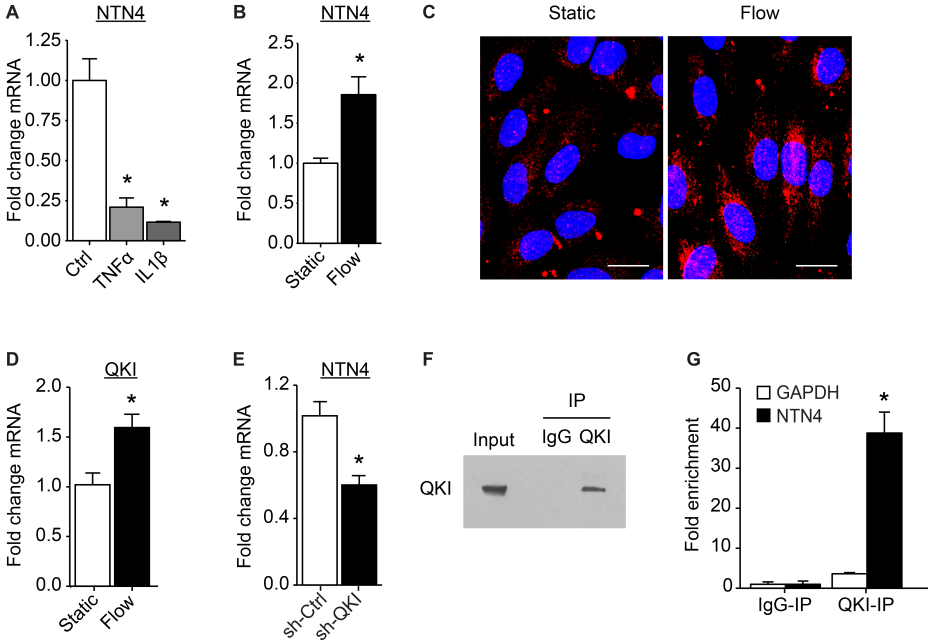

Figure 3. Regulation of NTN4 expression level in HUVECs

(A-B) qPCR analysis of NTN4 mRNA isolated from (A) HUVECs stimulated with the inflammatory factors, TNFα (10 ng/mL) or IL1β (20 ng/mL) for 24 hours, or (B) HUVECs cultured under static conditions or laminar flow (10 dynes/cm^2) conditions for seven days. Results are expressed as fold change of untreated cells (A) or static cultured cells (B), set to 1, Mean ± SEM, n = 3; * $p < 0.05$. (C) Immunofluorescence staining of NTN4 (red) and DNA (blue) in HUVECs cultured under static conditions or laminar flow (10 dynes/cm^2). Maximum intensity z -projection images from a series of confocal images. Scale bars = 20 µm (D) qPCR analysis of QKI mRNA isolated from HUVECs cultured under static or laminar flow conditions. Results are presented relative to static cultured cells. Mean ± SEM of n = 4. * $p < 0.05$. (E) qPCR analysis of NTN4 mRNA isolated from HUVECs transduced with anti-Qki shRNA (shQKI) or control shRNA (shCtrl). Results are presented relative to shCtrl. Mean ± SEM of n = 5. * $p < 0.05$. (F, G) RNA-immunoprecipitation in HUVEC using an IgG control or QKI-5 antibody. (F) Immunoblot of QKI confirming immunoprecipitation of QKI protein from endothelial cell lysates. (G) NTN4 and GAPDH mRNA abundance in the immune-precipitated fraction was determined by qPCR. Results are presented relative to IgG immunoprecipitation. Mean ± SEM of n = 4. * $p < 0.05$.

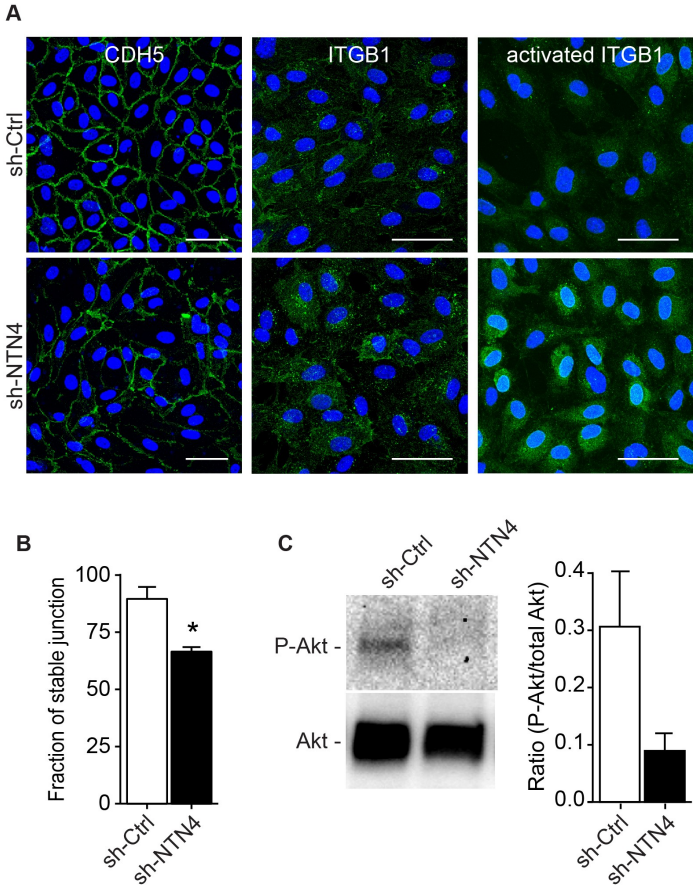

Figure 4. Reduction of NTN4 expression in endothelial cells reduces CDH5 junction localization and increases integrin β1 activity

(A) Immunofluorescence staining of CDH5, integrin β1 or activated integrin β1 (green) and DNA (blue) in HUVECs transduced with anti-NTN4 shRNA (sh-NTN4) or scrambled shRNA (sh-Ctrl). Representative images of n = 2-3. Maximum intensity z -projection images from series of confocal images. Scale bar = 50 μm. (B) Quantification of fraction of stable adherens junctions. Mean ± SEM of n = 3; * $p < 0.05$. (C) Immunoblots and quantification of phospho- and total Akt in sh-Ctrl and sh-NTN4 treated cells. Levels are expressed as ratio P-Akt/total Akt, Mean ± SEM of n = 3.

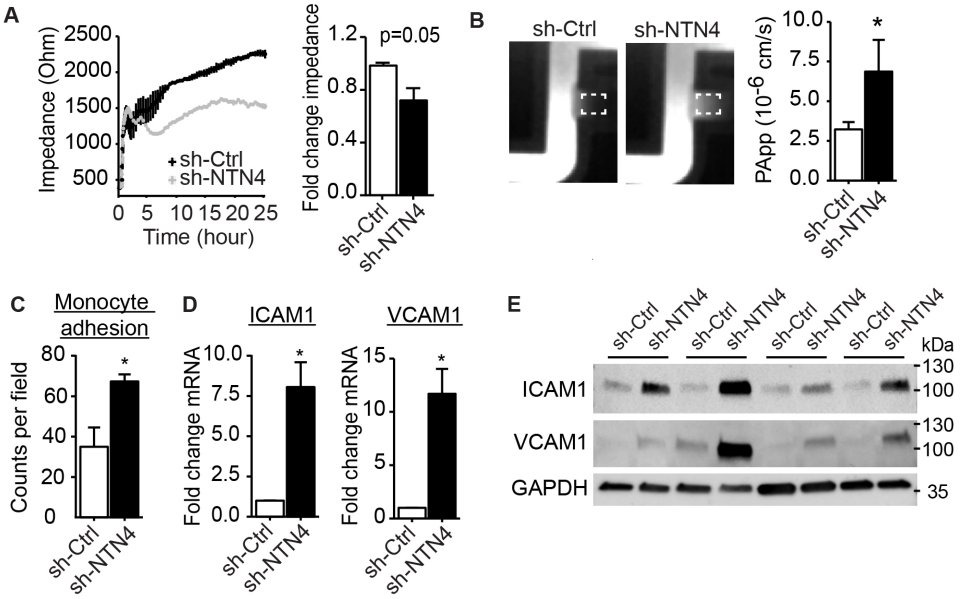

Figure 5. Reduction of NTN4 expression in endothelial cells diminishes endothelial barrier function and promotes an inflammatory phenotype

(A) Left graph shows transendothelial electrical resistance of scrambled shRNA (sh-Ctrl) or anti-NTN4 shRNA (sh-NTN4) transduced HUVECs seeded on electric cell–substrate impedance sensing (ECIS) electrodes (Mean ± SD of technical triplicates, representative of three independent experiments). Right graph shows the relative trans-endothelial electrical resistance of sh-Ctrl or sh-NTN4 HUVEC stable monolayer, sh-Ctrl set to 1. Mean ± SEM of n = 3. (B) HUVECs transduced with sh-Ctrl or sh-NTN4 were seeded in the vertical channel of a microfluidic device with collagen in the horizontal channel. At the start of the measurement, fluorescently labeled albumin was infused in the vessel lumen and after 10 minutes albumin leakage outside the vessel channel was visualized and quantified. Dotted box indicates the region used in quantification. Bar graph shows the permeability coefficient presented as Mean ± SEM of n = 3; * $p < 0.05$. (C) Quantification of adhesion of primary human monocytes to sh-Ctrl or sh-NTN4 transduced HUVECs. Mean ± SEM of n = 3; * $p < 0.05$ (D) ICAM1 and VCAM1 mRNA expression in sh-Ctrl or sh-NTN4 transduced HUVECs. Results are presented relative to sh-Ctrl. Mean ± SEM of n = 3; * $p < 0.05$. (E) Immunoblots of ICAM1, VCAM1 and GAPDH (housekeeping) in sh-Ctrl and sh-NTN4 treated cells. n=4.

cence by investigating expression levels of senescence- associated transcription factors. Up-regulation of senescence-associated transcription factors, CDKN1A and CDKN2A (encoding $p21^{Waf1/Cip1}$ and $p16^{Ink4a}$, respectively), but not CDKN1B (encoding $p27^{Kip1}$), was observed in endothelial cells with NTN4 knockdown (**Figure 6C**). For CDKN1A, the most abundantly expressed of these three genes, we performed immunofluorescence staining to look into protein expression, and observed also at protein level increased expression of the senescence marker CDKN1A upon NTN4 knockdown (**Figure 6D**). Furthermore, senescence-associated β-galactosidase (SA-β-gal) staining revealed a higher percentage of positively stained cells in NTN4 sh-RNA treated endothelial cells compared to scrambled sh-RNA (**Figure 6E**). To confirm the hypothesis that loss of NTN4 induced the endothelial senescence, we performed rescue experiment with human NTN4 protein. Indeed, NTN4 knockdown endothelial cells cultured on human NTN4 coating no longer showed increased β-galactosidase staining compared to control cells (**Figure 6E**).

4.3.5 NTN4 promotes endothelial cell survival

As introduced previously, NTN4 can interact with laminin gamma chain in the basement membrane[9, 10]. To study the consequence for endothelial cells of NTN4 interacting with extracellular matrix, we utilized sections of decellularized human kidney. Immunostaining confirmed NTN4 presence on the extracellular matrix, which could be increased by addition of NTN4 protein (**Figure 7A**). Next, we added endothelial cells to the kidney scaffold with or without extra loading of NTN4. We observed that more endothelial cells adhered to the kidney scaffolds loaded with NTN4, as quantified by CD31 staining and nucleus counting (**Figure 7B and 7C**).

4.4 Discussion

Shear stress, or the in vivo hemodynamic environment, is one of the most profound regulators of endothelial cell biology. Low shear stress or disturbed flow explains the increased vulnerability of certain vascular regions (bifurcations or inner wall of aorta) to pathophysiological changes, such as endothelial senescence, vascular wall inflammation and atherosclerosis [29]. In the current study, we found that the expression of NTN4 could be induced by prolonged laminar shear stress. Making use of NTN4 knockdown endothelial cells, we showed that a reduction of NTN4 resulted in a more inflammatory phenotype with impaired barrier function as well as increased monocyte adhesion due to increased expression of ad-

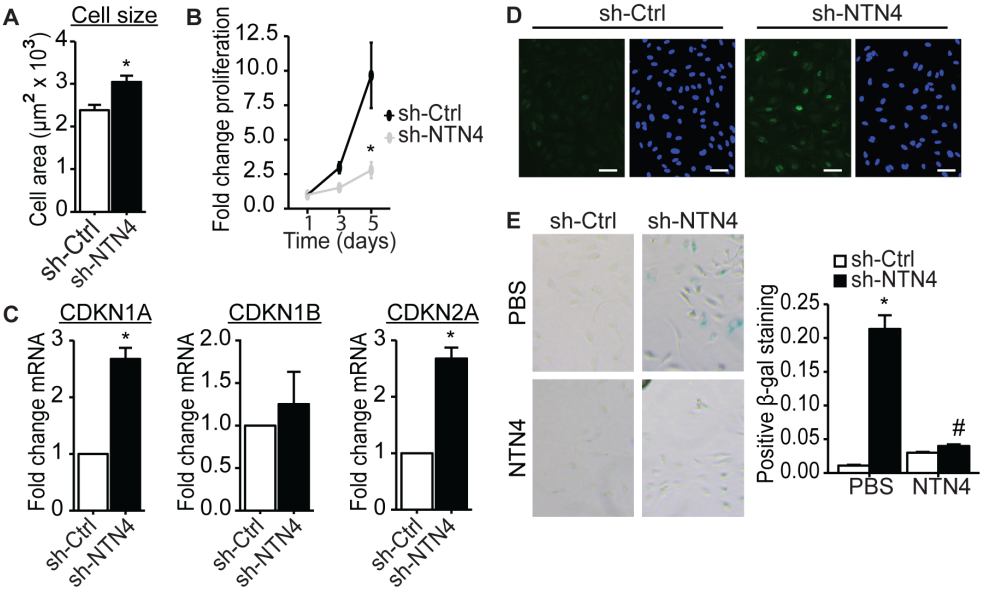

Figure 6. Loss of NTN4 results in endothelial cell senescence

(A) Cell surface area of scramble shRNA treated endothelial cells (sh-Ctrl) or endothelial cells treated with shRNA against NTN4 (sh-NTN4) cultured into confluent monolayer. Mean ± SEM of n = 3; * $p < 0.05$. (B) Proliferation of sh-Ctrl and sh-NTN4 endothelial cells. Results are expressed as fold change to day 0, sh-Ctrl. Mean ± SEM of n = 3; * $p < 0.05$. (C) CDKN1A, CDKN1B and CDKN2A mRNA expression in sh-Ctrl or sh-NTN4 endothelial cells. Results are presented relative to sh-Ctrl set to 1. Mean ± SEM of n = 3; * $p < 0.05$. (D) Immunofluorescence staining of CDKN1A (green) and DNA (blue) in HUVECs transduced with anti-NTN4 shRNA (sh-NTN4) or scrambled shRNA (sh-Ctrl). Representative images of n = 2. Maximum intensity z -projection images from series of confocal images. Scale bar = 50 μm. (E) Representative images of SA-β-gal staining of sh-Ctrl or sh-NTN4 cells cultured in wells pre-treated with PBS or NTN4. Bar graph shows the fraction of positively stained cells. Mean ± SEM of n = 3; * $p < 0.05$ for effect of shNTN4, #$p < 0.05$ for interaction effect of shNTN4 and NTN4 coating.

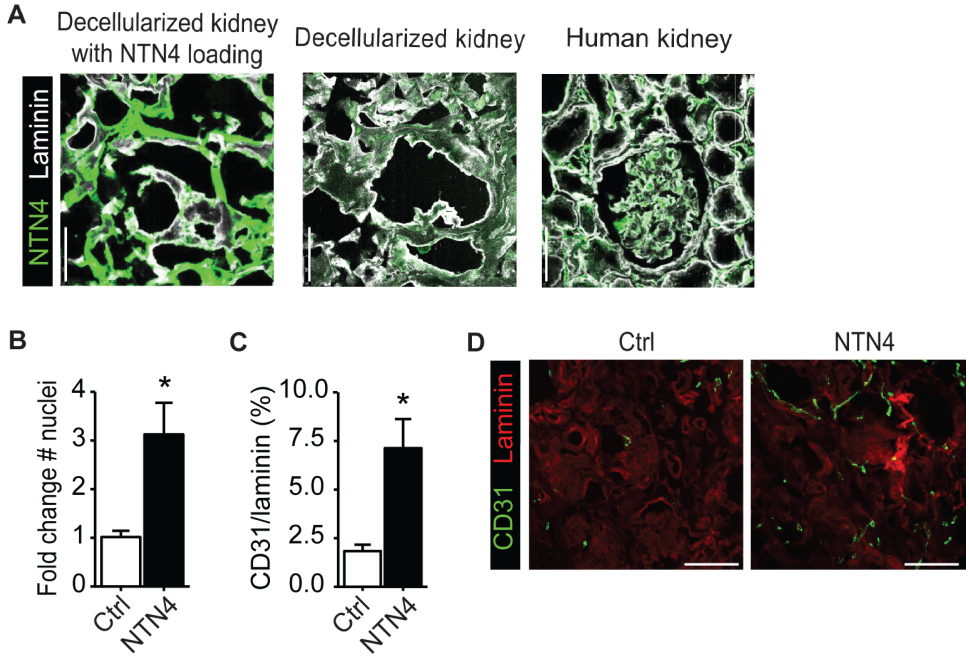

Figure 7. NTN4 on extracellular matrix supports endothelial survival

(A) Immunofluorescence staining of NTN4 (green) and laminin (white) of human kidney and decellularized kidney with and without preincubation of NTN4 protein. Representative images of n = 3. Scale bar = 100 µm. (B-C) Number of nuclei (B) or CD31+ area of human decellularized kidneys without (Ctrl) and with preincubation of NTN4 protein (NTN4) on which endothelial cells were added and cultured. Results are expressed as (B) fold change to Ctrl or (C) CD31+/laminin ratio. Mean ± SEM of n = 3; * $p < 0.05$. (D) Immunofluorescence staining of CD31 (green) and laminin (red) of human decellularized kidney with and without preincubation of NTN4 on which endothelial cells were added and cultured. Representative images of n = 3. Scale bar = 100 µm.

hesion molecules. Loss of NTN4 also led to a senescent endothelial phenotype, which can explain the inflammatory nature of these cells. Using decellularized human kidneys, we were able to illustrate the effect of NTN4 addition in promoting endothelial adhesion and survival to extracellular matrix. Collectively, these results indicate an important role for NTN4 in maintaining endothelial cell function. Cellular senescence can be induced by two mechanisms, namely replicative senescence and stress-induced senescence. Via these mechanisms, senescence of endothelial cells was shown to occur under circumstances of repetitive injuries (due to atherosclerosis or artificial injuries) or oxidative stress (reviewed in [30]). Replicative senescence results from shortening of telomeres during division of primary cells [31], while stress-induced senescence can be caused by reasons including DNA damage [32] and oxidative stress [33]. We saw senescent phenotypes of endothelial cells upon knockdown of NTN4 expression, which fits in the theoretical framework of stress-induced cellular senescence, since the replicative potential of the HUVECs was not exhausted. Work done by Li et al. showed that NTN4 was implicated in protection of glioblastoma cell line U251MG from senescence in an ITGB4-dependent manner [34]. Further investigations are needed to clarify the dependency of protective effect of NTN4 from senescence on integrin activity in endothelial cells. The presence of NTN4 has been shown to increase activity of Akt and ERK1/2[11, 35]. Increased levels of Akt phosphorylation result in decreased integrin activity[25, 26] and are associated with increased survival of endothelial cells [36]. In line with this, our NTN4 knockdown cells showed decreased Akt phosphorylation, increased integrin activity and decreased endothelial survival. In addition, integrin activity and binding to extracellular matrix also modulate endothelial cell cytoskeletal contractility and cell shape, thereby also affecting endothelial barrier function[37, 38]. ITGB1 gene inactivation impairs proper localization of VE-cadherin and thereby endothelial junction integrity [39]. In contrast, addition of NTN4 has been shown to be able to bind to and activate endothelial integrin alpha 6 beta 1[40]. As NTN4 is structurally homologous to laminin β chain and has been known as a guidance cue in extracellular matrix, it is able to regulate the structure of the laminin network in cellular basement membrane[9, 10]. We suggest that the local concentration of NTN4 is of much relevance. NTN4 has been shown to disassemble laminin networks and to disrupt endothelial basement membrane functions when given exogenously [9]. Here, we demonstrate for the first time that reduction of NTN4 expression from its normal level induces an inflammatory and senescent phenotype. In addition, reintroducing NTN4 can rescue the senescent phenotype and increase adhesion of endothelial cells to the

extracellular matrix. This suggests that modification of the matrix by NTN4 adapts the extracellular matrix properties in a more beneficial way, giving an essential role for NTN4 to regulate endothelial extracellular matrix properties under physiological condition. The relevance of such a modification in vivo is yet to be revealed. Together we identified NTN4 as an anti-senescence and anti-inflammatory protein. NTN4 is important in prevention of endothelial cells from pathophysiological consequences, such as decreased regeneration capacity and endothelial dysfunction.

Acknowledgements

We thank Mehdi Maanaoui and Zsofia Nagy for their technical support. This research was funded by Dutch Heart Foundation, grant number 2013T127, 2018T095, and RECONNECT CVON, European Research Area Network on Cardiovascular Diseases, grant number 038 MISsCVD, and ZonMW MKMD, grant number 114022501.

Conflicts of Interest

The authors declare no conflict of interest.

References

1. *Zhang, H., D. Vreeken, C.S. Bruikman, A.J. van Zonneveld, and J.M. van Gils, Understanding netrins and semaphorins in mature endothelial cell biology. Pharmacol Res, 2018. 137: p. 1-10.*
2. *Castets, M., M.M. Coissieux, C. Delloye-Bourgeois, L. Bernard, J.G. Delcros, A. Bernet, V. Laudet, and P. Mehlen, Inhibition of endothelial cell apoptosis by netrin-1 during angiogenesis. Dev Cell, 2009. 16(4): p. 614-20.*
3. *Toque, H.A., A. Fernandez-Flores, R. Mohamed, R.B. Caldwell, G. Ramesh, and R.W. Caldwell, Netrin-1 is a novel regulator of vascular endothelial function in diabetes. PLoS One, 2017. 12(10): p. e0186734.*
4. *van Gils, J.M., B. Ramkhelawon, L. Fernandes, M.C. Stewart, L. Guo, T. Seibert, G.B. Menezes, D.C. Cara, C. Chow, T.B. Kinane, E.A. Fisher, M. Balcells, J. Alvarez-Leite, A. Lacy-Hulbert, and K.J. Moore, Endothelial expression of guidance cues in vessel wall homeostasis dysregulation under proatherosclerotic conditions. Arterioscler Thromb Vasc Biol, 2013. 33(5): p. 911-9.*
5. *Lai Wing Sun, K., J.P. Correia, and T.E. Kennedy, Netrins: versatile extracellular*

cues with diverse functions. Development, 2011. 138(11): p. 2153-69.

6. *Podjaski, C., J.I. Alvarez, L. Bourbonniere, S. Larouche, S. Terouz, J.M. Bin, M.A. Lecuyer, O. Saint-Laurent, C. Larochelle, P.J. Darlington, N. Arbour, J.P. Antel, T.E. Kennedy, and A. Prat, Netrin 1 regulates blood-brain barrier function and neuroinflammation. Brain, 2015. 138(Pt 6): p. 1598-612.*
7. *Nacht, M., T.B. St Martin, A. Byrne, K.W. Klinger, B.A. Teicher, S.L. Madden, and Y. Jiang, Netrin-4 regulates angiogenic responses and tumor cell growth. Exp Cell Res, 2009. 315(5): p. 784-94.*
8. *Han, Y., Y. Shao, T. Liu, Y.L. Qu, W. Li, and Z. Liu, Therapeutic effects of topical netrin-4 inhibits corneal neovascularization in alkali-burn rats. PLoS One, 2015. 10(4): p. e0122951.*
9. *Reuten, R., T.R. Patel, M. McDougall, N. Rama, D. Nikodemus, B. Gibert, J.G. Delcros, C. Prein, M. Meier, S. Metzger, Z. Zhou, J. Kaltenberg, K.K. McKee, T. Bald, T. Tuting, P. Zigrino, V. Djonov, W. Bloch, H. Clausen-Schaumann, E. Poschl, P.D. Yurchenco, M. Ehrbar, P. Mehlen, J. Stetefeld, and M. Koch, Structural decoding of netrin-4 reveals a regulatory function towards mature basement membranes. Nat Commun, 2016. 7: p. 13515.*
10. *Schneiders, F.I., B. Maertens, K. Bose, Y. Li, W.J. Brunken, M. Paulsson, N. Smyth, and M. Koch, Binding of netrin-4 to laminin short arms regulates basement membrane assembly. J Biol Chem, 2007. 282(33): p. 23750-8.*
11. *Lambert, E., M.M. Coissieux, V. Laudet, and P. Mehlen, Netrin-4 acts as a pro-angiogenic factor during zebrafish development. J Biol Chem, 2012. 287(6): p. 3987-99.*
12. *Larrieu-Lahargue, F., A.L. Welm, K.R. Thomas, and D.Y. Li, Netrin-4 induces lymphangiogenesis in vivo. Blood, 2010. 115(26): p. 5418-26.*
13. *Dakouane-Giudicelli, M., S. Brouillet, W. Traboulsi, A. Torre, G. Vallat, S. Si Nacer, M. Vallee, J.J. Feige, N. Alfaidy, and P. de Mazancourt, Inhibition of human placental endothelial cell proliferation and angiogenesis by netrin-4. Placenta, 2015. 36(11): p. 1260-5.*
14. *Lejmi, E., L. Leconte, S. Pedron-Mazoyer, S. Ropert, W. Raoul, S. Lavalette, I. Bouras, J.G. Feron, M. Maitre-Boube, F. Assayag, C. Feumi, M. Alemany, T.X. Jie,*

T. Merkulova, M.F. Poupon, M.M. Ruchoux, G. Tobelem, F. Sennlaub, and J. Plouet, Netrin-4 inhibits angiogenesis via binding to neogenin and recruitment of Unc5B. Proc Natl Acad Sci U S A, 2008. 105(34): p. 12491-6.

15. *Hruz, T., O. Laule, G. Szabo, F. Wessendorp, S. Bleuler, L. Oertle, P. Widmayer, W. Gruissem, and P. Zimmermann, Genevestigator v3: a reference expression database for the meta-analysis of transcriptomes. Adv Bioinformatics, 2008. 2008: p. 420747.*
16. *Wickham, H., ggplot2: Elegant Graphics for Data Analysis. Springer-Verlag New York, 2016.*
17. *de Bruin, R.G., E.P. van der Veer, J. Prins, D.H. Lee, M.J. Dane, H. Zhang, M.K. Roeten, R. Bijkerk, H.C. de Boer, T.J. Rabelink, A.J. van Zonneveld, and J.M. van Gils, The RNA-binding protein quaking maintains endothelial barrier function and affects VE-cadherin and beta-catenin protein expression. Sci Rep, 2016. 6: p. 21643.*
18. *de Bruin, R.G., L. Shiue, J. Prins, H.C. de Boer, A. Singh, W.S. Fagg, J.M. van Gils, J.M. Duijs, S. Katzman, A.O. Kraaijeveld, S. Bohringer, W.Y. Leung, S.M. Kielbasa, J.P. Donahue, P.H. van der Zande, R. Sijbom, C.M. van Alem, I. Bot, C. van Kooten, J.W. Jukema, H. Van Esch, T.J. Rabelink, H. Kazan, E.A. Biessen, M. Ares, Jr., A.J. van Zonneveld, and E.P. van der Veer, Quaking promotes monocyte differentiation into pro-atherogenic macrophages by controlling pre-mRNA splicing and gene expression. Nat Commun, 2016. 7: p. 10846.*
19. *Guyette, J.P., S.E. Gilpin, J.M. Charest, L.F. Tapias, X. Ren, and H.C. Ott, Perfusion decellularization of whole organs. Nat Protoc, 2014. 9(6): p. 1451-68.*
20. *Leuning, D.G., F.M.R. Witjas, M. Maanaoui, A.M.A. de Graaf, E. Lievers, T. Geuens, C.M. Avramut, L.E. Wiersma, C.W. van den Berg, W. Sol, H. de Boer, G. Wang, V.L.S. LaPointe, J. van der Vlag, C. van Kooten, B.M. van den Berg, M.H. Little, M.A. Engelse, and T.J. Rabelink, Vascular bioengineering of scaffolds derived from human discarded transplant kidneys using human pluripotent stem cell-derived endothelium. Am J Transplant, 2018.*
21. *Hardy, R.J., Molecular defects in the dysmyelinating mutant quaking. J Neurosci Res, 1998. 51(4): p. 417-22.*
22. *Zearfoss, N.R., B.M. Farley, and S.P. Ryder, Post-transcriptional regulation of myelin formation. Biochim Biophys Acta, 2008. 1779(8): p. 486-94.*

23. *Luque, A., M. Gomez, W. Puzon, Y. Takada, F. Sanchez-Madrid, and C. Cabanas, Activated conformations of very late activation integrins detected by a group of antibodies (HUTS) specific for a novel regulatory region (355-425) of the common beta 1 chain. J Biol Chem, 1996. 271(19): p. 11067-75.*

24. *Tsuchida, J., S. Ueki, Y. Saito, and J. Takagi, Classification of 'activation' antibodies against integrin beta1 chain. FEBS Lett, 1997. 416(2): p. 212-6.*

25. *Somanath, P.R., E.S. Kandel, N. Hay, and T.V. Byzova, Akt1 signaling regulates integrin activation, matrix recognition, and fibronectin assembly. J Biol Chem, 2007. 282(31): p. 22964-76.*

26. *Virtakoivu, R., T. Pellinen, J.K. Rantala, M. Perala, and J. Ivaska, Distinct roles of AKT isoforms in regulating beta1-integrin activity, migration, and invasion in prostate cancer. Mol Biol Cell, 2012. 23(17): p. 3357-69.*

27. *Giaever, I. and C.R. Keese, Use of Electric Fields to Monitor the Dynamical Aspect of Cell Behavior in Tissue Culture. IEEE Transactions on Biomedical Engineering, 1986. BME-33(2): p. 242-247.*

28. *Junaid, A., A. Mashaghi, T. Hankemeier, and P. Vulto, An end-user perspective on Organ-on-a-Chip: Assays and usability aspects. Current Opinion in Biomedical Engineering, 2017. 1: p. 15-22.*

29. *Chistiakov, D.A., A.N. Orekhov, and Y.V. Bobryshev, Effects of shear stress on endothelial cells: go with the flow. Acta Physiol (Oxf), 2017. 219(2): p. 382-408.*

30. *Erusalimsky, J.D., Vascular endothelial senescence: from mechanisms to pathophysiology. J Appl Physiol (1985), 2009. 106(1): p. 326-32.*

31. *Harley, C.B., A.B. Futcher, and C.W. Greider, Telomeres shorten during ageing of human fibroblasts. Nature, 1990. 345(6274): p. 458-60.*

32. *Kaneko, T., S. Tahara, T. Taguchi, and H. Kondo, Accumulation of oxidative DNA damage, 8-oxo-2'-deoxyguanosine, and change of repair systems during in vitro cellular aging of cultured human skin fibroblasts. Mutat Res, 2001. 487(1-2): p. 19-30.*

33. *Chen, Q. and B.N. Ames, Senescence-like growth arrest induced by hydrogen peroxide in human diploid fibroblast F65 cells. Proc Natl Acad Sci U S A, 1994. 91(10): p. 4130-4.*

34. *Li, L., Y. Hu, I. Ylivinkka, H. Li, P. Chen, J. Keski-Oja, and M. Hyytiainen, NETRIN-4 protects glioblastoma cells FROM temozolomide induced senescence. PLoS One, 2013. 8(11): p. e80363.*

35. *Lange, J., Y. Yafai, A. Noack, X.M. Yang, A.B. Munk, S. Krohn, I. Iandiev, P. Wiedemann, A. Reichenbach, and W. Eichler, The axon guidance molecule Netrin-4 is expressed by Muller cells and contributes to angiogenesis in the retina. Glia, 2012. 60(10): p. 1567-78.*

36. *Cheng, H.W., Y.F. Chen, J.M. Wong, C.W. Weng, H.Y. Chen, S.L. Yu, H.W. Chen, A. Yuan, and J.J. Chen, Cancer cells increase endothelial cell tube formation and survival by activating the PI3K/Akt signalling pathway. J Exp Clin Cancer Res, 2017. 36(1): p. 27.*

37. *Geiger, B. and A. Bershadsky, Exploring the neighborhood: adhesion-coupled cell mechanosensors. Cell, 2002. 110(2): p. 139-42.*

38. *Juliano, R.L., Signal transduction by cell adhesion receptors and the cytoskeleton: functions of integrins, cadherins, selectins, and immunoglobulin-superfamily members. Annu Rev Pharmacol Toxicol, 2002. 42: p. 283-323.*

39. *Yamamoto, H., M. Ehling, K. Kato, K. Kanai, M. van Lessen, M. Frye, D. Zeuschner, M. Nakayama, D. Vestweber, and R.H. Adams, Integrin beta1 controls VE-cadherin localization and blood vessel stability. Nat Commun, 2015. 6: p. 6429.*

40. *Larrieu-Lahargue, F., A.L. Welm, K.R. Thomas, and D.Y. Li, Netrin-4 activates endothelial integrin alpha6beta1. Circ Res, 2011. 109(7): p. 770-4.*

Gene	Forward Sequence	Reverse Sequence
GAPDH	CCTGCACCACCAACTGCTTA	GGCCATCCACAGTCTTCTGAG
NTN1	GGGTGCCCTTCCAGTTCTAC	GCGAGTTGTCGAAGTCGTG
NTN3	GCCGTCGTCCCTTACTCCTA	TGAGGCATGTCCATTGCACTT
NTN4	GTACTTTGCGACTAACTGCTCC	TCCAGTGCATGGAAAAGGACT
NTN5	GGACCCATGCTACGATCCAC	AAGCGCAAGCTGACAGATGT
NTNG1	AAGTTTGGGATTACATGGCCTG	CGGAGGATCGAGTTTCACTTTC
NTNG2	GCGCCTGAAGGACTACGTC	CGTTGCTGCATAGGTAGGGAT
panQKI	CTGATGCTGTGGGACCTATTG	GTTGTTTGGCTGTAAGTCCTCT
ICAM-1	GGCCGGCCAGCTTATACAC	TAGACACTTGAGCTCGGGCA
VCAM-1	TCAGATTGGAGACTCAGTCATGT	ACTCCTCACCTTCCCGCTC
CDKN1A	ACTCTCAGGGTCGAAAACGG	CTTCCTGTGGGCGGATTAGG
CDKN1B	TCTGAGGACACGCATTTGGT	AAGAATCGTCGGTTGCAGGT
CDKN2A	GGAGGCCGATCCAGGTCAT	ACGGGTCGGGTGAGAGTG

Supplemental table 1. List of primers

Antibody	Company	Catalogue number
Rabbit anti-human Akt	Cell Signaling	4691
Rabbit anti-human P-Akt	Cell Signaling	4060
Mouse anti-human CD31	BD Biosciences	555446
Mouse anti-human CDH5	BD Biosciences	555661
Goat anti-human CDKN1A	Santa Cruz Biotechnology	sc-397
Rabbit anti-human GAPDH	Cell Signaling	5174
Rabbit anti-goat HRP	Dako	P0160
Donkey anti-goat alexa-488	Invitrogen	A-11055
Donkey anti-goat alexa-568	Invitrogen	A-11057
Donkey anti-goat alexa-647	Invitrogen	A-21447
Rabbit anti-human ICAM1	Cell signaling	4915
Mouse anti-activated integrin β1	Merck-Millipore	MAB2079Z
Mouse anti-integrin β1	Santa Cruz Biotechnology	sc-53711
Rabbit anti-human laminin	Sigma Aldrich	L9393
Goat anti-mouse alexa-488	Invitrogen	A-11001
Goat anti-human NTN4	R&D Systems	AF1254
Mouse anti-panQKI	NeuroMab	clone N147/6
Goat anti-rabbit HRP	Dako	P0448
Donkey anti-rabbit alexa-568	Invitrogen	A-11011
Rabbit anti-human VCAM1	Abcam	ab134047

Supplemental table 2. List of antibodies used

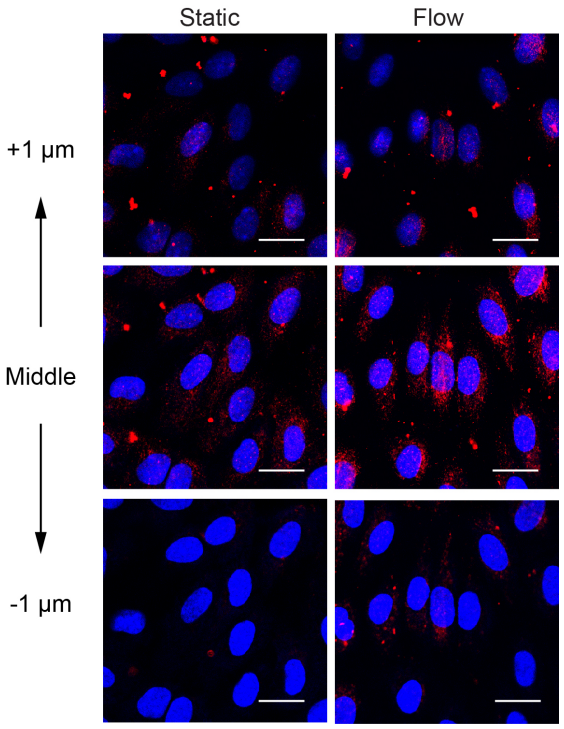

Supplementary Figure 1. Immunofluorescent images at different z plane of staining of NTN4 (red) and DNA (blue) in HUVECs cultured under static conditions or laminar flow (10 dynes/cm^2). Scale bar = 20 µm.

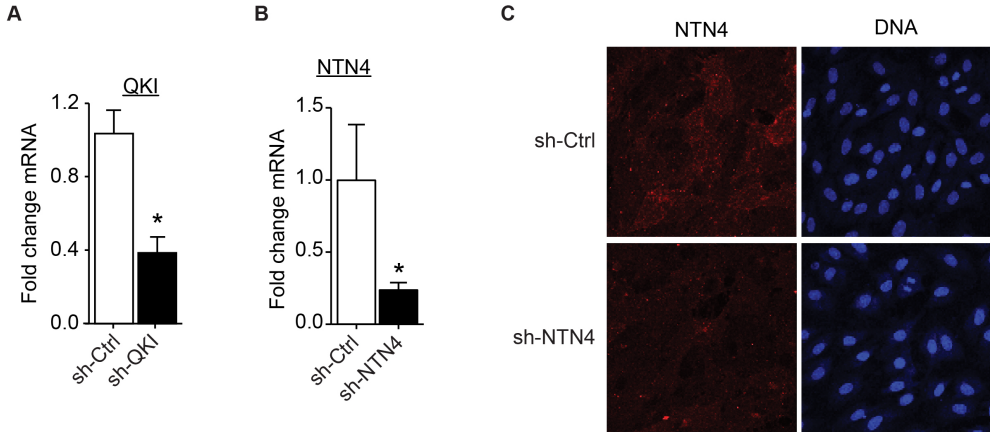

Supplementary Figure 2. (A) qPCR analysis of QKI mRNA isolated from HUVECs transduced with anti-Qki shRNA (sh-QKI) or control shRNA (sh-Ctrl). Results are presented relative to sh-Ctrl. Mean ± SEM of n = 5. * $p < 0.05$. (B) NTN4 mRNA expression in sh-RNA treated endothelial cells (sh-Ctrl) or endothelial cells treated with sh-RNA against NTN4 (sh-NTN4). Results are presented relative to scrambled. Mean ± SEM of n = 3; * $p < 0.05$. (C) Immunofluorescence staining of NTN4 (red) and DNA (blue) in HUVECs transduced with anti-NTN4 shRNA (sh-NTN4) or scrambled shRNA (sh-Ctrl).

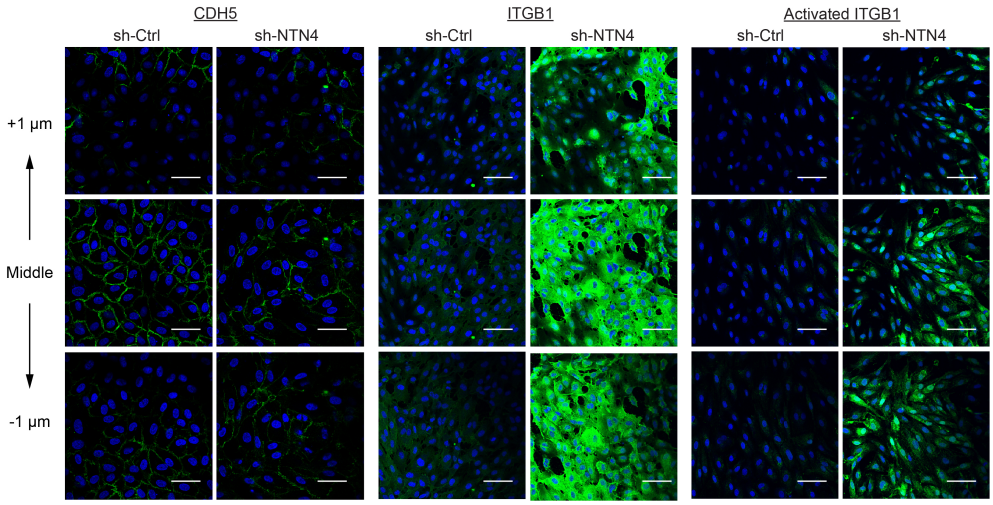

Supplementary Figure 3. Immunofluorescent images at different z plane of staining of CDH5, integrin β1 or activated integrin β1 (green) and DNA (blue) in HUVECs transduced with anti-NTN4 shRNA (sh-NTN4) or scrambled shRNA (sh-Ctrl). Representative images of n = 2-3. Scale bar = 50 µm.

Chapter 5

Comprehensive analysis of neuronal guidance cue expression regulation during monocyte to macrophage differentiation reveals post-transcriptional regulatory hotspot in Semaphorin7A 3'UTR

Zhang, H., Prins, J., Vreeken, D., Florijn, B. W., de Bruin, R. G., van Hengel,O. R., van Essen, M. F., Duijs, J. M., Van Esch, H., van der Veer, E. P., van Zonneveld, A. J. and Gils, J. M.

Innate Immunity, 2020;27.

Abstract

In response to inflammatory cytokines and chemokines, monocytes differentiate into macrophages. Recent research on neuronal guidance cues (NGCs) has expanded their function in the field of immunology. Nonetheless, a comprehensive analysis of gene expression regulation of NGC ligands and receptors in the monocyte to macrophage differentiation process was not available yet. We performed transcriptome profiling in both human primary periphery blood monocytes (PBMCs)/PBMC-derived macrophages and THP-1 cells/THP1-macrophages using microarray or RNAsequencing methods. Pathway analysis showed that the axonal guidance pathway is significantly regulated upon monocyte differentiation. We confirmed NGC ligands and receptors which were consistently regulated, including SEMA4D, SEMA7A, NRP1, NRP2, PLXNA1, PLXNA3. The involvement of RNA-binding protein quaking (QKI) in the regulation of NGC expression was investigated using monocytes and macrophages from a QKI haplo-insufficient patient and her healthy sibling. This revealed a positive correlation of SEMA7A expression with QKI expression. In silico analysis of 3'UTRs of NGCs proposed the competitive binding of QKI to proximal microRNA targeting sites as the mechanism of QKI-dependent regulation of SEMA7A. RNA-immunoprecipitation confirmed an interaction of QKI with the 3'UTR of SEMA7A. In addition, loss of SEMA7A resulted in monocyte differentiation towards a more anti-inflammatory macrophage. All taken together, the axonal guidance pathway is regulated during monocyte to macrophage differentiation and the regulation is in line with the necessary functional adaption for the specialized role of macrophages.

Keywords

monocyte, macrophage, semaphorin, quaking, microRNA

5.1 Introduction

Monocytes, with their ability to phagocytose, present antigens and produce cytokines, play important roles in immune surveillance. In response to inflammatory cytokines and chemokines, they are able to extravasate through endothelium and differentiate into macrophages, which are more specialized in phagocytosis and play a significant role in innate immunity [1]. Besides their important roles in various physiological processes, macrophages are responsible for the pathophysiology of various inflammatory diseases, including atherosclerosis, Crohn's disease, and various neurodegenerative diseases [2]. Upon monocyte to macrophage differentiation, the cells change their functionalities in multifaceted ways, which can partly be reflected by altered gene expressions in biological pathways. A comprehensive understanding of biological pathway regulations during monocyte/macrophage differentiation give insights to their functions in health and disease. Neuronal guidance cues (NGCs) are ligands in the axon guidance pathway that trigger downstream signaling by binding to their receptors. They consist of 4 classes, namely semaphorin (SEMA), netrin (NTN), ephrin (EFN) and slit (SLIT), with their receptors being plexin/neuropilin (PLXN/NRP), UNC5/DCC/NEO1, EPH and ROBO, respectively. Functionally, these guidance cues affect adhesion, migration and activation of cells. In recent years, we have come to the understanding that neuronal guidance cues play an important role in immunology and are also specifically shown to be involved in monocyte-macrophage biology. For example, SEMA7A was shown to stimulate production of pro-inflammatory cytokines in monocytes and potentially promote differentiation of monocytes to macrophages [3]. NTN1 and SEMA3A were found to inhibit migration of monocyte-like cell lines and adhesion of leukocytes to capillary endothelium [4]. In ApoE knockout mice fed a high fat diet, NTN1 inhibited emigration of macrophages from atherosclerotic lesions [5]. To better interpret the involvement of NGCs in monocyte-to-macrophage differentiation, we sought out to give an overall image of the expression of guidance cues and their regulations during monocyte-to-macrophage differentiation using multiple commonly used experimental models. Quaking (QKI), an RNA binding protein (RBP), has been identified as a central regulator of gene expression changes in the monocyte-to-macrophage differentiation process [6]. One of the mechanisms through which QKI performs its regulatory functions is that QKI binds to quaking response element (QRE) motif in mRNA stabilizing mRNA transcript [7, 8]. The QRE motif consists of the core sequence "ACUAA", often followed by a half site "UAAY" [7]. Despite the central role of QKI in monocyte-to-macrophage differentiation,

involvement of QKI in the regulation of NGCs is yet to be studied. In the current study, we found significant regulation of genes in the axonal guidance pathway during monocyte to macrophage differentiation by pathway analysis. Consistent regulation of gene expression was identified among multiple experimental models. In addition, we explored the involvement of QKI in the regulation of NGC ligands and receptors [6]. Using material from a QKI haplodeficient patient, we demonstrated the possibility that regulation of SEMA7A was dependent on the competitive binding of QKI to a microRNA (miRNA) targeting cluster in 3'UTR of SEMA7A.

5.2 Materials and Methods

5.2.1 Culture of human monocytes and THP-1 cells

THP-1 cells were obtained from ATCC (TIB202) and were cultured in RPMI 1640 medium with 10% fetal bovine serum (FBS) supplemented with 0.01 μg/mLL-glutamine, penicillin and streptomycin and 0.05 mM 2-mercaptoethanol. For differentiation of THP-1 cells to THP-1 macrophages, 100 nM of Phorbol 12-Myristate 13-Acetate (PMA, Sigma-Aldrich) was added to the medium. After 3 days, the PMA-containing medium was replaced by normal growth medium and the cells were cultured for another 5 days. Primary human monocytes were isolated from whole blood donated by the QKI haplo-deficiency patient and her sibling. Peripheral blood mononuclear cells were isolated by gradient centrifugation in Ficoll-Paque (Sigma-Aldrich). Monocyte fraction were then labeled with anti-CD14 antibody conjugated to magnetic beads (Miltenyi) and separated on a MACS magnetic column, according to manufacturer's instruction. The purity of the isolated monocytes was around 95% (**Supplementary Figure 1**). Isolated monocytes were either subjected directly to RNA isolation procedure or differentiated to pro-inflammatory macrophage in RPMI 1640 medium with 10% FBS supplemented with 5 ng/mLrecombinant human granulocyte-macrophage colony-stimulating factor (GM-CSF, Biosource). The medium was refreshed every 2 days until day 7. Ethics issues regarding utilization of patient-derived samples were described previously [6]. Briefly, informed consents were obtained prior to the experiments and the proposals were approved by relevant ethics committees in Maastricht University Medical Center, the Netherlands, and Leuven University Hospital, Belgium.

5.2.2 Omics data access

Transcriptome (GSE9820 [9], last downloaded on Jan 15, 2015) and miRNA (GSE52986, last downloaded on Oct 01, 2018 [10]) profiling data of human monocytes were obtained from Gene Expression Omnibus (GEO) repository using "GEOquery" package from R bioconductor, according the developer's manual [11]. QKI eCLIP data were downloaded from ENCODE website (ENCSR366YOG, last downloaded on Sept 23, 2018) [12]. A summary of in-house and online data used in this article is provided in **Supplementary table 1**.

5.2.3 Gene expression microarrays

Detailed method has been described before by de Bruin et al [6]. THP-1 cells and THP-1 macrophages were lysed in Trizol (Thermo Fisher Scientific). RNA was isolated using the RNeasy Mini Kit (Qiagen) according to the manufacturer's instructions. Complementary DNA synthesis was done with the WT Expression Kit (Affymetrics). Fragmentation and terminal labeling were done using the WT Terminal Labeling Kit (Affymetrics). The library was then hybridized to HJAY Chips (Affymetrix 540091). Chips were scanned using the Affymetrix Gene ChIP Scanner 3000 7G (Affymetrix). Probe intensity data were analyzed using the standard Affymetrix pipeline according to manufacturer's instructions. Data was deposited in GEO under the accession number GSE74887.

5.2.4 RNA sequencing

RNA sequencing analysis (RNAseq) was performed as previously described [6]. Briefly, ribosomal RNA was removed using Ribo-Zero rRNA Removal Kit (Illumina). Sequence libraries for mRNA were generated using TruSeq RNA Library Prep Kit (Illumina). The cDNA fragments of 300 bp in size were isolated and purified using 2% E-gel SizeSelect gels (Invitrogen). The libraries were then pair-end sequenced on Illumina HiSEQ platform to a depth of 41-70 million reads per sample. The sequencing results were mapped using Tophat2 software to GRCh37/UCSC-hg19 genome assembly with the gene model provided by "hg19 UCSC Known Genes" [13]. Guidance cues with non-zero counts were included for subsequent analyses.

5.2.5 Pathway analysis

Pathway analysis was done using annotation of Kyoto Encyclopedia of Genes and Genomes (KEGG) [14] with R package "gage" [15]. Gene symbols are converted to En-

trez ID using data base provided in R package "org.Hs.eg.db". Pathway "Axon guidance" (KEGG accession: hsa04360) was tested under the null hypothesis that this pathway is not significantly regulated. A p-value of less than 0.05 was considered enough for rejecting the null hypothesis. The analysis was visualized using R package "pathview".

5.2.6 Quantitative polymerase chain reaction

RNA isolation was done as described for the gene expression microarray method. Briefly, RNA isolation was done using the miRNeasy Mini Kit (Qiagen), while random hexamers served as primers for first strand cDNA synthesis. The polymerase chain reaction (PCR) was run on a CFX384 Real-Time PCR Detection System and SYBRgreen (Applied Biosystems) was used to detect amplification of the PCR product. A list of primer sequences can be found in **Table 1**. We analyzed 4 housekeeping genes in the THP-1 monocytes and macrophages. Three out of four were unchanged by differentiation (**Supplementary Figure 2A**). From this GAPDH was chosen for the analysis of primary monocytes differentiated to macrophages. Comparing different donors, showed that GAPDH mRNA did not change upon differentiation (**Supplementary Figure 2B**). Therefore, the presented change in mRNA expression was calculated by the comparative copies per GAPDH.

5.2.7 Mapping of "ACUAA" 5mer and miRNA target sites in 3'UTR of transcripts

Genome coordinates of 3'UTRs of NGC transcripts were retrieved from Ensembl annotation "EnsDb.Hsapiens.v75" [16] using R package "GenomicFeatures" [17]. Sequences of 3'UTRs were obtained using R package "ensembldb" [18]. Motif "ACUAA" was matched against 3' UTR sequence using R package "Biostrings" [19]. Counts of the 5mer were stored and related to the regulation of NGCs. Genome coordinates of QRE motifs were also stored for subsequent analysis. To examine the possibility that QKI could protect 3'UTRs of NGCs from targeting of miRNA, we collected genomic coordinates of miRNA target sites from "miRbase.org" [20] and of QRE 5mers from the previous mapping. The miRNA target sites were filtered by the miRNA expression levels given from the monocyte miRNA microarray (GSE52986 [10]; **Supplementary table 1 Dataset 4**; expression level in top 50%) and by miRNA targeting strength score (miRsvr score ¡ -1). QRE mappings were cross-validated by experimentally confirmed interaction of QKI and target mRNA using eCLIP-seq method (ENCSR366YOG [12]) by overlaying genomic range of narrow peak signals to QRE mappings. Next, we scanned for proximity of validated QRE and filtered miRNA targeting sites

Symbol	Forward Primer (5' ->3')	Reverse Primer (5' ->3')
ACTB	TGCGTGACATTAAGGAGAAG	TGAAGGTAGTTTCGTGGATG
ADORA2B	GGGCTTCTGCACTGACTTCT	CCCGTGACCAAACTTTTATACCTG
EPHB3	GTCATCGCTATCGTCTGCCT	AAACTCCCGAACAGCCTCATT
GAPDH	TTCCAGGAGCGAGATCCCT	CACCCATGACGAACATGGG
IL10	GCGCTGTCATCGATTTCTTCC	GTAGATGCCTTTCTCTTGGAGCTTA
NRP1	GGCGCTTTTCGCAACGATAAA	TCGCATTTTTCACTTGGGTGAT
NRP2	AAGTTCACCTCCGACTACGC	CATGCACGTTTCAAGCCCTC
PLXNA1	TGTGCAGTACACGTCCTGTG	GCTCGTCTGCTCGCTCAC
PLXNA3	CGGACATGTTCAGTCTCGTGTA	CGCTGACGAAGCCGTAGAT
PLXND1	CTGTGCATGTGGAGTGATGG	GTTCCTTCCTCGGATGGTCAG
QKI5	GACTGGCATTTCAATCCAC	GATGGACACGCATATCGTG
RHOA	GATTGGCGCTTTTGGGTACAT	AGCAGCTCTCGTAGCCATTTC
RPS18	CCTGCGGCTTAATTTGACTC	AGACAAATCGCTCCACCAAC
SEMA3C	TGTGAAAGGATCTTCCCAGCC	GATGGTGGGAAAGGCTGAAGT
SEMA4A	CTCCCCACATCTACGCAGTC	AGAGAGAAGGCACAAACCGC
SEMA4B	GAGCGGCCATTCCTCAGATTC	CACCCACGTACAGGGTCCT
SEMA4D	GACAGCGATGGCATTTGCAC	CCTCCCGGGCACCTATGTA
SEMA4F	TCCAATCTCTGAGGCTGACTC	GGGATAAAGCGAAGATGGTGTC
SEMA7A	ATCTTCGCCGTCTGGAAAGG	TAGTTCTCGCAGTCCGTGC
SEMA7A 3'UTR	GGCATCGATGACCCAAGACT	TGGGAGCATCGCTGCATTTA
TNFA	CCTCTCTCTAATCAGCCCTCTG	GAGGACCTGGGAGTAGATGAG

Table 1. List of primers used

using R package "GenomicRanges" [17]. We considered a physical distance of less than 20 nucleotide as proximity. Final results were visualized with R package "Gviz" [21].

5.2.8 RNA immunoprecipitation

HEK293T cells were transfected with a human QKI5 and human SEMA7A 3'UTR-reporter plasmid (SwitchGear Genomics) through the use of polyethylenimine (3 µg/1µg DNA; Polysciences Inc). Twenty-four hours after transfection RNA-immunoprecipitation was performed using Millipore's validated RIPAb+QKI-5 kit according to manufacture instructions.

5.2.9 Immunoblot analysis

Suspended cells were collected, spun down, washed with cold PBS and lysed in 100ul of Novex Tris-Glycine SDS sample buffer (ThermoFisher, LC2676). Adhered cells were washed with cold PBS, lysed in another 100 µL of sample buffer, collected and combined with lysates from suspended cells. After sonication, samples were centrifuged at 14000 rpm for 10 minutes at 4°C. Equal amounts of protein samples, measured with Nanodrop (Thermo Fisher), were denatured using DTT and heating at 95°C for 10 minutes, followed by size separation on a 10% Mini-PROTEAN gel (Biorad, 4561033). Proteins were transferred to PVDF membranes (Biorad, 1074156) using the Trans-Blot Turbo system (Biorad) after which membranes were blocked in TBST-5% Milk. Membranes were incubated with human SEMA7A antibody (1:10000, AF 2068, R&D systems) or GAPDH antibody (1:1000, 5174, Cell signaling Technology) in blocking buffer overnight at 4°C. Thereafter membranes were shortly washed and incubated with HRP-labeled secondary antibodies (1:5000, Dako) for 1 hour at room temperature. After thorough washing with TBST, protein bands were visualized using Western lightning ECL (PerkinElmer, NEL1030001EA) and the ChemiDoc Touch Imaging System (Biorad).

5.2.10 Statistical analysis

Comparison between 2 means were done with 2-tailed unpaired Student's t-test. A p-value less than 0.05 was considered significant.

5.3 Results

5.3.1 Axonal guidance pathway is significantly altered in monocyte to macrophage differentiation

In order to assess the relevance of the axon guidance pathway in monocyte to macrophage differentiation, we extracted transcriptome profiling data of human peripheral blood monocytes and monocyte-derived macrophages (**Supplementary Table 1 Dataset 1**) and of THP-1 cells and THP-1 macrophages (**Supplementary Table 1 Dataset 2**). KEGG pathway analysis on the 2 datasets (**Supplementary Figure 3 and 4**) showed significant (p=0.016 and 0.007 respectively) regulation of gene expression in the axon guidance pathway (KEGG: hsa04360) during monocyte-to-macrophage differentiation (**Table 2**). Since downstream signaling in the axon guidance pathway is initiated by binding of guidance cues and their receptors on the cell surface, we next focused on the regulation of NGC ligands and their receptors during monocyte-to-macrophage differentiation.

Pathway	Accession	Biological Process	P value
Axon guidance	KEGG: hsa04360	Human monocyte-macrophage	0.016
Axon guidance	KEGG: hsa04360	THP1-THP1 macrophage	0.007

Table 2. Pathway analysis of the transcriptome change in experimental monocyte-macrophage differentiation

5.3.2 Detectable expression of NGCs in monocytes and macrophages

To gain insight in the genes with significant expression, we summarized the transcriptome data obtained from both microarray and RNAseq methods. Significant expression of NGCs from different classes was detected in primary human monocytes and macrophages (**Figure 1A, Supplementary table 1 Dataset 1**) and in THP1 cells and THP1 macrophages (**Supplementary Figure 5**, **Supplementary table 1 Dataset 2**). To examine the comparability between observations of the 2 methods, we plotted the relative probe signal intensity representing expression of NGCs in descending order and differentially labeled the ones that were detectable in RNAseq data (**Figure 1B and 1C**). As we have n = 3 in microarray method, the signals from microarray methods gives good overview of the expression of NGCs and its variation. The RNAseq experiment, as a method with better sensitivity and

larger dynamic range, provides extra information on the likelihood of whether NGCs with borderline expression are actually expressed. Several NGCs, including SEMA4D, SEMA7A, NRP1, NRP2, PLXNA1, PLXNA3 and NTN1 that are known to be involved in monocyte-macrophage physiology, could be detected with both the micro array and RNAseq. However, some NGCs like EPHA4 and UNC5B were detected with RNAseq but have a low expression in the microarray. This might be due to the intrinsic character of a higher dynamic range of RNAseq. Overall it can be concluded that numerous NGCs are expressed by monocytes and macrophages.

5.3.3 Regulation of NGCs in monocyte to macrophage differentiation

Next we assessed the changes in expression of NGCs in monocyte-to-macrophage differentiation in vitro in 3 datasets (Mono-macro RNAseq, Mono-macro microarray and THP-1 microarray). Fold changes in NGC expression in macrophages relative to monocytes are depicted in a heatmap and shown in **Figure 2A**. Around half of all NGCs were detectable with RNAseq (36/74, **Figure 2B**). Of the detected NGCs, 12.2% were upregulated (9/74), while 10.8% were downregulated (8/74) in at least 2 of the 3 datasets (**Figure 2A and 2B**). Regulation of NGC expression was confirmed by qPCR (**Figure 3 and Supplementary Figure 6**). The list of regulated genes is shown in **Table 3** and a brief annotation of the known relevant functions are also provided. Overall can be concluded that the results obtained from different methods had good agreement with each other.

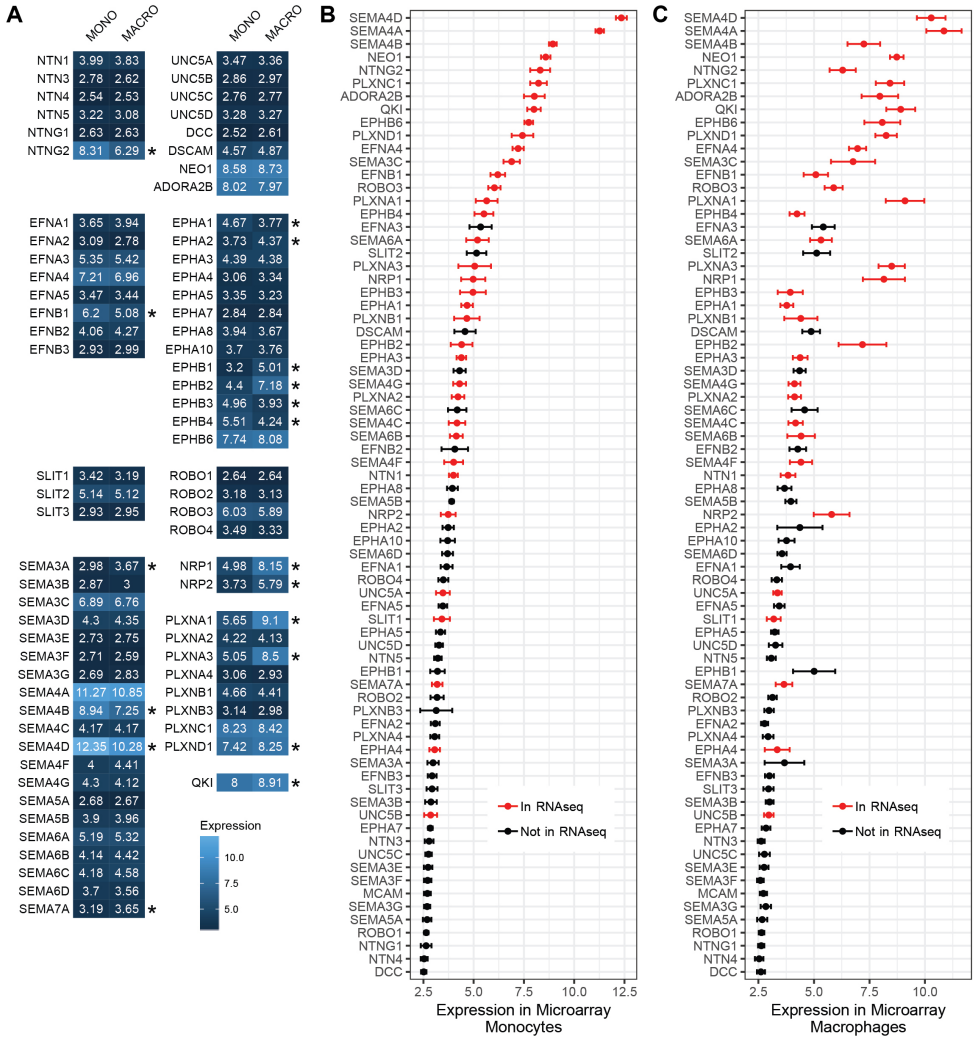

Figure 1. Expression of NGCs in human monocytes/macrophages

(A) Heatmap of mRNA expression of NGCs in human monocytes/macrophages detected by microarray expressed in log2 scale. (Lighter blue indicates higher expression; n=12; * $p < 0.05$) (B, C) Average expression levels of mRNA NGCs in human monocytes (B) or macrophage (C) detected by microarray ranked by expression in monocytes from high to low. RED: detectable in RNAseq. Data are Mean ± SEM; n=12.

Gene	Mono-mφ RNAseq	Mono-mφ Microarray	THP-1 Microarray	Expression	Type	Annotation
NTNG2	Down	Down*	-	++	Netrin	Function unknown
ADORA2B	Up	-	Up*	++	Netrin Receptor	ADORA2B has a pro-inflammatory role through production of cAMP. [22]
EPHA1	Down	Down*	Down*	++	Ephrin Receptor	EPHA1 is a receptor for EFNA1, which promotes monocyte adhesion. [23]
EPHB3	Down	Down*	-	+/-	Ephrin Receptor	EPHB3 is a receptor for EFNB2, which promotes monocyte adhesion. [24]
EPHB4	Down	Down*	Down*	+	Ephrin Receptor	EPHB4 is a receptor for EFNB2, which promotes monocyte adhesion. [24]
SEMA3C	Up	-	Up*	+++	Semaphorin	SEMA3C enhances deformability of DCs, promoting migration of DCs. [25]
SEMA4A	Down	Down	Down	++++	Semaphorin	SEMA4A promotes expression of VEGFA in monocytes. [26]
SEMA4B	Down	Down*	-	+++	Semaphorin	Function unknown
SEMA4D	Down	Down*	Down*	++++	Semaphorin	AntiSEMA4D treatment augments pro-inflammatory function of mφ [27]; SEMA4D itself also promote differentiation of monocyte to alternatively activated mφ [28].
SEMA4F	Up	Up*	Up*	-	Semaphorin	Function unknown
SEMA6A	Down	-	Down*	+	Semaphorin	SEMA6A signals via PLXNA4 leading to repulsion of cell migration. [29]
SEMA7A	Up	Up*	Up*	+/-	Semaphorin	SEMA7A works as a stimulator of monocytes, promoting the production of GM-CSF. [3]
NRP1	Up	Up*	Up*	++	Neuropilin	NRP1 is a co-receptor of Class III semaphorins, which are repellents for monocyte adhesion and migration.[4] NRP1+ mφ migrate towards SEMA3A expressed in hypoxic niches of tumors. [30]
NRP2	Up	Up*	Up*	++	Neuropilin	NRP2 is a co-receptor of Class III semaphorins, which are repellents for monocyte adhesion and migration. [4] NRP2 is required for phagocytosis of mφ. [31]
PLXNA1	Up	Up*	Up*	++	Plexin	PLXNA1 is a receptor of Class III semaphorins, which are repellents for monocyte adhesion and migration. [4] PLXNA1 facilitates migration of tumor associated mφ into hypoxic niche. [30]
PLXNA3	Up	Up*	Up*	+	Plexin	PLXNA3 is a receptor of Class III semaphorins, which are repellents for monocyte adhesion and migration. [4]
PLXND1	-	Up*	Up*	+++	Plexin	SEMA3E-PLXND1 axis promotes mφ infiltration in adipose tissue. [32]

(Continued from previous page)

Table 3. Overview of regulated genes and their known relevant function

Annotation of functions of the NGCs that showed consistent changes in at least 2 of the 3 monocyte-to-macrophage differentiation datasets. (* $p < 0.05$; mφ: macrophages)

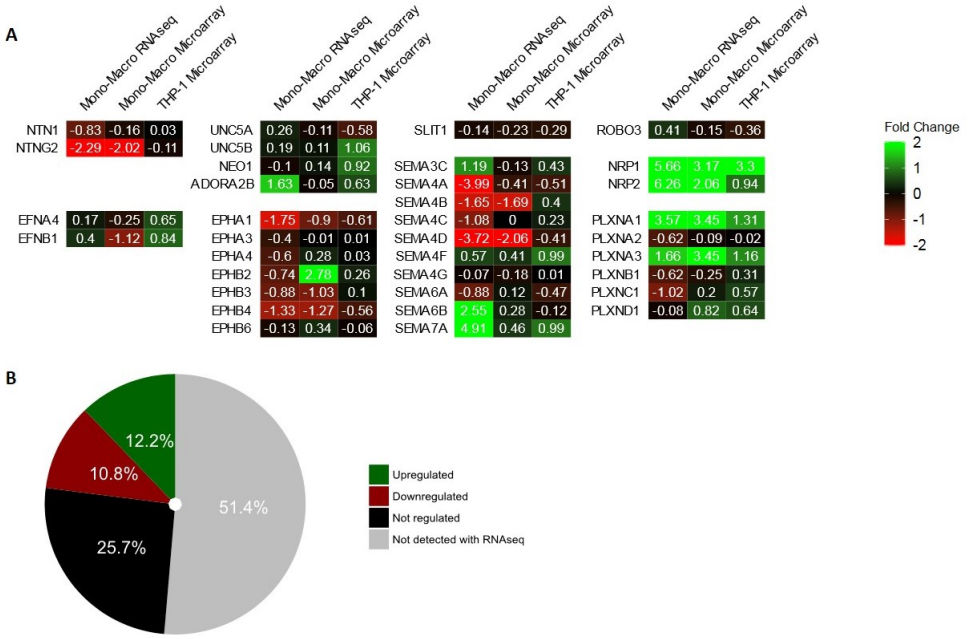

Figure 2. Change of NGC expression during monocyte to macrophage differentiation
(A) Heatmap of fold change of NGC expression in log2 scale (GREEN: upregulation; RED: downregulation). (Mono-macro RNAseq n=1; mono-macro microarray n=12; THP-1 microarray n=3) (B) Summary of NGC expression regulation during monocyte/macrophage differentiation.

5.3.4 Quaking contributes to the regulation of NGCs

Next we investigated the role of the RNA-binding protein QKI in the regulation of NGC expression. Similar to NGCs, QKI was originally identified for its function in the central and peripheral nervous system, while further studies revealed that QKI was ubiquitously expressed [8]. In addition, QKI is known as one of the key master regulators controlling gene expression change during monocyte-to-macrophage differentiation [6]. QKI is upregulated

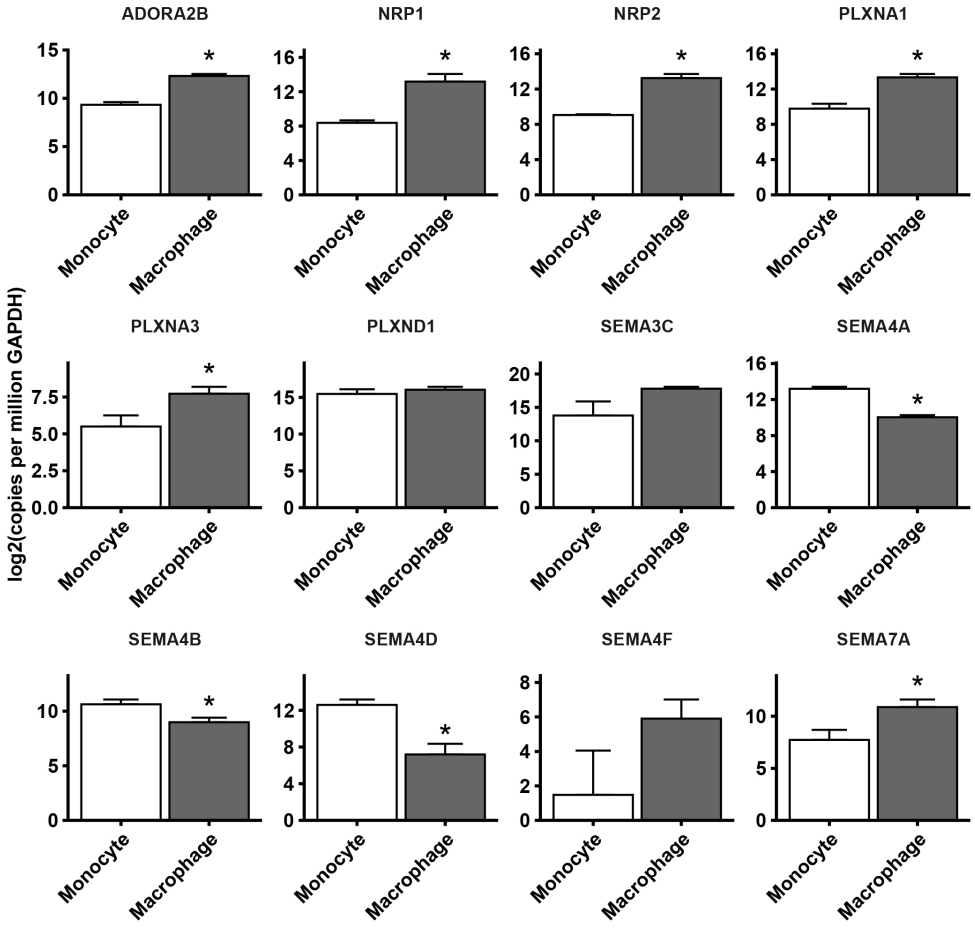

Figure 3. Confirmation of regulation of NGC expression

Quantitative PCR analysis of NGCs mRNA isolated from human monocytes or macrophages. Gene expression is expressed as copies per GAPDH in a log2 scale. Data Mean ± SEM; n=3; * $p < 0.05$).

in pro-inflammatory macro-phages, modulating the expression of various genes that have important functions in macrophage biology. To gain insight into whether QKI is implicated in regulating NGC expression in monocyte-to-macrophage differentiation, we exploited material from a patient with a haplo-deficiency of QKI (patient) and her unaffected sibling. The haplo-deficiency is caused by chromosomal translocation that occurred in the intron of the QKI gene. The transcription of a complete QKI gene is disrupted leading to reduced QKI expression. Transcriptome profiling was done using RNAseq method in both freshly isolated peripheral blood monocytes and monocyte-derived macrophages (**Figure 4A, Supplementary table 1 Dataset 3**). Due to the limitation of numbers of samples by nature, we could only examine change of NGC expression by putting an arbitrary threshold (±log¬20.4¬). Fold changes of NGC expression comparing the patient and her sibling showed SEMA7A to be consistently regulated in monocytes and monocyte-derived macrophages (**Figure 4B**). Expression of SEMA7A was decreased in both patient monocytes and macrophages compared to monocytes and macrophages from her sibling. To extend results obtained with the QKI haploinsufficient patient, we reduced QKI expression in primary human monocytes harvested from healthy controls using GapmeR antisense oligonucleotides that either targeted QKI for degradation or are scrambled as a control [6]. The GapmeR antisense oligonucleotides were present during the differentiation of the primary monocytes to macrophages. Although the GapmeR-mediated reduction in QKI expression varied a lot per donor, it nonetheless enabled us to validate a positive correlation between QKI and SEMA7A expression (**Figure 4C**).

5.3.5 QKI binds to cluster of miRNA target sites in SEMA7A 3'UTR

One of the well-defined mechanisms by which QKI affects gene expression is to stabilize gene transcripts by binding to quaking response element (QRE) motifs on their 3' UTRs [7, 8]. A QRE consists of a core sequence "ACUAA" and a half site "UAAY" [7]. We therefore explored the fold change of NGC expression between the patient and her sibling in relation to the number of "ACUAA" core sequences in 3'UTRs of NGCs (**Figure 5A, B**). Surprisingly, the analysis revealed no clear correlations between the fold change of the NGCs and QRE counts, so that existence of QRE sequence alone did not explain the effect of QKI to enhance expression of SEMA7A. We then explored the possibility whether binding of QKI to 3' UTRs of mRNAs might mask the sites for microRNA (miRNA) interactions by scanning proximal pairs of miRNA targeting sites and QRE motifs in 3'UTRs of NGC genes.

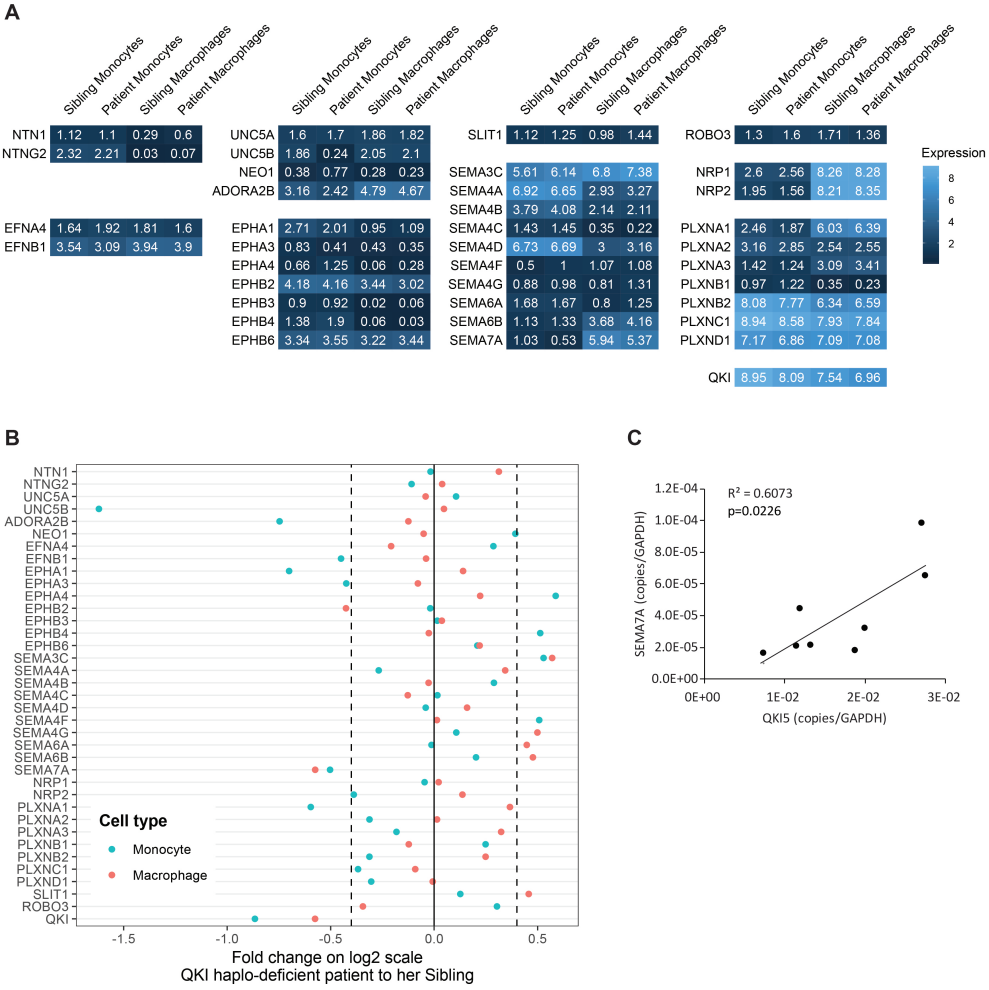

Figure 4. Regulation of NGC expression by QKI

(A) Heatmap of expression of NGCs in monocytes and macrophages determined by RNAseq from QKI patient and sibling in log2 scale (Lighter blue indicates higher expression; n=1). (B) Fold change of NGC expression comparing QKI patient's monocyte and macrophage to her sibling's. (C) In macrophages treated with GapmeR antisense oligonucleotides, there is a significant positive correlation between QKI and SEMA7A expression, measures by quantitative PCR analysis. Gene expression is expressed as copies per GAPDH.

The scanning results revealed that only in the 3'UTR of the SEMA7A gene such proximity between QREs and miRNA targeting sites was present (**Figure 6**). The QRE at the very end of SEMA7A's 3'UTR overlaps with QKI-DNA interactions sites from both duplicates from eCLIP-seq, increasing the confidence that this QRE is actively used. In proximity of the QRE, a targeting site of a cluster of miRNAs exists. It is therefore probable that QKI and miRNAs antagonistically regulate expression of SEMA7A in a proposed broader concept of RBP-miRNA interaction. Moreover, the QRE was experimentally verified with CLIP-seq methods in the K562 myeloid cell line (**Figure 6, Supplementary table 1 Dataset 5**). This observation further supported our theory that QKI enhances SEMA7A transcript stability by competing with the binding of miRNAs in the 3'UTR of SEMA7A. We next sought to determine whether QKI can directly bind to 3'UTR of SEMA7A using RNA-immunoprecipitation experiment. For this we used Hek293T cells in which we overexpressed both QKI and a construct containing the 3'UTR of SEMA7A. QKI is known to bind RNA of QKI itself, which we also observed (**Figure 7A**). When analyzing the SEMA7A 3' UTR indeed, RNA of SEMA7A 3'UTR was highly enriched in the QKI-antibody precipitated RNA fraction (**Figure 7B**), indicating binding of QKI to the 3' UTR of SEMA7A.

5.3.6 SEMA7A induced monocyte differentiation to pro-inflammatory macrophage

Before further exploring the functional important of SEMA7A for macrophages, we validated the increase of SEMA7A upon monocyte into macrophage differentiation seen at mRNA level at protein level (**Figure 8A-B**). To gain insight into the function of SEMA7A in monocyte differentiation into macrophage we silenced SEMA7A expression in monocytes using lentiviral shRNA vectors targeting the SEMA7A mRNA and non-SEMA7A targeting control shRNA. These monocytes were differentiated into macrophages. Targeted reduction of SEMA7A in monocytes did not seems to affect the capacity of the monocytes to differentiate into macrophages, but did show more elongated anti-inflammatory macrophage morphology (**Figure 8C**). To confirm the hypothesis that loss of SEMA7A induced a more anti-inflammatory phenotype, we investigated expression levels of TNFα (pro-inflammatory macrophage cytokine) and IL-10 (anti-inflammatory macrophage cytokine). Indeed, SEMA7A knockdown macrophages showed a ratio that was more anti-inflammatory compared to control macrophages (**Figure 8D**).

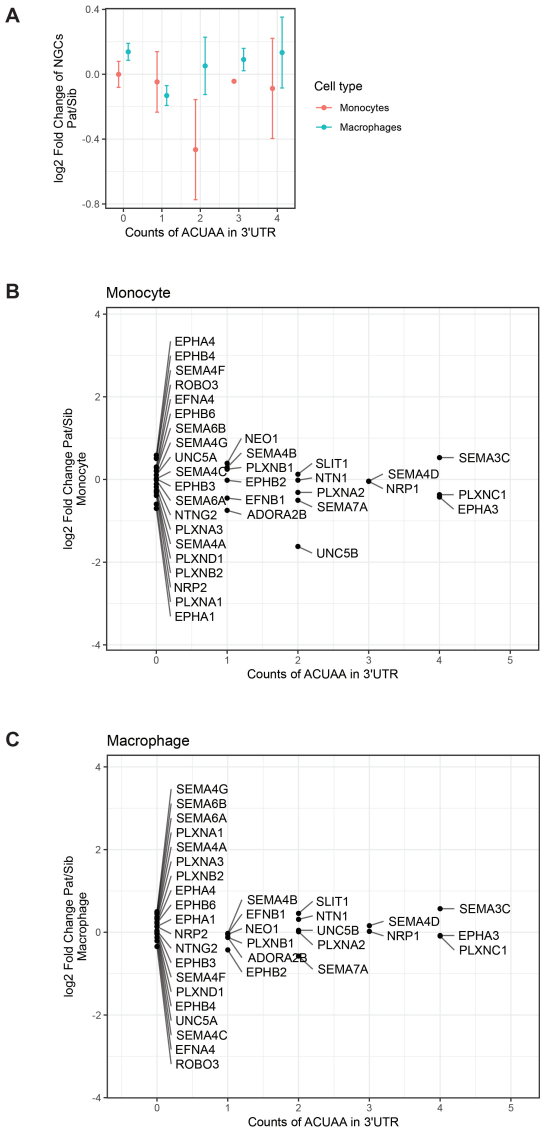

Figure 5. QKI response elements in NGC transcripts

(A-C) Scatter plots of QRE motif counts in the 3'UTRs of NGCs against log2 fold change of NGC expression in monocytes and macrophages. In A monocytes and macrophages combined. In B and C monocyte shown separately with individual NGCs. Existence of quaking response element (QRE/ACUAA motif) did not correspond with the fold change of NGC expression in the QKI haplo-deficient patients.

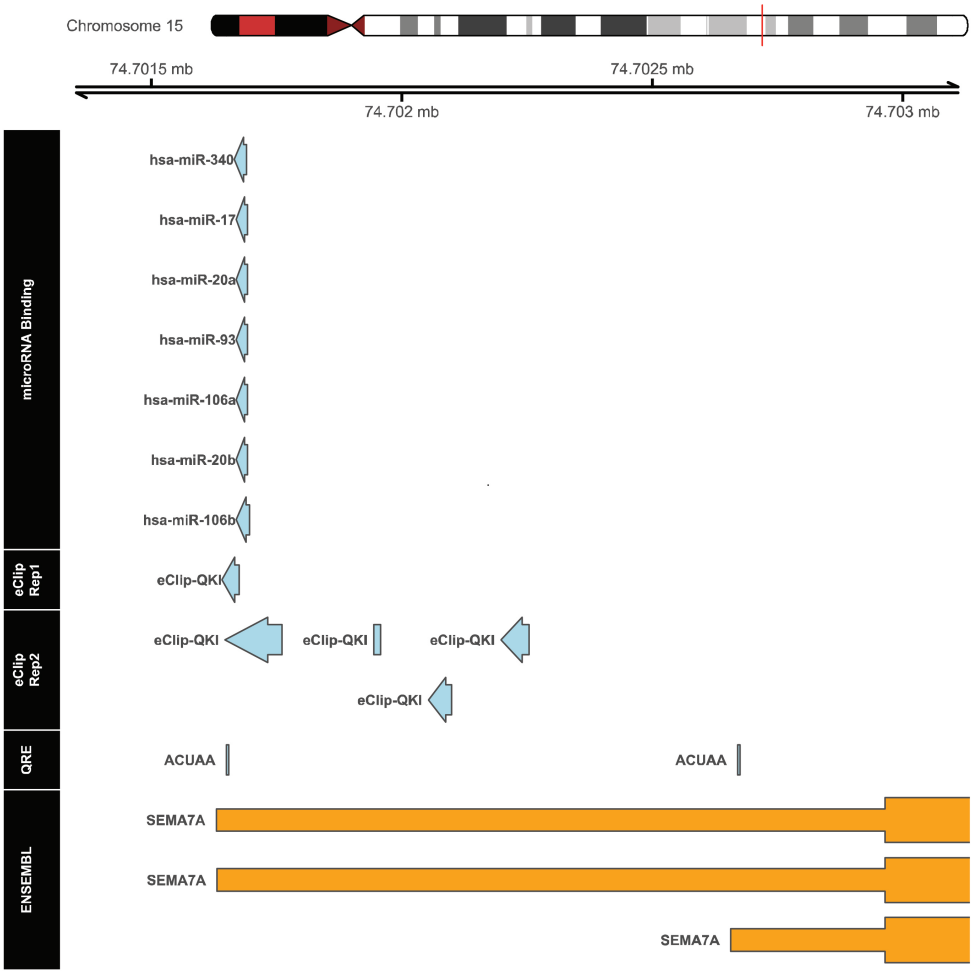

Figure 6. Visualization of genomic annotations in 3'UTR region of SEMA7A gene
The region in 3'UTR region of SEMA7A in the human genome (hg19 Chromosome 15 q24.1, bp 74,701,500 – 74,703,000) is annotated with aspects of miRNA binding sites, QKI targeting sites (experimental evidence based), QKI response element (QRE, in silico alignment of "ACUAA motif") and SEMA7A exon. The microRNA binding information was extracted from "miRbase" and was filtered by expression in monocytes/macrophages and miRNA interaction score. Interactions between RNA binding proteins (RBPs) to genomic DNA were obtained from technique duplicates of eCLIP-seq in the myelogenous K562 cells.

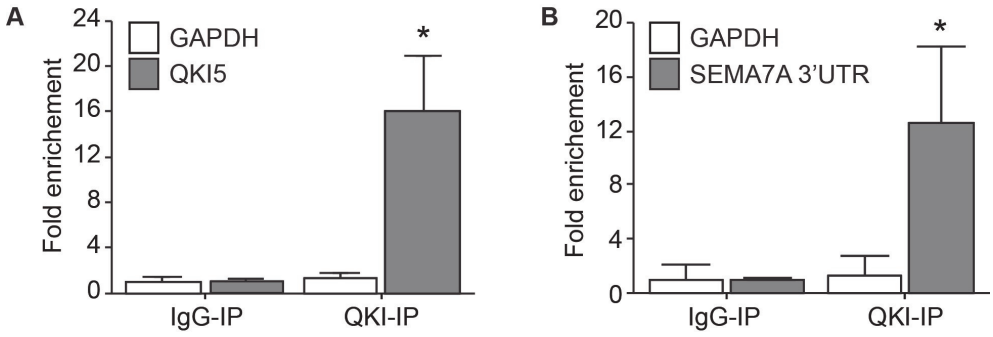

Figure 7. RNA-immunoprecipitation showing quaking protein binding to the 3'UTR of SEMA7A

(A) RNA-immunoprecipitation in Hek293T cells overexpression QKI5 using an IgG control or QKI5 antibody. QKI5 and GAPDH mRNA abundance in immune-precipitated fraction was determined by qPCR. Results are presented relative to IgG immunoprecipitation. Data Mean ± SEM; n = 5; * $p < 0.05$. (B) RNA-immunoprecipitation in Hek293T cells overexpression QKI5 and 3'UTR of SEMA7A using an IgG control or QKI5 antibody. SEMA7A 3'UTR and GAPDH mRNA abundance in immune-precipitated fraction was determined by qPCR. Results are presented relative to IgG immunoprecipitation. Data Mean ± SEM; n=3; * $p < 0.05$.

5.4 Discussion

In this study, we identified the axon guidance pathway as a novel pathway regulated in the monocyte-macrophage differentiation process. We illustrated the regulation of NGCs and annotated the shift in functionality contributed by the regulation of axon guidance pathway based on the currently available knowledge from the literature. We also investigated the involvement of QKI in regulation of SEMA7A in a miRNA dependent manner. The different platforms analyzed to detect NGC gene expression in human monocytes and macrophage showed numerous NGCs expressed. NTN1 was low, but significant expressed, it was detectable with the RNAseq method and had a signal above background in the microarray. The relevance of NTN1 secreted from macrophages has been shown to inhibit their emigration in autocrine or paracrine manner [5]. NGCs like EPHA4 and UNC5B were detected with RNAseq but had low expression in microarray. This could be due to the intrinsic character of RNAseq that it has a larger dynamic range. We found many members of the semaphorin family expressed by monocytes and macrophages, both ligands and receptors. For example SEMA4D (CD100), an immune semaphorin, was identified with both

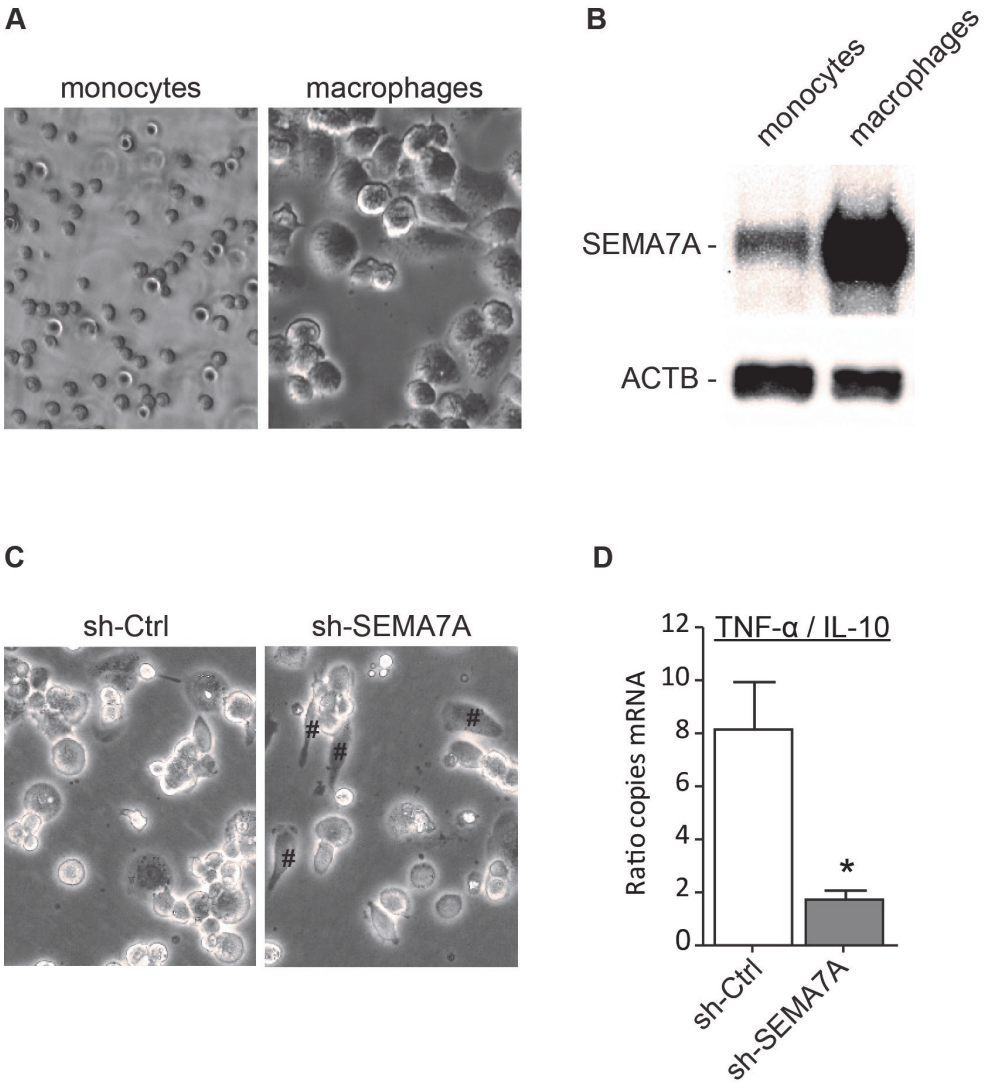

Figure 8. Role for SEMA7A in monocyte differentiation into pro-inflammatory macrophages

(A) Bright field microscope images from THP1 monocytes and macrophages. (B) Representative immunoblot analysis of SEMA7A or ACTB (loading control) in protein lysates THP1 monocytes and macrophages. (C) Bright field microscope images from THP1 macrophages transduced with anti-SEMA7A shRNA (sh-SEMA7A) or scrambled shRNA (sh-Ctrl). Elongated phenotype indicated by #. (D) Ratio of TNF-α and IL-10 mRNA expression of sh-SEMA7A or sh-Ctrl THP1 macrophages. Data Mean ± SEM; n=4; * $p < 0.05$.

methods and has been shown to mediate monocyte adhesion and differentiation [28, 33]. Expression of the SEMA7A-PLXNC1 ligand-receptor pair, which was recently shown to be involved in atherogenesis [34], was also detected. During the differentiation of both human primary monocytes to macrophages and THP-1 cells to THP-1 macrophages, upregulation of receptors for Class III semaphorins, namely NRP1, NRP2, PLXNA1 and PLXNA3, was observed. Previous studies have shown that activation of the SEMA3-PLXNA-NRP axis is reduced in monocyte-endothelium interactions, although SEMA3A-NRP1 binding could sustain directed migration of macrophages under hypoxic condition in tumor tissues [4, 30]. Upregulation of these receptors could sensitize the response of macrophages to the guidance signals provided by Class III semaphorins. In addition, we observed downregulation of membrane bound Class IV semaphorins, namely SEMA4A, SEMA4B and SEMA4D in macrophages compared to monocytes. SEMA4D is known to promote differentiation of alternatively activated macrophages, while anti-SEMA4D treatment increases the population of classically activated macrophages in mammary carcinoma tissue and induces the production of inflammatory cytokines [27, 28]. This is in line with our finding of SEMA4D downregulation in macrophages, considering GM-CSF stimulation is a model of monocyte-to-classical-macrophage differentiation. In contrast to SEMA4D, SEMA7A expression was increased in monocyte to macrophage differentiation. Our studies indicate that SEMA7A itself serves as a stimulator for monocytes to differentiated into a pro-inflammatory macrophage. These observation are in line with the findings of Holmes et al, that SEMA7A results in an increased production of inflammatory cytokines and GM-CSF, which could be a potential positive feedback mechanism for monocyte activation and differentiation [3]. Indeed, neutralization of SEMA7A using an antibody reduced the number of pro-inflammatory macrophages in a murine viral myocarditis model [35]. QKI was shown to be a critical regulator of monocyte to macrophage differentiation [6]. During the differentiation, expression of QKI increases, triggering a range of effects, including transcript stabilization and alternative splicing. We investigated whether regulation of some NGCs could be mediated by QKI by comparing the NGC expression in monocytes and macrophages of the QKI haplodeficient patient and her sibling. As described previously, SEMA7A was upregulated in monocyte-to-macrophage differentiation. The comparison of the patient and her sibling revealed that SEMA7A was decreased in both monocytes and macrophages. QRE motifs were found in 3'UTR of the SEMA7A transcript, which are necessary for the transcript stabilization effect of QKI. However, counts of QRE motifs alone could not explain the regulation of SEMA7A expression

by QKI activity, indicating that extra factors are involved in the regulation of SEMA7A by QKI. It has been proposed that QKI could stabilize transcripts of miRNAs thereby regulating gene expression [36]. However, such mechanism is unlikely to be applicable in our case, since SEMA7A would have been upregulated in patients if any miRNA targeting SEMA7A was stabilized by QKI. Therefore, we explored the QRE motif region and found a cluster of miRNA target sites in proximity of QRE. This observation pointed to the possibility that the competitive binding of QKI to miRNA targeting sites is the underlying mechanism for regulation of SEMA7A by QKI. Such a concept has been reported for other RBPs before [37, 38], but not yet for QKI. We now show that QKI binds to the 3'UTR of SEMA7A. Further studies are needed to confirm the competitive access of QKI and miRNA to 3'UTR of SEMA7A to be responsible for the observed changes in SEMA7A expression. In summary, during monocyte-to-macrophage differentiation, axonal guidance pathway was significantly regulated with changes in expression of several NGC ligands and receptors. Regulation of NGCs in monocyte-to-macrophage differentiation fits the functional adaption that is necessary for the specialized role of macrophages. So far, a role for SEMA7A in regulating macrophage polarization into an pro-inflammatory macrophage. In the future, the changes in gene expression can be further studied in the context of diseases where monocyte-macrophage biology plays a role.

Acknowledgements

The research in this paper was supported by a grant from the Netherlands Heart Foundation (2013T127 to J.M.v.G.) and from European Research Area Network on Cardiovascular Diseases (grant number 038 MISsCVD to J.M.v.G.).

Conflict of interest

The authors declare no conflicts of interest.

References

1. *Italiani, P. and D. Boraschi, From Monocytes to M1/M2 Macrophages: Phenotypical vs. Functional Differentiation. Frontiers in immunology, 2014. 5: p. 514-514.*

2. *Shapouri-Moghaddam, A., S. Mohammadian, H. Vazini, et al., Macrophage plasticity, polarization, and function in health and disease. J Cell Physiol, 2018. 233(9): p. 6425-6440.*

3. *Holmes, S., A.M. Downs, A. Fosberry, et al., Sema7A is a potent monocyte stimulator. Scand J Immunol, 2002. 56(3): p. 270-5.*

4. *van Gils, J.M., B. Ramkhelawon, L. Fernandes, et al., Endothelial expression of guidance cues in vessel wall homeostasis dysregulation under proatherosclerotic conditions. Arterioscler Thromb Vasc Biol, 2013. 33(5): p. 911-9.*

5. *van Gils, J.M., M.C. Derby, L.R. Fernandes, et al., The neuroimmune guidance cue netrin-1 promotes atherosclerosis by inhibiting the emigration of macrophages from plaques. Nat Immunol, 2012. 13(2): p. 136-43.*

6. *de Bruin, R.G., L. Shiue, J. Prins, et al., Quaking promotes monocyte differentiation into pro-atherogenic macrophages by controlling pre-mRNA splicing and gene expression. Nat Commun, 2016. 7: p. 10846.*

7. *Hafner, M., M. Landthaler, L. Burger, et al., Transcriptome-wide identification of RNA-binding protein and microRNA target sites by PAR-CLIP. Cell, 2010. 141(1): p. 129-41.*

8. *Chenard, C.A. and S. Richard, New implications for the QUAKING RNA binding protein in human disease. J Neurosci Res, 2008. 86(2): p. 233-42.*

9. *Schirmer, S.H., J.O. Fledderus, A.M. van der Laan, et al., Suppression of inflammatory signaling in monocytes from patients with coronary artery disease. J Mol Cell Cardiol, 2009. 46(2): p. 177-85.*

10. *Dang, T.M., W.C. Wong, S.M. Ong, et al., MicroRNA expression profiling of human blood monocyte subsets highlights functional differences. Immunology, 2015. 145(3): p. 404-16.*

11. *Davis, S. and P.S. Meltzer, GEOquery: a bridge between the Gene Expression Omnibus (GEO) and BioConductor. Bioinformatics, 2007. 23(14): p. 1846-7.*

12. *An integrated encyclopedia of DNA elements in the human genome. Nature, 2012. 489(7414): p. 57-74.*

13. *Kim, D., G. Pertea, C. Trapnell, et al., TopHat2: accurate alignment of transcriptomes in the presence of insertions, deletions and gene fusions. Genome Biol, 2013. 14(4): p. R36.*

14. *Kanehisa, M., Y. Sato, M. Kawashima, et al., KEGG as a reference resource for gene and protein annotation. Nucleic Acids Res, 2016. 44(D1): p. D457-62.*

15. *Luo, W., M.S. Friedman, K. Shedden, et al., GAGE: generally applicable gene set enrichment for pathway analysis. BMC Bioinformatics, 2009. 10: p. 161.*

16. *J., R., EnsDb.Hsapiens.v75: Ensembl based annotation package. R package version 2.99.0. 2017.*

17. *Lawrence, M., W. Huber, H. Pages, et al., Software for computing and annotating genomic ranges. PLoS Comput Biol, 2013. 9(8): p. e1003118.*

18. *J., R., ensembldb: Utilities to create and use Ensembl-based annotation databases. R package version 2.4.1. 2018.*

19. *Zhang, H., D. Vreeken, C.S. Bruikman, et al., Understanding netrins and semaphorins in mature endothelial cell biology. Pharmacol Res, 2018. 137: p. 1-10.*

20. *Kozomara, A., M. Birgaoanu, and S. Griffiths-Jones, miRBase: from microRNA sequences to function. Nucleic Acids Res, 2019. 47(D1): p. D155-D162.*

21. *Hahne, F. and R. Ivanek, Visualizing Genomic Data Using Gviz and Bioconductor. Methods Mol Biol, 2016. 1418: p. 335-51.*

22. *Sciaraffia, E., A. Riccomi, R. Lindstedt, et al., Human monocytes respond to extracellular cAMP through A2A and A2B adenosine receptors. J Leukoc Biol, 2014. 96(1): p. 113-22.*

23. *Jellinghaus, S., D.M. Poitz, G. Ende, et al., Ephrin-A1/EphA4-mediated adhesion of monocytes to endothelial cells. Biochim Biophys Acta, 2013. 1833(10): p. 2201-11.*

24. *Zhang, C., J. Song, Y. Xu, et al., [Ephrin B2 is involved in Porphyromonas gingivalis infection-enhanced adhesion of THP-1 to human umbilical vein endothelial cells]. Zhonghua Kou Qiang Yi Xue Za Zhi, 2014. 49(10): p. 614-8.*

25. *Curreli, S., B.S. Wong, O. Latinovic, et al., Class 3 semaphorins induce F-actin reorganization in human dendritic cells: Role in cell migration. J Leukoc Biol, 2016. 100(6): p. 1323-1334.*

26. *Meda, C., F. Molla, M. De Pizzol, et al., Semaphorin 4A exerts a proangiogenic effect by enhancing vascular endothelial growth factor-A expression in macrophages. J Immunol, 2012. 188(8): p. 4081-92.*

27. *Evans, E.E., A.S. Jonason, Jr., H. Bussler, et al., Antibody Blockade of Semaphorin 4D Promotes Immune Infiltration into Tumor and Enhances Response to Other Immunomodulatory Therapies. Cancer Immunol Res, 2015. 3(6): p. 689-701.*

28. *Chen, Y., L. Zhang, R. Lv, et al., Overexpression of Semaphorin4D indicates poor prognosis and prompts monocyte differentiation toward M2 macrophages in epithelial ovarian cancer. Asian Pac J Cancer Prev, 2013. 14(10): p. 5883-90.*

29. *Wolf, Y., S. Boura-Halfon, N. Cortese, et al., Brown-adipose-tissue macrophages control tissue innervation and homeostatic energy expenditure. Nat Immunol, 2017. 18(6): p. 665-674.*

30. *Casazza, A., D. Laoui, M. Wenes, et al., Impeding macrophage entry into hypoxic tumor areas by Sema3A/Nrp1 signaling blockade inhibits angiogenesis and restores antitumor immunity. Cancer Cell, 2013. 24(6): p. 695-709.*

31. *Roy, S., A.K. Bag, R.K. Singh, et al., Multifaceted Role of Neuropilins in the Immune System: Potential Targets for Immunotherapy. Front Immunol, 2017. 8: p. 1228.*

32. *Shimizu, I., Y. Yoshida, J. Moriya, et al., Semaphorin3E-induced inflammation contributes to insulin resistance in dietary obesity. Cell Metab, 2013. 18(4): p. 491-504.*

33. *Chabbert-de Ponnat, I., A. Marie-Cardine, R.J. Pasterkamp, et al., Soluble CD100 functions on human monocytes and immature dendritic cells require plexin C1 and plexin B1, respectively. Int Immunol, 2005. 17(4): p. 439-47.*

34. *Hu, S., Y. Liu, T. You, et al., Vascular Semaphorin 7A Upregulation by Disturbed Flow Promotes Atherosclerosis Through Endothelial beta1 Integrin. Arterioscler Thromb Vasc Biol, 2018. 38(2): p. 335-343.*

35. *Wu, X., Y. Meng, C. Wang, et al., Semaphorin7A aggravates coxsackievirusB3-induced viral myocarditis by increasing alpha1beta1-integrin macrophages and subsequent enhanced inflammatory response. J Mol Cell Cardiol, 2018. 114: p. 48-57.*

36. *Lange, J., Y. Yafai, A. Noack, et al., The axon guidance molecule Netrin-4 is expressed by Muller cells and contributes to angiogenesis in the retina. Glia, 2012. 60(10): p. 1567-78.*

37. *Gardiner, A.S., J.L. Twiss, and N.I. Perrone-Bizzozero, Competing Interactions of RNA-Binding Proteins, MicroRNAs, and Their Targets Control Neuronal Development and Function. Biomolecules, 2015. 5(4): p. 2903-18.*

38. *Zhao, X., D. Chen, Y. Cai, et al., RBPvsMIR: A Computational Pipeline to Identify Competing miRNAs and RNA-Binding Protein Pairs Regulating the Shared Transcripts. Genes (Basel), 2018. 9(9).*

No.	Material	Description	Type
1	Human monocyte	Patients with atherosclerosis and healthy controls	online
2	THP-1 cell line	THP-1 cells and THP-1 macrophage	in house
3	Human monocyte	QKI haploinsufficiency patient and her sibling	in house
4	Human monocyte	Healthy controls	online
5	K562 cell line	Isogenic duplicates of QKI eCLIP-seq in K562 cells	online

No.	Accession	Differentiation Method	Profiling Method
1	GSE9820	20h Plastic Culture	Microarray (mRNA)
2	GSE74887	PMA (100 nM) for 8 days	Microarray (mRNA)
3	GSE74978	GM-CSF (5 ng/ml) for 7 days	RNAseq (mRNA)
4	GSE52986	NA	Microarray (miRNA)
5	ENCSR366YOG	NA	eCLIP-seq

Supplementary table 1. Summary of the data accessions used in relation to the experimental materials and the profiling methods.

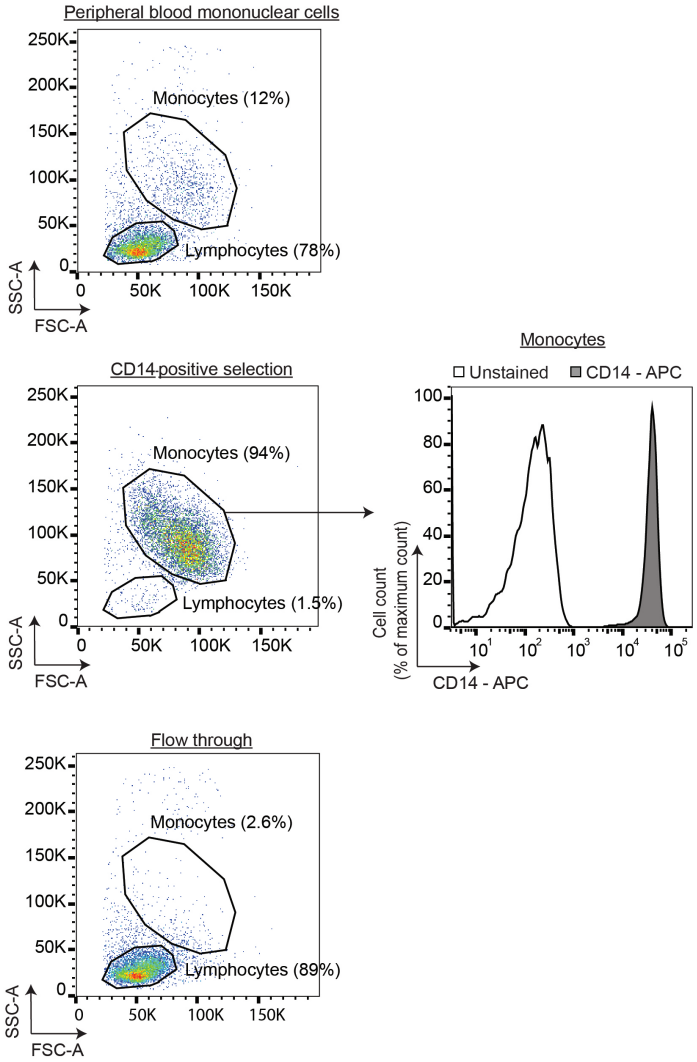

Supplementary Figure 1

Assessing purity of monocyte isolation. A sample of peripheral blood mononuclear cells (top), of which the CD14-positive selected cells (middle) where isolated and the non-selected cells (bottom) were incubated with anti-human CD14 (APC, 1:200, Clone Mφ P9, cat no. 345787, BD), measured by flow cytometry LSR-II (BD Biosciences, Vianen, The Netherlands), and analyzed using FlowJo Software version 10 (Tree Star, Ashland, OR, USA).

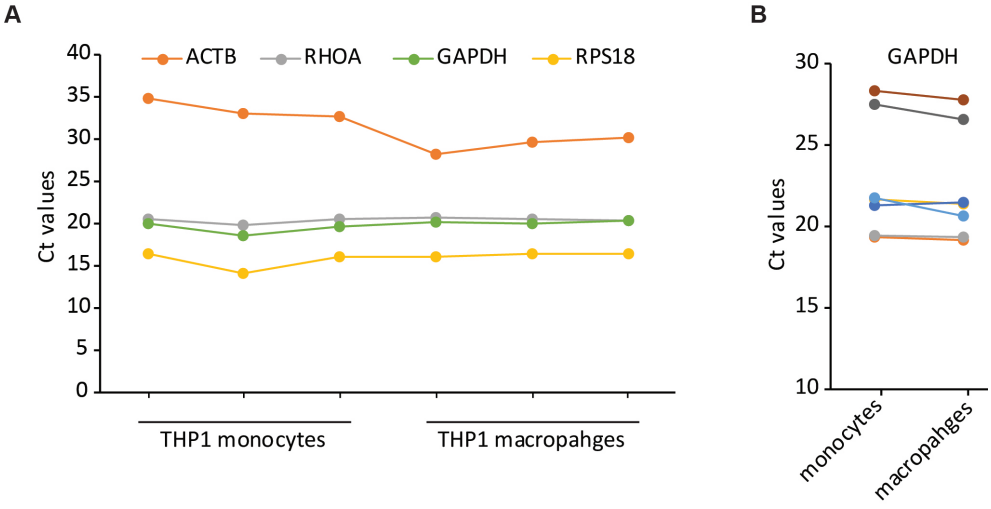

Supplementary Figure 2

Assessing multiple housekeeping genes. Quantitative PCR analysis of different housekeeping mRNA isolated from THP1-monocytes or -macrophages (A) or primary monocytes or macrophages (B). Gene expression is expressed Ct values. (A) each color is different housekeeping gene measured in 3 independent THP1 monocytes and 3 independent THP1 macrophages samples. (B) each color represents a different donor of primary monocytes or macrophages, n=7.

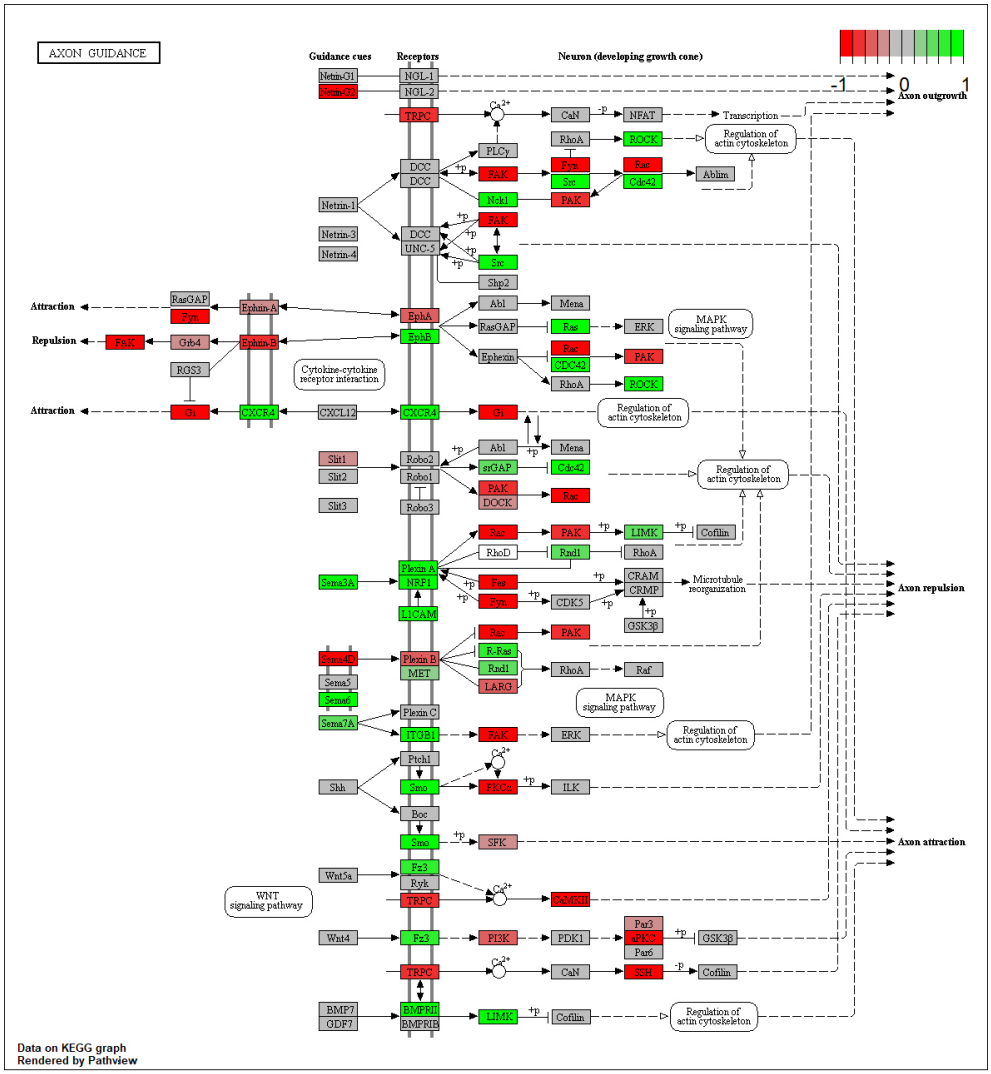

Supplementary Figure 3

Visualization of the axon guidance pathway and the gene expression changes during human monocyte-to-macrophage differentiation. The gene expression in monocytes and macrophages was obtained from GEO database (Accession: GSE9820, Supplementary table 1 Dataset 1). Data from 12 individuals were pooled for each cell type.

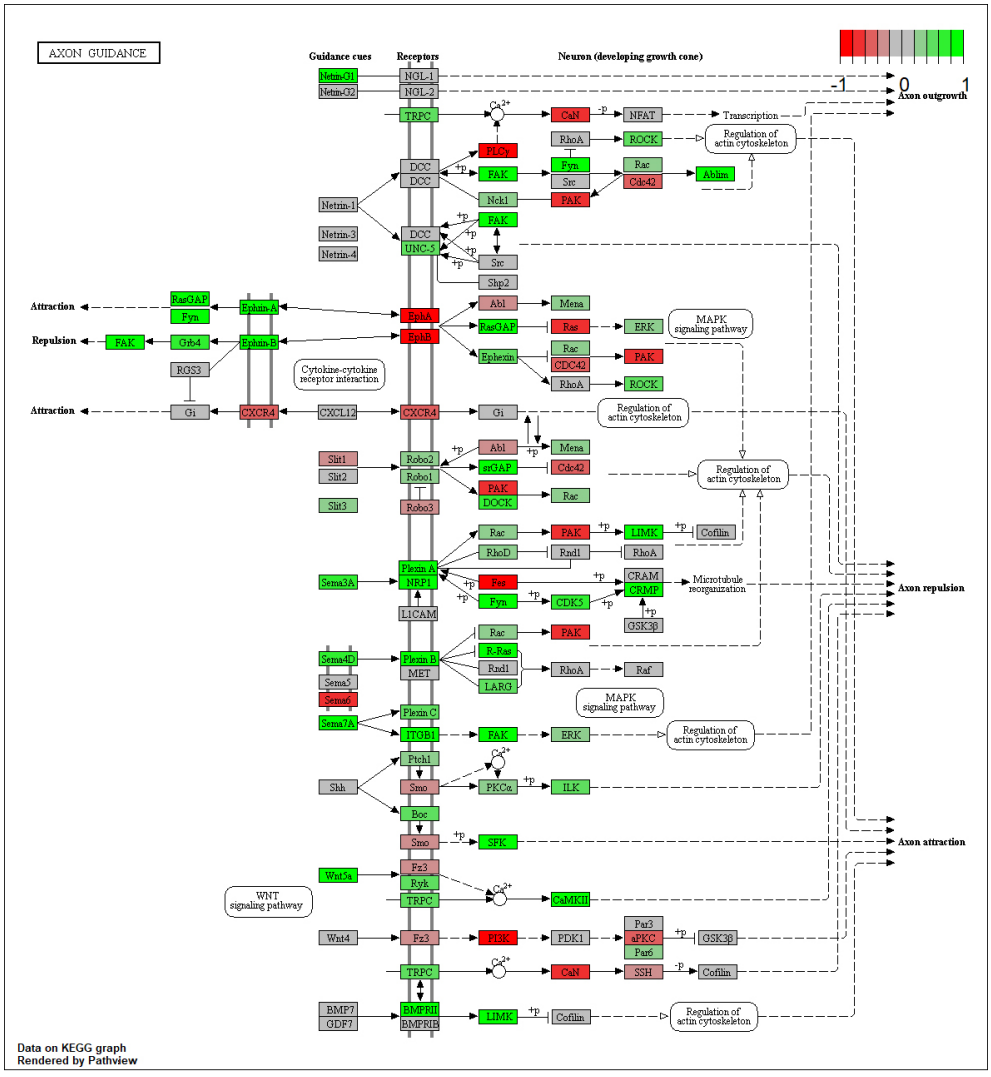

Supplementary Figure 4

Visualization of the axon guidance pathway and the gene expression change during THP-1 cell to THP-1 macrophage differentiation. The changes in gene expression in THP-1 cells to THP-1 macrophages were profiled in on the "Affymetrix GeneChip Human HJAY Array" (Accession: GSE74887, Supplementary table 1 Dataset 2). Data from 3 technical replicates were pooled for each cell type.

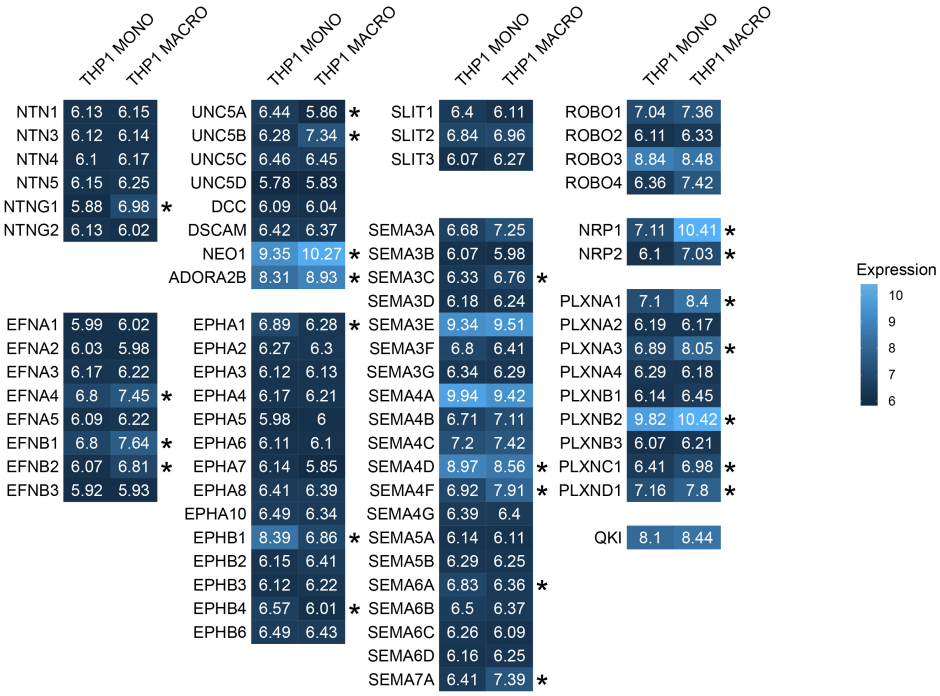

Supplementary Figure 5

Expression of NGCs in human monocyte/macrophage cell line. Heatmap of expression of NGCs in THP1 cells/THP1 macrophages in a log2 scale. Light blue: higher expression; dark blue: lower expression; n=3; * $p < 0.05$.

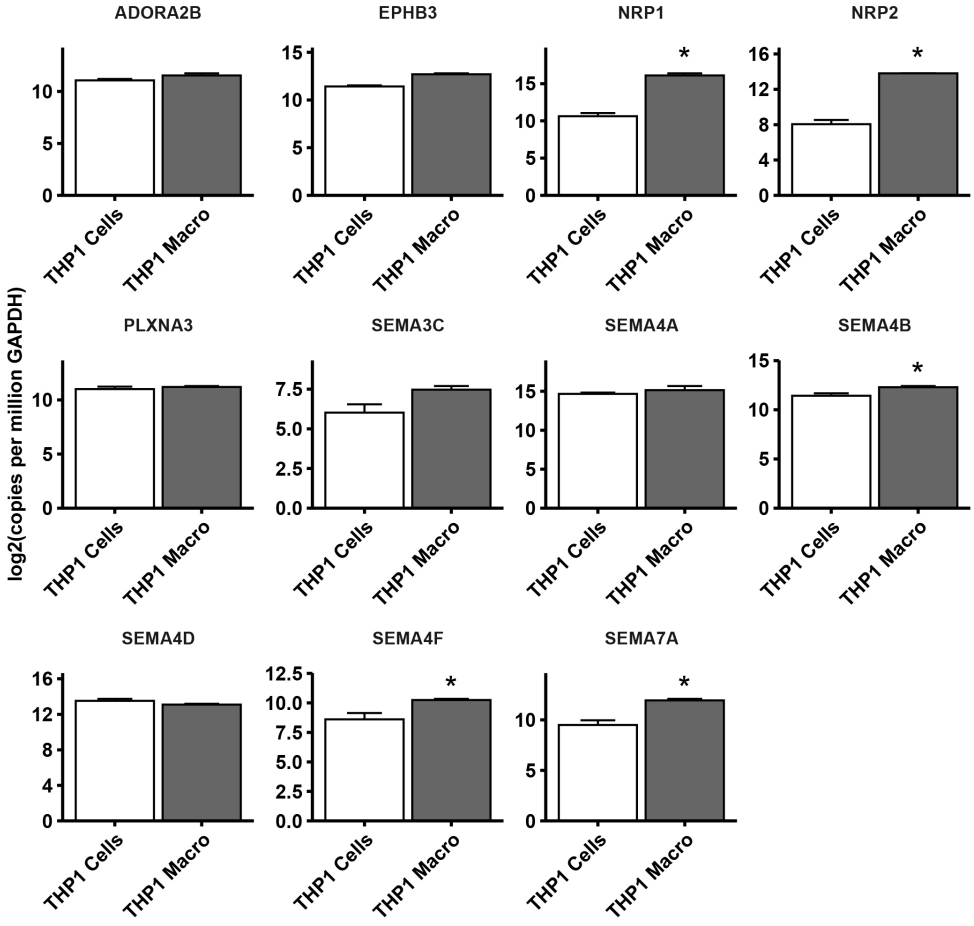

Supplementary Figure 6

Confirmation of regulation of NGC expression. Quantitative PCR analysis of NGCs mRNA isolated from THP1-monocytes or -macrophages. Gene expression is expressed as copies per GAPDH in a log2 scale. Graphs show the mean ± S.E.M. n=3 * $p < 0.05$.

Chapter 6

Prediction power on cardiovascular disease of neuroimmune guidance cues expression by peripheral blood monocytes determined by machine learning methods

Zhang, H., Bredewold, E. O. W., Vreeken, D., Duijs, J., de Boer, H. C., Kraaijeveld,A. O., Jukema, J. W., Pijls, N. H., Waltenberger, J., Biessen, E. A. L., van der Veer,E. P., van Zonneveld, A. J. and van Gils, J. M.

International Journal of Molecular Science, 2020;21.

Abstract

Atherosclerosis is the underlying pathology in a major part of cardiovascular disease, the leading cause of mortality in developed countries. The infiltration of monocytes into the vessel walls of large arteries is a key denominator of atherogenesis, making monocytes accountable for the development of atherosclerosis. With the development of high-throughput transcriptome profiling platforms and cytometric methods for circulating cells, it is now feasible to study in-depth the predicted functional change of circulating monocytes reflected by changes of gene expression in certain pathways and correlate the changes to disease outcome. Neuroimmune guidance cues comprise a group of circulating- and cell membrane-associated signaling proteins that are progressively involved in monocyte functions. Here, we employed the CIRCULATING CELLS study cohort to classify cardiovascular disease patients and healthy individuals in relation to their expression of neuroimmune guidance cues in circulating monocytes. To cope with the complexity of human datasets featured by noisy data, nonlinearity and multidimensionality, we assessed various machine-learning methods. Of these, the linear discriminant analysis, Naïve Bayesian model and stochastic gradient boost model yielded perfect or near-perfect sensibility and specificity and revealed that expression levels of the neuroimmune guidance cues SEMA6B, SEMA6D and EPHA2 in circulating monocytes were of predictive values for cardiovascular disease outcome.

Keywords

cardiovascular diseases; monocytes; machine-learning methods; neuroimmune guidance cues

6.1 Introduction

Cardiovascular diseases (CVD) remain a leading cause of death in the more economically developed countries, despite improvements in surgical and drug treatments. Much of the CVD-related mortality and morbidity is attributable to atherosclerosis [1]. Atherosclerosis is a systemic chronic inflammatory and immune disease [2,3]. Monocytes and their derived macrophages play a key role in the development of atherosclerosis. Under conditions of dyslipidemia and chronic systemic inflammation, circulating monocytes and the endothelium become activated, resulting in monocyte infiltration and differentiation into macrophages in the vessel wall. Upon the excessive uptake of lipids, these macrophages become foam cells and participate decisively in the development and exacerbation of atherosclerosis, coronary stenosis and its clinical sequela, such as acute myocardial infarctions [3-7]. Neuroimmune guidance cues (NGCs) comprise the netrin, semaphorin, ephrin and slit families of proteins of ligands and receptors, which were originally characterized to direct cell and axon migration during neural development. In the last two decades, it has become increasingly clear that these proteins can also play a major role in (pathological) immune responses by directly regulating leukocyte trafficking and directly impacting the pathogenesis of atherosclerosis [8-10]. Indeed, numerous studies using murine atherosclerosis models have found multifaceted roles of NGCs in the development of atherosclerosis [11-15]. In addition, several observations also support a role for NGCs in human CVD. For instance, three NGC genes are located on human chromosome 1, in the locus that has been identified as the premature myocardial infarction susceptibility locus [16]. In addition, the axonal guidance pathway is found enriched with genetic variants that have significant associations with CVD, and several novel genetic risk loci for CVD contain NGCs genes [17,18]. However, whether the monocytic expression of NGCs is informative for human CVD has not been described yet. Transcriptomics can reveal key alterations in biological processes causing human diseases, thereby present novel instruments that are not only useful for the understanding of the disease mechanisms but, also, for molecular diagnosis and clinical therapy [19]. Since monocytes are among the culprit cells of atherosclerosis development, monocytic expression levels of NGCs could provide insights into the underlying mechanisms in atherosclerosis development and can be used to improve the evidence-based treatment of CVD to reduce the global burden of this disease. The CIRCULATING CELLS study was designed to study the role of several cellular mediators of atherosclerosis as biomarkers of CVD to predict the suscep-

tibility of patients to the progression of CVD [20]. By applying different machine-learning methods (also known as predictive modeling methods) on the gene expression data of peripheral monocytes from the CIRCULATING CELLS study cohort, we investigated whether monocytic NGC expression is informative to distinguish between healthy individuals and CVD patients. As machine-learning methods are developed to explore complex relationships between predictors and outcomes, they are suitable tools to tackle the difficulties due to the complexity of human datasets featured by noisy data, nonlinearity and multidimensionality. Some machine-learning methods take simplistic approaches and work with linear relationships between features and outcomes, while other methods are more complex and are able to capture nonlinear patterns and to tolerate a low information-noise ratio, owing to the difference of their pre-assumptions and learning logics. We compared the performance of multiple modeling methods to explore the best predicting potential of our dataset. In our study, we included commonly used models like logistic regression and linear discriminant analysis, as well as more complex nonlinear models and tree-based models. Linear models, like partial least square, have supervised dimension reduction functionality, which benefits model performances in the case of high between-feature correlations. Nonlinear models, like Naïve Bayesian, make probabilistic calls based on the information provided by the features independently, possibly performing better in situations when between-feature correlations are low. In addition to modeling of the data itself, stochastic gradient boost also models the residuals, thereby increasing the learning ability when the information-noise ratio is low. We compared the results of the different modeling methods to gain insights on the nature of the dataset. Altogether, this allowed us to give a proof of concept that the expression of a small set of functional genes can be a prediction value for complex diseases like CVD.

6.2 Materials and Methods

6.2.1 Study Population

The study population consists of a subgroup of 369 patients from the CIRCULATING CELLS study cohort [20] (**Figure 1**). In brief, CIRCULATING CELLS was a prospective multicenter study in which patients scheduled for coronary angiography due to CVD were included. For this subgroup, extensive clinical characteristics were recorded (**Table 1**), and the transcriptomes of purified circulating CD14+ monocytes were profiled. To minimize the potential influence of the presence of profound acute myocardial ischemia on monocytic gene expression profiles, patients with ST-elevation myocardial infarction (STEMI) were excluded.

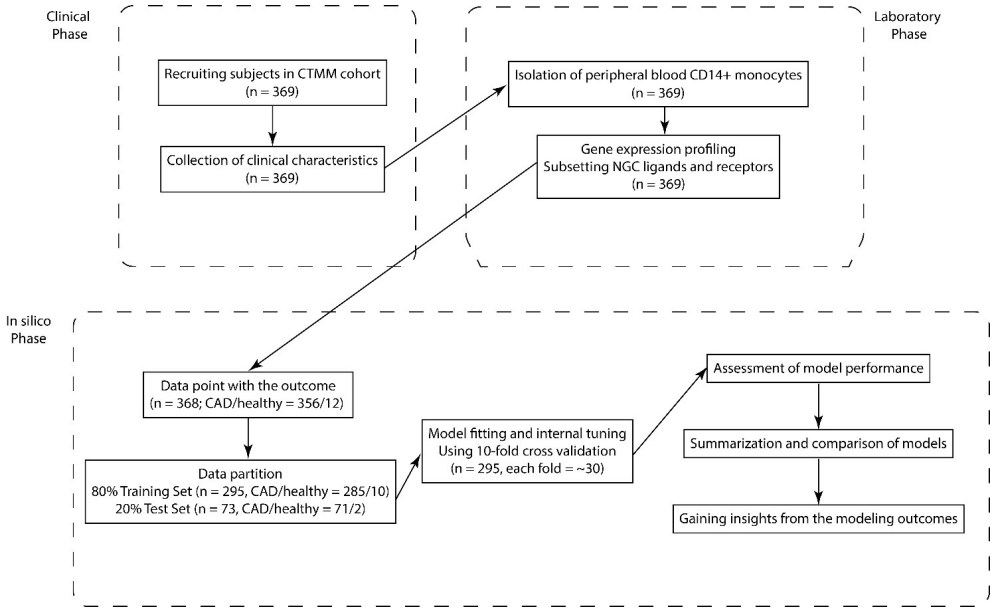

Figure 1. Flowchart of predictive modeling using neuroimmune guidance cues (NGCs) Subjects in the CIRCULATING CELLS cohort were recruited based on inclusion criteria. The clinical characteristics were collected, peripheral blooded CD14-positive monocytes were isolated, and their transcriptomes were profiled. The expression of neuronal guidance cues was subset. The individuals were randomly assigned to the Training Set or Test Set for external assessment of the model performance. Classification models that were built on the Training Set data and model performance were internally assessed with cross-validation. Finally, we made comparisons between the models and gained insights on the choice of model and features.

Clinical Characteristics	All	CVD	Healthy
Demographic data			
Number (male/female)	368 (273/95)	356 (264/92)	12 (9/3)
Age	61.8 (±10.4)	62.2 (±10.3)	49.2 (±6.3)
BMI	27.3 (±4.3)	27.4 (±4.3)	23.7 (±2.3)
Coronary risk factors			
Hypertension	231 (63%)	231 (0.65)	0 (0)
Hypercholesterolemia	70 (19%)	65 (0.18)	5 (0.42)
Diabetes	77 (21%)	77 (0.22)	0 (0)
Current smoker	73 (20%)	73 (0.21)	0 (0)
Family MI history	141 (39%)	137 (0.39)	4 (0.33)
Previous MI	112 (30%)	112 (0.31)	0 (0)
Positive family history	157 (43%)	152 (0.43)	5 (0.42)
Therapeutic decision			
PTCA	130 (35%)	130 (0.37)	0 (0)
CABG	32 (9%)	32 (0.09)	0 (0)
NYHA Classification			
NYHA Class I	248 (67%)	236 (0.66)	12 (1)
NYHA Class II	78 (21%)	78 (0.22)	0 (0)
NYHA Class III	26 (7%)	26 (0.07)	0 (0)
NYHA Class IV	16 (4%)	16 (0.04)	0 (0)
Current medication			
β-blocker	228 (69%)	228 (0.72)	0 (0)
Ca-antagonist	95 (29%)	95 (0.30)	0 (0)
Aspirin	260 (79%)	260 (0.82)	0 (0)
Vitamin K antagonist	29 (9%)	29 (0.09)	0 (0)
Low molecular weight heparin	10 (3%)	10 (0.03)	0 (0)
ADP receptor blocker	168 (51%)	168 (0.53)	0 (0)
ACE inhibitor	116 (35%)	116 (0.36)	0 (0)
ATII receptor blocker	71 (22%)	71 (0.22)	0 (0)
Diuretic	76 (23%)	76 (0.24)	0 (0)
Statins	252 (77%)	252 (0.79)	0 (0)

Table 1. Clinical characteristics of the CTMM patient cohort

Values are N ± SD or N (%). Abbreviations: BMI—body mass index, MI—myocardial infarction, PTCA—percutaneous transluminal coronary angioplasty, CABG—coronary artery bypass graft, NYHA—New York Heart Association, and CVD—cardiovascular disease.

Additional exclusion criteria were age ¡ 18 years, inability to give informed consent, suspected drug or alcohol abuse, serious concomitant disease, serious recent infectious disease in the last 6 weeks or suspected elevated state of the immune system and noncooperativeness. The study was approved by the medical ethical committees of the participating centers and conformed to the Declaration of Helsinki. All patients received oral and written information about the objectives of the study and provided written informed consent.

6.2.2 Isolation of Peripheral Blood CD14-Positive Monocytes

The full procedures for the isolation of peripheral blood CD14-positive monocytes were described previously [20]. Briefly, 60 mLof EDTA blood was collected from patients via the arterial sheath catheter. Peripheral blood mononuclear cells (PBMCs) were isolated by density gradient centrifugation over Ficollpaque Plus (GE Healthcare, Diegem, the Netherlands). For further purification of monocytes, the PBMC fraction was incubated with magnetic beads coated with anti-CD14 antibodies (BD Biosciences, Breda, the Netherlands), and monocytes were purified with a MACS separation system according to the manufacturer's instructions (BD Biosciences, Breda, the Netherlands). Cells in CD14-positive fraction were resuspended, lysed in Trizol and aliquoted. The aliquots were stored at -80 °C for RNA isolation.

6.2.3 RNA Isolation and Microarray Analysis

Monocyte samples were shipped to Eurofins Genomics for semiautomated extraction of RNA using RNeasy 96-well plates (Qiagen). RNA samples were quantified using a Beckman Coulter DTX880 system, and only samples that displayed RIN values > 9 (Agilent Bioanalyzer) were included. Labeled RNA was prepared and used on the array for hybridization. Hybridized chips were scanned by Illumina BeadStation (Illumina, Inc., San Diego, CA, USA). Raw image analysis and signal extraction was performed with Illumina Beadstudio Gene Expression software with default settings (no background subtraction). Data were exported as text files. The gene expression profiling data were integrated and archived using the self-developed software "Circucel" [20]. The expressions of NGC ligands and receptors were extracted along with the phenotypic profiles of the patients. We excluded patient records without the required outcome parameter—in this case, a "confirmed diagnosis". For NGC expression profiles, there were no missing values. Therefore, data imputation was not necessary.

6.2.4 Statistical Analysis

Univariate correlation of NGC expressions (or other continuous variables) with a categorical variable was tested by 2 mean Student's t-tests. p-values were obtained from t-statistics. Univariate correlation of NGC expressions (or other continuous variables) with a continuous variable was tested with linear regression. p-values were obtained from the t-statistic of the coefficient of the variable. Correlation of 2 categorical variables was tested using Pearson's chi-squared test of the cross-tabulation. p-values were obtained from the chi-square statistics. For all the tests, a p-value of less than 0.05 was considered significant.

6.2.5 Model Fitting and Assessment of Model Performance

We used R package "caret" and its multiple dependencies (summarized in **Table 2**) for modeling the predicting power of NGCs to the disease status of patients [33]. Performance statistics for binary classification models were calculated, including accuracy, Cohen's kappa ($\varkappa$), sensitivity and specificity. The Cohen's kappa ($\varkappa$) value is given by formula

$$\frac{P_{observed} - P_{expected}}{1 - P_{expected}} \tag{6.1}$$

which indicates the performance gain from the modeling over random guessing (the higher, the better). Since this data set features a smaller number of healthy individuals, we set the models to aim for picking up healthy individuals as events. The sensitivity (true positive prediction) and specificity (true negative prediction) values were also calculated in accord to this principle. For the external assessment of model performance, data partitions were created to have a training set (90% of the dataset) and a test set (10% of the dataset). This was done using the "createDataPartition" function in the "caret" package to ensure proportional and representative coverage of individuals in both the training and test sets. Data in the training set were used for model building, and the data in the test set were held out in the training process and were used to determine the model performance pseudo-externally by comparing the prediction on the test set with the actual outcome of the test set. The distributions of NGC expressions in the training set and test set were illustrated in **Figure S3**. For the internal assessment of model performance and stability, 10-fold cross-validations were done, which means 10% of the training data were kept out of each iteration to evaluate the model generated by the other 90% training data over 10 iterations. Similar performance statistics were calculated at each iteration. The average values and standard deviations of the parameters were summarized to assess the model performance and

stability, respectively. Some models were tuned in ranges of tuning parameters to control their complexity and adaptivity (**Table 2**). Tuning parameters giving the best performance statistics in the cross-validation were chosen as optimal tuning of the model, and a final model was built using these parameters on the complete training data.

6.3 Results

6.3.1 NGC Expressions in Monocytes and Feature Selections

We made use of the CIRCULATING CELLS study cohort [20] to address the question of whether NGC expression profiles of circulating blood cells can be related to cardiovascular health. From 368 subjects out of this cohort (CVD patients and healthy controls), the transcriptomes of their CD14-positive monocytes were profiled (**Figure 1**). The individuals received different treatments and medications, and some of them suffered from other diseases, resembling the reality of complexity of most human cohorts (**Table 1**). Next, we aimed to classify CVD patients and healthy individuals using the differential expression of the NGC transcripts. To that end, we first sought to include NGCs with high expression levels and good univariate correlation with the outcome. **Figure 2A** shows the expression of NGCs in the cohort. Based on the detection threshold of the profiling platform, NGCs with signals higher than 6.75 (log2 scale unless specified otherwise) were unconditionally included in the modeling as potential features. To validate the microarray analysis, we compared the monocytic NGC expression profile obtained by microarray to that obtained by real-time PCR. Both methods showed a similar expression profile, with the exception of SEMA3E (**Figure S1**). To gain understanding of univariate correlation of the features to the outcome, violin plots of the NGC expressions were created to compare the distribution of NGC expression levels in both the CVD group and healthy group (**Figure 2B and Table S1**). The ranges of expressions showed overlaps in both groups, suggesting that the univariate prediction power will be minimal. In addition, with the ranges being widespread, the information to noise ratio is relatively low in this dataset. To quantify the univariate correlation of NGC expressions to the disease status, we calculated the p-value with two mean t-tests between the CVD group and healthy group. A volcano plot was created to observe the t-test p-value in relation to the fold change (**Figure 3A**). We identified several NGC ligands and receptors to be significantly different between CVD patients and healthy individuals, although with small fold changes. Among the significantly different genes, 10 had expression signals lower than 6.75. These 10 were added to the modeling procedure despite

Model Name	**Abbr.**	**Type**	**Best tuning parameter (Tuning Range)**	**R Package Dependency**
Boosted Logistic Regression	Logit	Linear	$n_iter = 41(11, 101)$	"caTools"
Linear Discriminant Analysis	Lda	Linear	NA	"MASS"
Partial Least Squares	Pls	Linear	$n_comp = 1(1, 10)$	"pls"
Support Vector Machines	Svm	Nonlinear	$Cost = 0.25(2^{-2}, 2^{-7})$	"kernlab"
Nearest Shrunken Centroids	Pam	Linear	$Threshold = 0(0, 25)$	"pamr"
Mixture Discriminant Analysis	Mda	Nonlinear	$Subclasses = 11(2, 16)$	"mda"
Flexible Discriminant Analysis	Fda	Nonlinear	$Degree = 4(1, 5)$ $n_pruning = 5(2, 5)$	"earth", "mda"
k-Nearest Neighbors	Knn	Nonlinear	$n_neighbor = 5(5, 23)$	"class"
Naive Bayesian	Nb	Nonlinear	$Laplacecorrection = 1(1, 3)$ $Kernalfunction = F(F, T)$ $BandwidthAdj = 1(1, 3)$	"naivebayes"
Bagged CART	BagCart	Tree/Rule-based	NA	"ipred", "plyr" "e1071"
Random Forest	Rf	Tree/Rule-based	$n_param = 2(2, 37)$	"randomForest"
Stochastic Gradient Boosting	Gbm	Tree/Rule-based	$Interactiondepth = 1(1, 7)$ $n_trees = 450(100, 1000)$ $Shrinkage = 0.1(0.01, 0.1)$ $Minnodesize = 5(5, 7)$	"gbm", "plyr"
C5.0 Tree	C5	Tree/Rule-based	NA	"C50", "plyr"

Table 2. Summary of model names, types and tuning parameters

their low expression levels. In total, 35 NGC genes were further to be used as features in subsequent modeling. Finally, to avoid instability caused by between-feature collinearity in some models, we calculated between-feature correlations of the expressions of selected NGCs (**Figure 3B**). No pairwise correlations of NGC expressions exceeded the threshold of 0.75, suggesting that there would be a minimal influence of collinearity. Therefore, none of the selected NGCs were eliminated based on between-feature correlations.

6.3.2 Gender and Age are Unlikely to be Confounding Factors in the Current Study

Gender and age are conventional confounding factors in clinical situations when revealing relationships between measurements of phenotypes and diseases. For machine learning, if age or gender affect both the features and the outcome, they would be confounding factors by definition. Firstly, we examined the relationship of age to NGC expressions and disease outcome. NGC expressions plotted against age in scatterplots with linear fittings showed no significant correlation between age and the NGC expressions (**Figure 4A**). The age ranges of both groups overlap, although the younger age dominates in the healthy group (**Figure 4B**). These observations suggested that age would add an additional prediction power in our modeling but would not be a confounding factor, as it does not link directly to NGC expressions. Next, we examined the relationship of sex to NGC expressions and disease outcomes. Using violin plots, we compared the distribution of NGC expressions in both sexes (**Figure 5A**). The distribution of NGC expressions was barely affected by sex, including the X-linked PLXNA3, PLXNB3 and EFNB1 genes (**Figure 5A**). There were six NGCs with significantly different expressions comparing males to females, albeit with a very small fold change relative to the variations (**Figure 5B**). Cross-tabulations of sex and disease outcomes were made, and the frequency distribution of both genders was similar among CVD patients and healthy individuals (**Figure 5C**). Therefore, sex was also unlikely to be a confounding factor in this study. Regardless, sex and age were included in our modeling process, as it is common practice to control for these conventional confounding factors.

6.3.3 Performance of Different Models

Different machine-learning methods were applied, and optimal tuning was obtained for each model listed in **Table 2**. The performance statistics for each of the models was calculated and summarized in **Figure 6**. As measurements for model stability, we examined standard deviations of the cross-validations for accuracies and Cohen's Kappa. Model per-

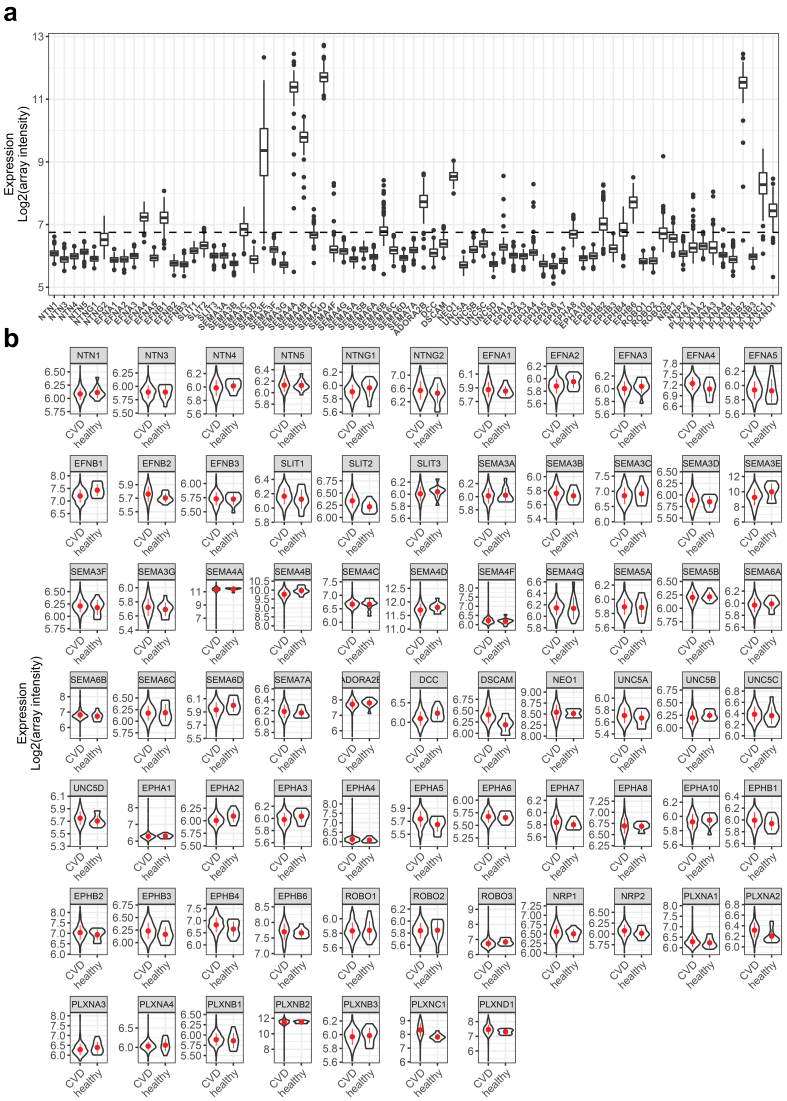

Figure 2. NGC expressions in patients and healthy subjects

(a) Box plots with quartiles were created using NGC expressions from all individuals. Baseline signal of the platform (6.75) was indicated with the dashed line. (b) Violin plots of all NGC expressions were created for cardiovascular disease (CVD) patients and healthy individuals. The violin shapes represent the density distribution of NGC expressions in the groups. The NGC expressions of CVD patients overlap with those of healthy individuals. Due to the small number of healthy individuals, their NGC expressions were sometimes not normally distributed.

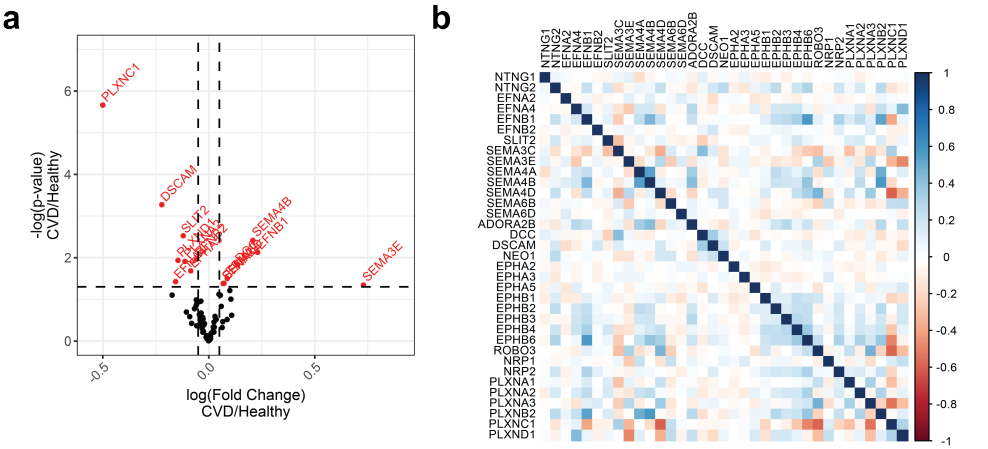

Figure 3. Univariate correlation of NGC expressions with disease phenotypes and pairwise correlations of NGC expressions

(a) Volcano plot showing the fold changes and the significance of difference in the 2 mean Student's t-tests between NGC expressions in CVD patients and healthy individuals. NGCs with significant differences ($p < 0.05$) are labeled with gene names and red color. For most NGCs, the univariate correlation determined by the 2 mean Student's t-tests with the outcomes is minimal. (b) Pairwise covariances of NGC expressions were illustrated in the heatmap to examine the between-feature correlations. Blue color indicates a positive correlation, whereas red color indicates a negative correlation. There are no absolute pairwise covariances higher than 0.75, the common cutoff for highly correlated features.

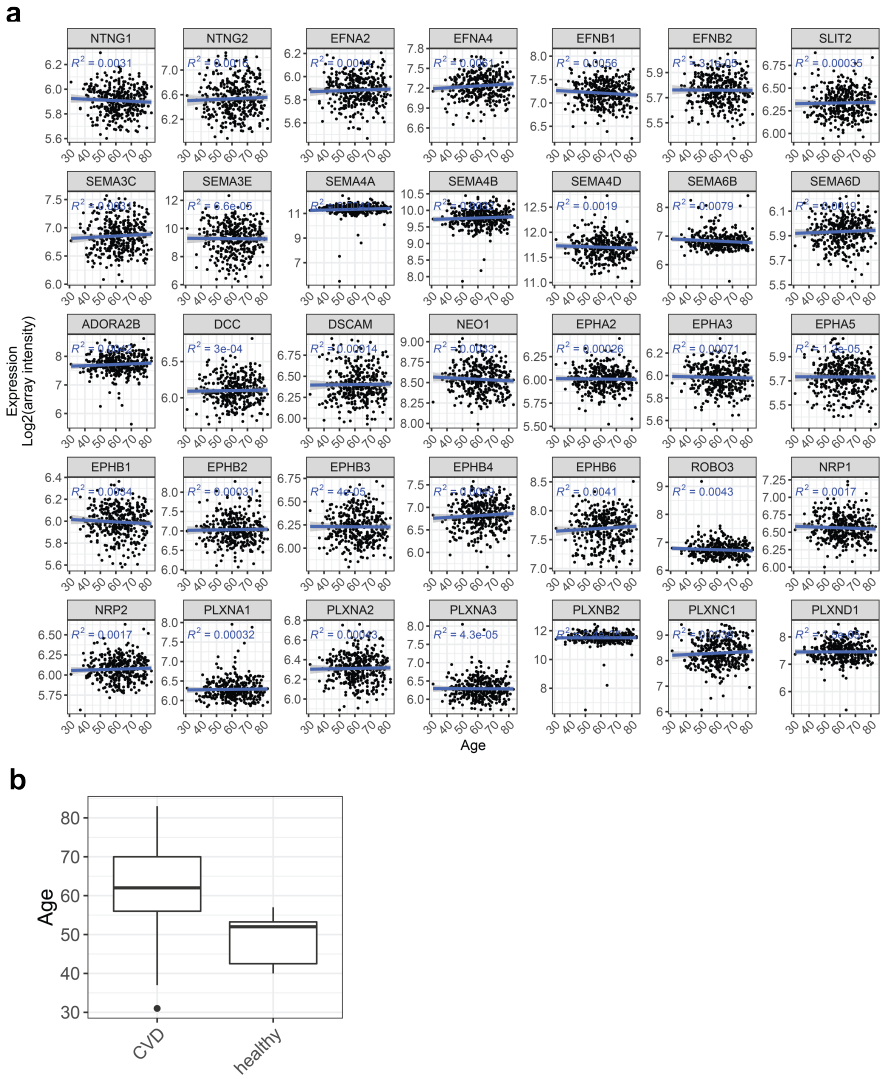

Figure 4. Influence of age as a potential confounding factor

(a) Scatter plots of expressions of selected NGCs in relation to age were made to show the influence of age on NGC expressions. Linear regressions were done with age being the dependent variable providing the fitted trend line (blue line), the 95% confidence interval of the trend (gray area) and the regression R-squared. Correlations of NGC expressions and age are minimal, as indicated by the R-squared values. (b) Boxplot of age distribution in CVD patients and healthy individuals. Young age dominates in the healthy individuals.

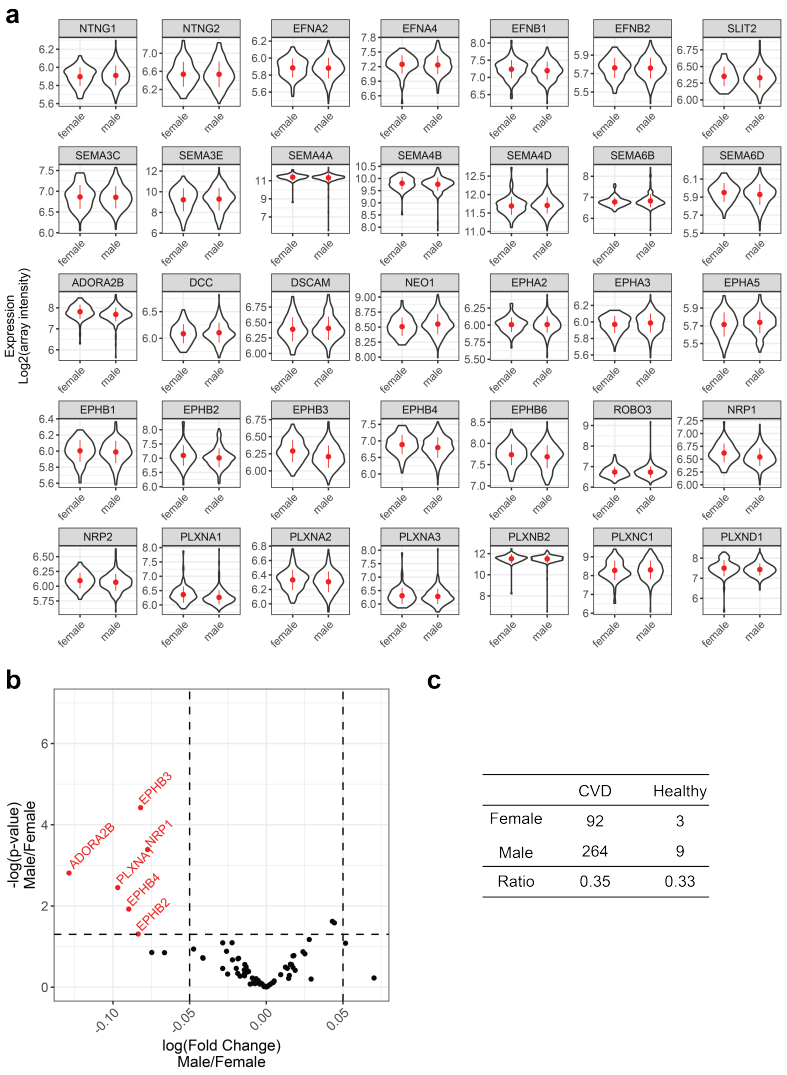

	CVD	Healthy
Female	92	3
Male	264	9
Ratio	0.35	0.33

Figure 5. Inspection of the influence of sex as a potential confounding factor

(a) Violin plots to show the distribution of expressions of selected NGCs in males and females. To be noticed is that distributions of selected NGC expressions are similar between sexes. (b) A volcano plot was made showing the fold change and the significance of differences in a 2 mean Student's t-tests between NGC expressions in males and females. NGCs with significant differences ($p < 0.05$) were labeled with gene names and red color. (c) Contingency table showing that the ratio of sexes is not biased in relation to the outcomes.

formance could be categorized in four groups (**Figure 6A-D**). (1) Partial least squares, support vector machine and nearest shrunken centroids models failed entirely to model the informative part of the gene expression data, as was revealed by having bottom-line accuracy (not better than predicting all the individuals to be CVD) and zero Cohen's Kappa value in the cross-validation, training set and test set. (2) Most models—namely, logistic regression, k-nearest neighbors, mixture discriminant analysis, flexible discriminant analysis, bagged CART (classification and regression tree), random forest and single C5.0 tree—suffered from overfitting, as was characterized by far better performances of models in the training set than in the test set. This can be explained by the modeling process trying to polish these models to perfectly predict the outcome based on the information in the training dataset. However, the modeling for the training set could not be generalized to the test set data. (3) K-nearest neighbors and flexible discriminant models had overall better prediction powers over random guesses but were still not up to standard. (4) Linear discriminant analysis, Naïve Bayesian and stochastic gradient boosting models performed best compared with the other models, within both the training set and test set at an accuracy of more than 0.98 and Cohen's Kappa more than 0.75 in the test set. These results indicate that the linear discriminant analysis, Naïve Bayesian and stochastic gradient boosting models were able to translate the informative part of NGC expression data into disease outcome. The three best-performing models all reached a sensitivity of 1 in the test set, meaning that they were able to discriminate healthy individuals from CVD patients (**Figure 6C**). Cohen's kappa ($\varkappa$) values were 0.79, 0.79 and 1 for the linear discriminant analysis, Naïve Bayesian model and stochastic gradient boost model, respectively (**Figure 6B**). The lower Cohen's kappa ($\varkappa$) for the former two models were due to the misclassification of one healthy individual as a CVD patient (**Table 3**). In the prediction of the training set, the linear discriminant analysis had lower sensitivity in the training set due to the misclassification of three healthy individuals to the CVD group (**Table 3**). Interestingly, the three misclassified healthy individuals still had higher modeled probability to be healthy than all but one misclassified CVD patient, suggesting that the sensitivity problem can be solved by an alternative cutoff value of the classification probability. When the cutoff value was altered from the original 0.5 to 0.28, the linear discriminant analysis achieved the same ideal sensitivity as the Naïve Bayesian model (**Figure S2A,B**). However, to prove the external efficiency of the alternative cutoff, another independent test set would be necessary, which is not feasible considering the size of this study.

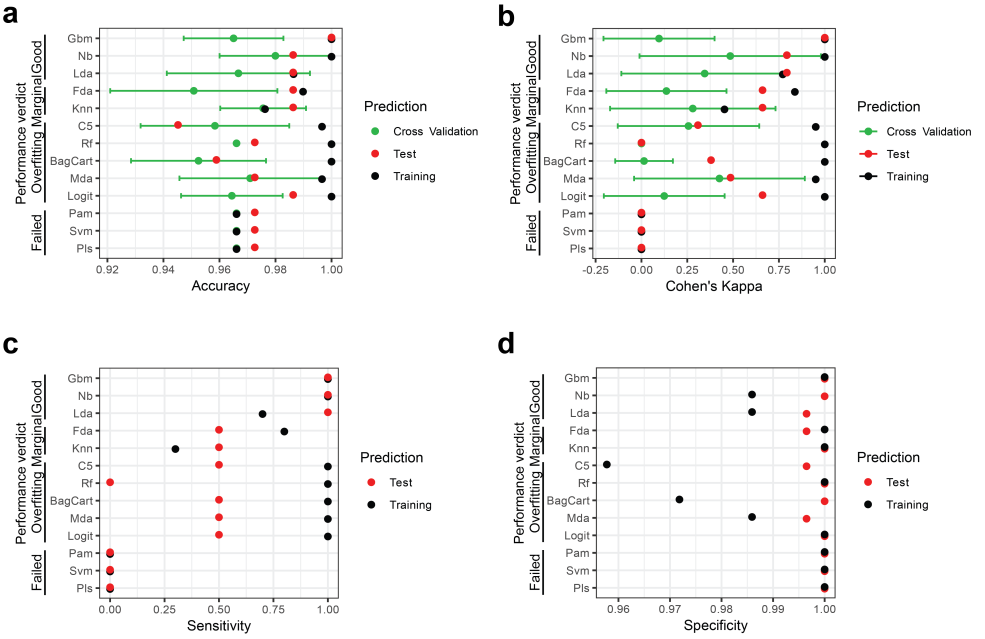

Figure 6. Model performance

(a-d) Model performance metrics—namely, accuracy (a), Cohen's Kappa (b), sensitivity (c) and specificity (d)—were illustrated in cross-validations (green dots and error bars), Training Set (black dots) and Test Set (red dots) for all models. Models are categorized into 4 groups based on their performances.

	Training	**Reference**		**Test**	**Reference**	
Model	Prediction	CVD	Healthy	Prediction	CVD	Healthy
Linear Discriminant	CVD	284	3	CVD	70	0
Analysis	Healthy	1	7	Healthy	1	2
Naive Bayesian	CVD	285	0	CVD	70	0
	Healthy	0	10	Healthy	1	2
Stochastic Gradient	CVD	285	0	CVD	71	0
Boosting	Healthy	0	10	Healthy	0	2

Table 3. Confusion matrices of the linear discriminant analysis, Naive Bayesian and stochastic gradient boosting models

6.3.4 Features with the Most Importance in the Models

Apart from age, the most important three features determined by the linear discriminant analysis and Naïve Bayesian model were PLXNC1, DSCAM and DCC, while the most important three features determined by stochastic gradient boost were SEMA6B, SEMA6D and EPHA2 (**Figure 7A-C**). As we noted before, age was determined to be important contributor to the model but was hardly a confounding factor, considering the weak correlation of age with NGC expressions (**Figure 7A-C**). The functional relevance of the top features will be discussed in the Discussion section.

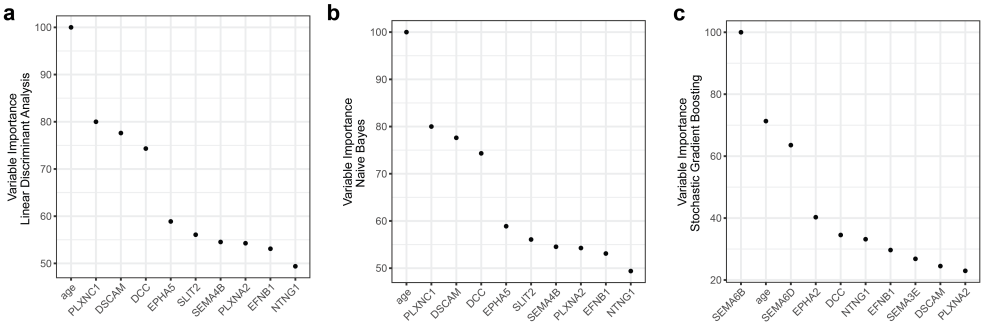

Figure 7. Variable importance of the models

(a-c) Variable importance measured in the linear discriminant analysis (a), Naïve Bayesian model (b) and stochastic gradient boost model (c). The importance of the most important feature was scaled to 100.

6.4 Discussion

In this study, we used NGC expressions of peripheral blood monocytes for the prediction of CVD. To reveal the true prediction power of monocytic NGC expression profiles, we performed cross-validation and validation using a pseudo-external test set with conventional confounding factors controlled. Of the models, Naïve Bayesian model and stochastic gradient model had satisfactory discrimination in both the training test and test set. The stochastic gradient model with a residual modeling mechanism was able to achieve 100% accuracy. Therefore, we have established the proof of concept that a small set of functional genes, NGCs, is of sufficient prediction power for the classification of CVD patients and healthy individuals. There are several challenging factors in the prediction of CVDs using monocytic NGC expressions. Firstly, nonlinearity is common in the biological effect of proteins.

Taking NTN1 as an example, the repellent effect of NTN1 on monocyte and macrophage migration has an optimal concentration of around 250 ng/ml; higher or lower concentrations are both less effective [3,14]. The biological effect also depends on its target, as NTN1 also has opposite roles acting on smooth muscle cells or macrophages [15]. Secondly, concomitant physiological processes in certain disease conditions can systemically cancel out the change of average gene expressions if they alter the gene expression in the opposite direction. In our case, CVD patients experience changes in the monocyte subpopulations, with increased lipopolysaccharide receptors and the low-affinity FC γ receptor-positive monocytes, referred to as intermediate monocytes [21,22]. These intermediate monocytes have been shown to predict cardiovascular events in subjects referred for elective coronary angiography [23]. At the same time, there is increased mobilization of lipopolysaccharide receptor-positive and low-affinity FC γ receptor-negative naïve classical monocytes from bone marrow, a process termed monocytosis. For any changes induced by monocyte activation/differentiation, monocytosis will cancel out the change because of the added naïve classical monocyte population. Moreover, human measurements in general can be very heterogenic by nature. Even proved biomarkers suffer from false positives and false negatives because of large variations in human measurements. In this study, we sought to tackle these problems by applying multiple modeling methods, each of which incorporates special features in the aspects of the linearity requirements or the learning mechanisms. Machine-learning methods are different from each other in various ways, including learning mechanisms and the assumptions made on the features. For a given dataset, choosing a model with suitable learning mechanisms and proper assumptions of the features can benefit the performance of modeling. In the current dataset, the linear discriminant analysis and the Naïve Bayesian model both adopted the same features, with identical weights on each feature, but the Naïve Bayesian model had better performance (**Figure 6 and 7A,B**). As both models are based on multivariate probability densities, the difference of the model performance should result from the different intrinsic assumptions and learning mechanisms of the models. The linear discriminant analysis assumes a multidimensional Gaussian distribution of the feature data, while the Naïve Bayesian model works with a more flexible distribution. Instead, the Naïve Bayesian model makes a strong assumption that all features are independent, so that the conditional probability of one class will be simply the product of the probability densities of all features. In addition, Naïve Bayesian could model nonlinear relationships between features and the outcome. Due to smaller numbers of individuals in the healthy group, distributions were

sometimes non-normal (**Figure 2B**). As previously described, the features in this dataset have relatively low pairwise covariance (**Figure 3B**), so that the independent-feature assumption required by the Naïve Bayesian model is very likely to be acceptable. Taken together, the structure in the current dataset favors the Naïve Bayesian model, which explains its better performance. The top 10 important NGCs chosen in the linear discriminant analysis and Naïve Bayesian models were all significantly differently expressed in the two mean t-tests, except NTNG1 (**Figure 3A and 7A,B**). This suggests that these two models favored features that have primarily different values in CVD and healthy groups, while the inclusion of NTNG1 served as a supplement to address the remaining variations that had not been explained by the other factors. Stochastic gradient boosting got the ideal classification of CVD and healthy individuals in both the training set and test set with a superior discrimination of CVD and healthy probability than the linear discriminant analysis and Naïve Bayesian model (**Figure 6 and Table 2**). The stochastic gradient boosting model is a classification tree-based model that incorporates functionalities that allows iterations over different choices of features and the modeling of residuals at costs until the residual is smaller than a certain threshold. From our modeling practice, the complexity of the stochastic gradient boosting paid off in comparison to the other two tree-based models—namely, the bagged CART model and the random forest model (**Figure 6** and **Figure S2C-E**). The bagged CART model, which does not iterate among different sets of features, suffered from a larger variation of predicted probabilities (**Figure S2C,D**), suggesting that randomized feature selection did benefit the modeling stability. On the other hand, the random forest model had the ability to produce probability predictions with less variation but failed to deliver a probability above the cutoff in the test set, confirming the extra learning ability made possible by the gradient boosting process (**Figure S2C,E**). Notably, the stochastic gradient boosting model picked considerably different NGCs as features. The most important three features in this model, SEMA6B, SEMA6D and EPHA2, are not included in the top 10 features in the linear discriminant analysis and Naïve Bayesian models (**Figure 7**). The most important feature, SEMA6B, was not even significant in the two mean t-tests (**Figure 3A**). Variable importance in the stochastic gradient boosting model took both the importance of a variable in the building of a decision tree and the subsequent modeling of residuals into account. It is likely that SEMA6B performed well in the modeling of the residual, since the univariate prediction power of SEMA6B should be minimal. The modeling of residuals often improves datasets with lower information-to-noise ratios, which is the case in the current

dataset. The importance of a feature in certain models could sometimes inform us with the relevance of the feature to the outcome. In the current setup, the importance of an NGC in the prediction models might suggest the functional importance of NGC in the development of CVD via monocytes. The linear discriminant analysis and Naïve Bayesian model picked up PLXNC1 as the most important feature. PLXNC1 mediates monocyte migration, adhesion and differentiation in response to its ligand SEMA7A [24]. At regions experiencing disturbed blood flow (atheroprone), an increase of SEMA7A in endothelial cells exacerbates inflammation and atherosclerotic plaque size [12]. SEMA6D and EPHA2 were chosen as the second and third most important features in the stochastic gradient boost model. SEMA6D has a role in immunology as being costimulatory molecule-expressed by dendritic cells [25]. The function of SEMA6D in monocytes is not known yet. EPHA2 promotes the adhesion and differentiation of monocytes [26,27]. In an apolipoprotein E knockout murine atherosclerosis model, the knockdown of EPHA2 using adenovirus-carrying short hairpin RNA resulted in the attenuation of atherosclerotic lesion development [28]. However, the amount of contribution from EPHA2 knockdown on monocytes could not be distinguished from that of endothelial cells. A limitation of this study is that the number of individuals is small in the healthy group, meaning the models were less trained by features of individuals with a healthy phenotype. This also led to some degree of instability of the models in the cross-validation. Another limitation is that the healthy individuals were younger than patients in the CVD group. Although, the ranges of ages in the two groups overlapped, it is to be determined whether the model could discriminate between the two phenotypes when the age range in the healthy group is extended. Future studies should recruit more age-matched individuals. To fully reveal the prediction power of NGC expressions, future works should focus on whether NGC expressions could discriminate between classes with more subtle differences, e.g. between stable and unstable angina. It should also be noted that the pathogenesis of CVD is rather complex. In this article, we focused on the association of NGC expressions to CVD, although multiple pathways are involved, leading to the identification of an incomplete risk gene set. The complex pathogenesis also dampens our ability to draw conclusions on causality, since it is possible that mechanisms that are implicated in CVD also alter the functional states of monocytes, reflected by monocytic gene expressions. In general, the development of clinical risk prediction models often faces certain hurdles, which could lead to less-defined results. Some studies only examined the univariate prediction value and ignored the combined prediction value of all features [29], while other studies did examine the

multivariate prediction value of features but used models that made strong assumptions on the data structure and covariance between features [30,31]. It is also common that studies have accessed the models in a descriptive way, but the external prediction potential is not determined [29,31,32]. In our study, we have incorporated multiple NGCs as features based on both statistical examinations and biological insights. We assessed the performances with cross-validation in the training data and independent prediction in the held-out data, thereby controlling the models on overfitting. Moreover, the models were shown to be not only a descriptive tool to confirm the correlations between NGC expression and CVD outcome but, also, a prediction method that can be applied to new datasets. In addition, we applied one of the complex models, the stochastic gradient boosting, which makes little assumptions on the characteristics of the data structure and returned a better performance. Taken together, this study gave the proof of principle on how machine-learning methods could be applied to the prediction of disease outcomes using the expression of a set of functional genes in circulating cells and allowed us to identify SEMA6B, SEMA6D and EPHA2 as predictive genes for CVD in the current cohort.

Acknowledgement

This research was funded by the Netherlands Heart Foundation, grant number 2013T127, European Research Area Network on Cardiovascular Diseases, grant number 038 MISsCVD and Centre for Translational Molecular Medicine, grant number 01C-102.

Conflicts of Interest

The authors declare no conflicts of interest.

References

1. *Frostegard, J., Immunity, atherosclerosis and cardiovascular disease. BMC Med, 2013. 11: p. 117.*
2. *Ross, R., Atherosclerosis–an inflammatory disease. N Engl J Med, 1999. 340(2): p. 115-126.*
3. *Hansson, G.K. and P. Libby, The immune response in atherosclerosis: a double-edged sword. Nat Rev Immunol, 2006. 6(7): p. 508-519.*
4. *Lessner, S.M., H.L. Prado, E.K. Waller, and Z.S. Galis, Atherosclerotic lesions grow through recruitment and proliferation of circulating monocytes in a murine model. Am*

J Pathol, 2002. 160(6): p. 2145-2155.

5. *Osterud, B. and E. Bjorklid, Role of monocytes in atherogenesis. Physiol Rev, 2003. 83(4): p. 1069-1112.*
6. *Hansson, G.K., Inflammation, atherosclerosis, and coronary artery disease. N Engl J Med, 2005. 352(16): p. 1685-1695.*
7. *Ley, K., Y.I. Miller, and C.C. Hedrick, Monocyte and macrophage dynamics during atherogenesis. Arterioscler Thromb Vasc Biol, 2011. 31(7): p. 1506-1516.*
8. *Funk, S.D. and A.W. Orr, Ephs and ephrins resurface in inflammation, immunity, and atherosclerosis. Pharmacol Res, 2013. 67(1): p. 42-52.*
9. *Mirakaj, V. and P. Rosenberger, Immunomodulatory Functions of Neuronal Guidance Proteins. Trends Immunol, 2017. 38(6): p. 444-456.*
10. *Zhang, H., D. Vreeken, C.S. Bruikman, A.J. van Zonneveld, and J.M. van Gils, Understanding netrins and semaphorins in mature endothelial cell biology. Pharmacol Res, 2018. 137: p. 1-10.*
11. *Ramkhelawon, B., Y. Yang, J.M. van Gils, B. Hewing, K.J. Rayner, S. Parathath, L. Guo, S. Oldebeken, J.L. Feig, E.A. Fisher, and K.J. Moore, Hypoxia induces netrin-1 and Unc5b in atherosclerotic plaques: mechanism for macrophage retention and survival. Arterioscler Thromb Vasc Biol, 2013. 33(6): p. 1180-1188.*
12. *Hu, S., Y. Liu, T. You, J. Heath, L. Xu, X. Zheng, A. Wang, Y. Wang, F. Li, F. Yang, Y. Cao, H. Zhang, J.M. van Gils, A.J. van Zonneveld, H. Jo, Q. Wu, Y. Zhang, C. Tang, and L. Zhu, Vascular Semaphorin 7A Upregulation by Disturbed Flow Promotes Atherosclerosis Through Endothelial beta1 Integrin. Arterioscler Thromb Vasc Biol, 2018. 38(2): p. 335-343.*
13. *Zhu, L., T.J. Stalker, K.P. Fong, H. Jiang, A. Tran, I. Crichton, E.K. Lee, K.B. Neeves, S.F. Maloney, H. Kikutani, A. Kumanogoh, E. Pure, S.L. Diamond, and L.F. Brass, Disruption of SEMA4D ameliorates platelet hypersensitivity in dyslipidemia and confers protection against the development of atherosclerosis. Arterioscler Thromb Vasc Biol, 2009. 29(7): p. 1039-1045.*
14. *Wanschel, A., T. Seibert, B. Hewing, B. Ramkhelawon, T.D. Ray, J.M. van Gils, K.J. Rayner, J.E. Feig, E.R. O'Brien, E.A. Fisher, and K.J. Moore, Neuroimmune*

guidance cue Semaphorin 3E is expressed in atherosclerotic plaques and regulates macrophage retention. Arterioscler Thromb Vasc Biol, 2013. 33(5): p. 886-893.

15. *van Gils, J.M., M.C. Derby, L.R. Fernandes, B. Ramkhelawon, T.D. Ray, K.J. Rayner, S. Parathath, E. Distel, J.L. Feig, J.I. Alvarez-Leite, A.J. Rayner, T.O. McDonald, K.D. O'Brien, L.M. Stuart, E.A. Fisher, A. Lacy-Hulbert, and K.J. Moore, The neuroimmune guidance cue netrin-1 promotes atherosclerosis by inhibiting the emigration of macrophages from plaques. Nat Immunol, 2012. 13(2): p. 136-143.*
16. *Wang, Q., S. Rao, G.Q. Shen, L. Li, D.J. Moliterno, L.K. Newby, W.J. Rogers, R. Cannata, E. Zirzow, R.C. Elston, and E.J. Topol, Premature myocardial infarction novel susceptibility locus on chromosome 1P34-36 identified by genomewide linkage analysis. Am J Hum Genet, 2004. 74(2): p. 262-271.*
17. *Ghosh, S., J. Vivar, C.P. Nelson, C. Willenborg, A.V. Segre, V.P. Makinen, M. Nikpay, J. Erdmann, S. Blankenberg, C. O'Donnell, W. Marz, R. Laaksonen, A.F. Stewart, S.E. Epstein, S.H. Shah, C.B. Granger, S.L. Hazen, S. Kathiresan, M.P. Reilly, X. Yang, T. Quertermous, N.J. Samani, H. Schunkert, T.L. Assimes, and R. McPherson, Systems Genetics Analysis of Genome-Wide Association Study Reveals Novel Associations Between Key Biological Processes and Coronary Artery Disease. Arterioscler Thromb Vasc Biol, 2015. 35(7): p. 1712-1722.*
18. *van der Harst, P. and N. Verweij, Identification of 64 Novel Genetic Loci Provides an Expanded View on the Genetic Architecture of Coronary Artery Disease. Circ Res, 2018. 122(3): p. 433-443.*
19. *Casamassimi, A., A. Federico, M. Rienzo, S. Esposito, and A. Ciccodicola, Transcriptome Profiling in Human Diseases: New Advances and Perspectives. Int J Mol Sci, 2017. 18(8).*
20. *Hoefer, I.E., J.W. Sels, J.W. Jukema, S. Bergheanu, E. Biessen, E. McClellan, M. Daemen, P. Doevendans, P. de Groot, M. Hillaert, S. Horsman, M. Ilhan, J. Kuiper, N. Pijls, K. Redekop, P. van der Spek, A. Stubbs, E. van de Veer, J. Waltenberger, A.J. van Zonneveld, and G. Pasterkamp, Circulating cells as predictors of secondary manifestations of cardiovascular disease: design of the CIRCULATING CELLS study. Clin Res Cardiol, 2013. 102(11): p. 847-856.*
21. *Thomas, G.D., A.A.J. Hamers, C. Nakao, P. Marcovecchio, A.M. Taylor, C. McSkimming, A.T. Nguyen, C.A. McNamara, and C.C. Hedrick, Human Blood Mono-*

cyte Subsets: A New Gating Strategy Defined Using Cell Surface Markers Identified by Mass Cytometry. Arterioscler Thromb Vasc Biol, 2017. 37(8): p. 1548-1558.

22. *Moroni, F., E. Ammirati, G.D. Norata, M. Magnoni, and P.G. Camici, The Role of Monocytes and Macrophages in Human Atherosclerosis, Plaque Neoangiogenesis, and Atherothrombosis. Mediators Inflamm, 2019. 2019: p. 7434376.*

23. *Rogacev, K.S., B. Cremers, A.M. Zawada, S. Seiler, N. Binder, P. Ege, G. Grosse-Dunker, I. Heisel, F. Hornof, J. Jeken, N.M. Rebling, C. Ulrich, B. Scheller, M. Bohm, D. Fliser, and G.H. Heine, CD14++CD16+ monocytes independently predict cardiovascular events: a cohort study of 951 patients referred for elective coronary angiography. J Am Coll Cardiol, 2012. 60(16): p. 1512-20.*

24. *Holmes, S., A.M. Downs, A. Fosberry, P.D. Hayes, D. Michalovich, P. Murdoch, K. Moores, J. Fox, K. Deen, G. Pettman, T. Wattam, and C. Lewis, Sema7A is a potent monocyte stimulator. Scand J Immunol, 2002. 56(3): p. 270-275.*

25. *O'Connor, B.P., S.Y. Eun, Z. Ye, A.L. Zozulya, J.D. Lich, C.B. Moore, H.A. Iocca, K.E. Roney, E.K. Holl, Q.P. Wu, H.W. van Deventer, Z. Fabry, and J.P. Ting, Semaphorin 6D regulates the late phase of CD4+ T cell primary immune responses. Proc Natl Acad Sci U S A, 2008. 105(35): p. 13015-13020.*

26. *Mukai, M., N. Suruga, N. Saeki, and K. Ogawa, EphA receptors and ephrin-A ligands are upregulated by monocytic differentiation/maturation and promote cell adhesion and protrusion formation in HL60 monocytes. BMC Cell Biol, 2017. 18(1): p. 28.*

27. *Saeki, N., S. Nishino, T. Shimizu, and K. Ogawa, EphA2 promotes cell adhesion and spreading of monocyte and monocyte/macrophage cell lines on integrin ligand-coated surfaces. Cell Adh Migr, 2015. 9(6): p. 469-482.*

28. *Jiang, H., X. Li, X. Zhang, Y. Liu, S. Huang, and X. Wang, EphA2 knockdown attenuates atherosclerotic lesion development in ApoE(-/-) mice. Cardiovasc Pathol, 2014. 23(3): p. 169-174.*

29. *Zawadzki, M., M. Krzystek-Korpacka, A. Gamian, and W. Witkiewicz, Serum cytokines in early prediction of anastomotic leakage following low anterior resection. Wideochir Inne Tech Maloinwazyjne, 2018. 13(1): p. 33-43.*

30. *Shimanuki, M., Y. Imanishi, Y. Sato, N. Nakahara, D. Totsuka, E. Sato, S. Iguchi, Y. Sato, K. Soma, Y. Araki, S. Shigetomi, S. Yoshida, K. Uno, Y. Ogawa, T. Tominaga,*

Y. Ikari, J. Nagayama, A. Endo, K. Miura, T. Tomioka, H. Ozawa, and K. Ogawa, Pretreatment monocyte counts and neutrophil counts predict the risk for febrile neutropenia in patients undergoing TPF chemotherapy for head and neck squamous cell carcinoma. Oncotarget, 2018. 9(27): p. 18970-18984.

31. *Machado, G.P., G.N. Araujo, C.K. Carpes, M. Lech, S. Mariani, F.H. Valle, L.C.C. Bergoli, S.C. Goncalves, R.V. Wainstein, and M.V. Wainstein, Comparison of neutrophil-to-lymphocyte ratio and mean platelet volume in the prediction of adverse events after primary percutaneous coronary intervention in patients with ST-elevation myocardial infarction. Atherosclerosis, 2018. 274: p. 212-217.*

32. *Guaricci, A.I., V. Lorenzoni, M. Guglielmo, S. Mushtaq, G. Muscogiuri, F. Cademartiri, M. Rabbat, D. Andreini, G. Serviddio, N. Gaibazzi, M. Pepi, and G. Pontone, Prognostic relevance of subclinical coronary and carotid atherosclerosis in a diabetic and nondiabetic asymptomatic population. Clin Cardiol, 2018. 41(6): p. 769-777.*

33. *Kuhn., M., Contributions from Jed Wing and Steve Weston and Andre Williams and Chris Keefer and Allan Engelhardt and Tony Cooper and Zachary Mayer and Brenton Kenkel and the R Core Team and Michael Benesty and Reynald Lescarbeau and Andrew Ziem and Luca Scrucca and Yuan Tang and Can Candan and Tyler Hunt. caret: Classification and Regression Training. R package version 6.0-80, 2018. https://CRAN.R-project.org/package=caret.*

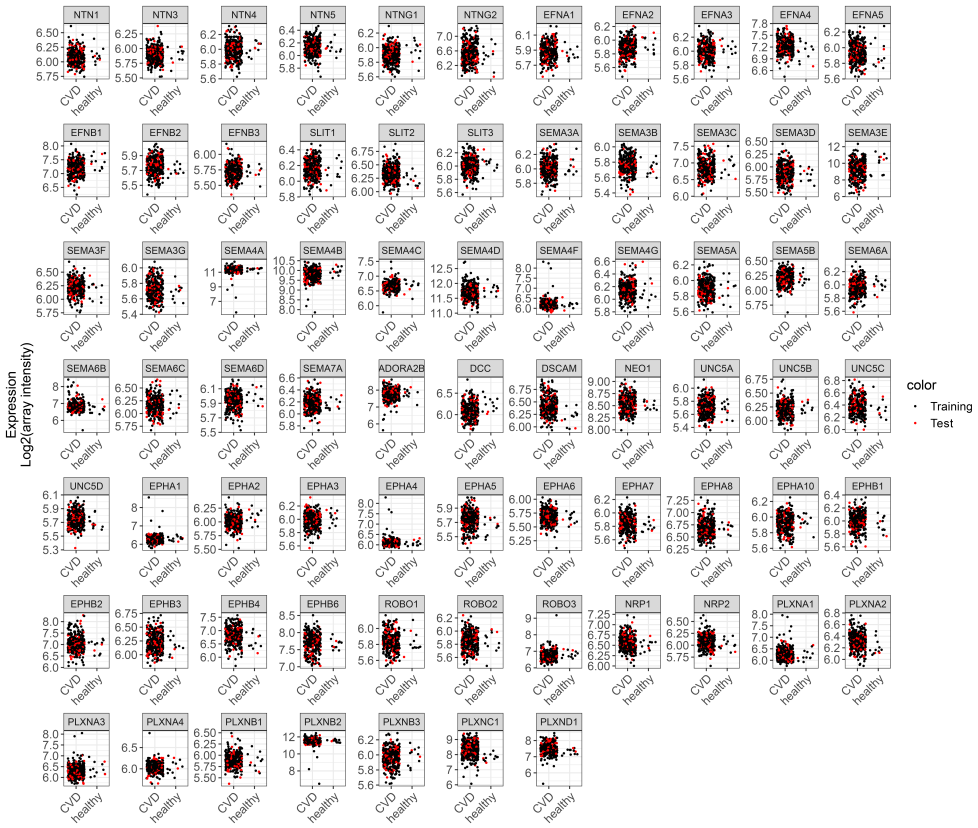

Supplementary Figure 1. Visualization of data partition

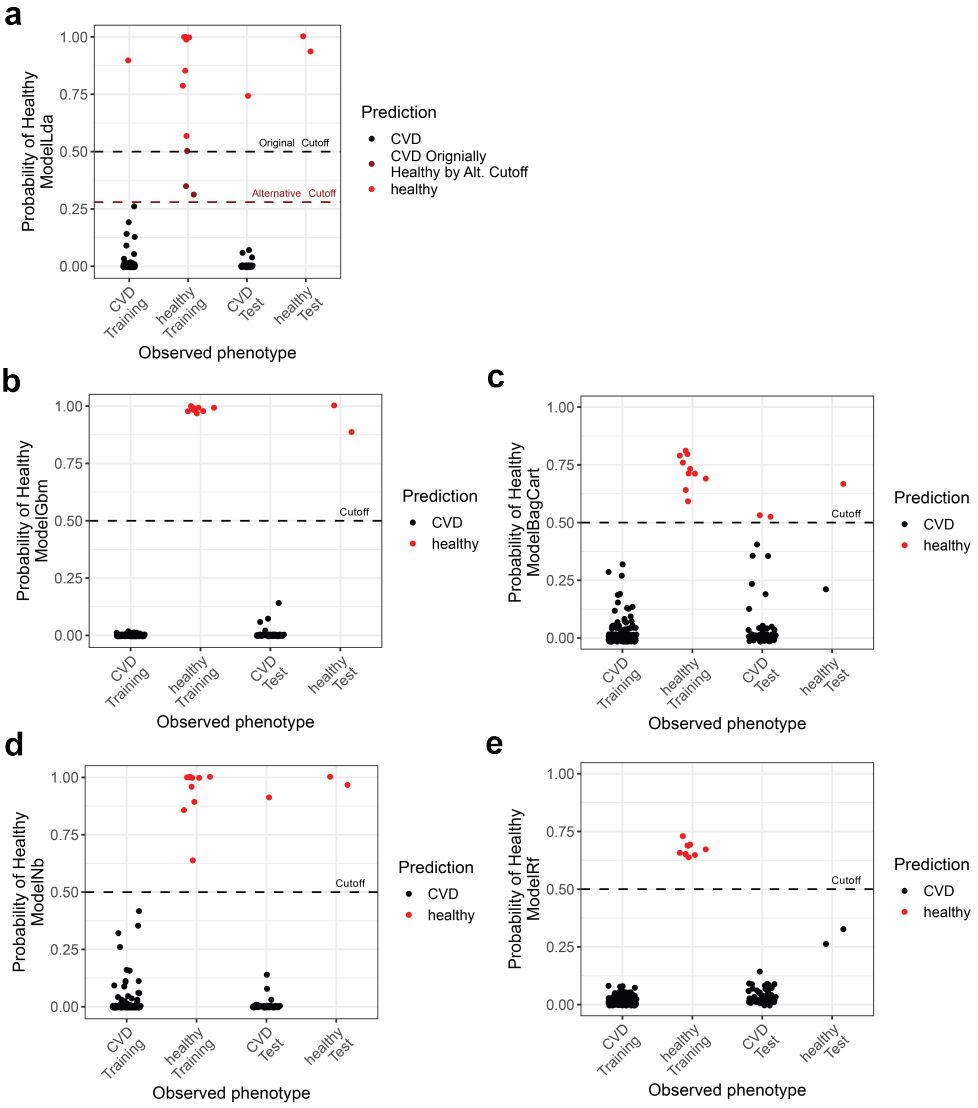

Supplementary Figure 2. Visualization of cutoffs for classification

Chapter 7

Summary and General Discussion

7.1 Key findings in this thesis

This thesis aimed to provide evidence that supports a central role for NGCs in CVD by studying the expression, regulation and function of neuronal guidance cues (NGCs) in endothelial cells and monocytes, the 2 cells types that play main role in development of atherosclerosis. The findings laid the foundation for future research of NGCs as novel targets for intervention of atherosclerosis. Following a short introduction in **Chapter 1**, in **Chapter 2**, we started with an overall review of the expression profiles and known functions of semaphorins and netrins in mature vascular endothelial cells. Average expression of semaphorins and netrins were listed, based on the transcriptomic data on GPL570 platform. Roles of semaphorins and netrins in survival, renewal potential, response to vessel wall shear stress, barrier function and controlling of vascular tone were summarized. From the literature review and preliminary experiments, we spotted high expression of SEMA3F and NTN4 in almost all types of endothelial cells. However, less was known about the function of these two guidance cues in mature and quiescent endothelial cells. There was also a lack of knowledge of function of SEMA3F and NTN4 in physiological concentration range. Therefore, in **Chapter 3 and 4**, functions of SEMA3F and NTN4 in endothelial cells were investigated in a reductionist approach. In **Chapter 3**, we observed impaired barrier function, resulting from change of cytoskeleton arrangement, if expression of SEMA3F was reduced using shRNA in human primary endothelial cells. The monocytic cell line THP-1 were shown to express the SEMA3F receptors NRP2, PLXNA1 and PLXNA3. In the presence of SEMA3F, monocyte migrations were inhibited. In **Chapter 4**, we made the observation that reduced level of NTN4 led to a senescence phenotype in endothelial cells. Presence of NTN4 in extracellular matrix derived from decellularized human kidney increased ability of endothelial cell to adhere to the matrix by promoting endothelial cell survival. These studies demonstrate the necessity of the 2 NGCs in endothelial cell biology. In **Chapter 5**, we perform a gene expression meta-analysis of NGCs during the monocyte to macrophage differentiation process, which is the critical process that occurs during development of atherosclerosis. Our pathway analysis confirmed the implication of axon guidance pathway in monocyte to macrophage differentiation process. The change of NGC expression profile corresponds to the function adaptions required for classically activated macrophages. Pro-inflammatory guidance cues, like SEMA7A, are upregulated in macrophage, while anti-inflammatory guidance cues, like SEMA4D, are downregulated. NGC receptors that were responsible for direction

of cell migration were upregulated. We further investigated the regulation of NGCs by the RNA-binding protein quaking (QKI) and found a regulatory hotspot in 3'UTR of SEMA7A transcript. QKI and a cluster of microRNAs possibly antagonize each other's effect by competitive binding at this hotspot. Given the implication of NGCs in monocyte function, we went one step further to validate the relevance of monocytic NGC expression in human using a coronary artery disease patient cohort. In **Chapter 6**, we determined prediction power of NGC expression of circulating CD14-positive monocytes. Using predictive modeling methods, we were able to find models, which correctly distinguished CVD patients from healthy individual. Therefore, monocytic expression of NGCs contains sufficient information for the disease status in our cohort. This gives the first link of between monocytic NGC expression and clinical phenotype in CVD patients.

7.2 NGCs are among the mediators of endothelial functional adaption to vessel wall shear stress

Atherosclerotic plaques profoundly develop at regions with disturbed flow or lower vascular wall shear stress [1]. This evidence has led to recognition of unfavorable hemodynamic environment as a key driver of endothelial dysfunction and subsequently atherogenesis. Vessel wall shear stress is the coplanar force applied to the vascular endothelium by the blood flow. Laminar shear stress (> 10 dyn/cm^2) provokes endothelial quiescence, which denotes the state of endothelial cells being mature and functional. Quiescence endothelial cells have a good barrier function, less coagulant activity and higher eNOS function (higher bioavailability of NO) and are anti-inflammatory. Therefore, laminar shear stress is believed to be atheroprotective, while disturbed flow (turbulence, oscillatory flow) is believed to be atherogenic. Genes that are regulated by shear stress are interesting, because they could be potential mediators of functional adaption to shear stress in endothelial cells, which may subsequently affect development of atherosclerosis. Previously it has been reported that NTN1, SEMA3A and EFNB2 expression is regulated by different flow conditions in both aortic arch of LDLR knockout mice and cell culture. With expression of NTN1 and SEMA3A being higher in atheroprotective flow condition (outer curvature of aortic arch and laminar flow), while expression of EFNB2 being higher in atherogenic flow condition (inner curvature of aortic arch and oscillatory flow) [2]. In **Chapter 3 and 4**, we found that SEMA3F and NTN4 were also upregulated by laminar shear stress, adding 2 more guidance cues that are regulated by shear stress. As reviewed in **Chapter 2**, NTN1 could serve as repellents of

monocyte migration and leukocyte adhesion, thus adding to the anti-inflammatory property of quiescent endothelial cells [3]. Passacquale et al observed downregulation of endothelial NTN1 in ApoE knockout mouse and showed that counteracting the downregulation with aspirin resulted in reduced atherosclerotic plaque progression by reducing monocyte infiltration [4]. Serum levels of NTN1 have been found to correlate with grades of atherosclerosis in human. In contrast to NTN1, EFNB2 could serve as monocyte attractant, so that low expression of EFNB2 in quiescent endothelial cells is intuitive [2]. Despite various studies confirming the involvement of SEMA3A and EFNB2 in cell types related to atherosclerosis, no in vivo evidence showing direct role in atherogenic has been published. In **Chapter 3**, we found SEMA3F was essential for stability of endothelial adherens junction and subsequently endothelial barrier function. Like SEMA3A and NTN1, SEMA3F was found to inhibit monocyte migration, although the inhibitory effect was not directional. Under baseline condition, global knockout of SEMA3F in mice do not display atherosclerotic phenotype [5]. Evidence of atheroprotective effect of SEMA3F in partial ligation mouse model is just emerging [6] (unpublished data suggesting 48% increase of lesion size in SEMA3F knockout mice compared to WT littermates following partial ligation procedure). In a Japanese population, a polymorphism in SEMA3F was associated with decreased risk of myocardial infarction. In **Chapter 4**, we demonstrated that NTN4 deficiency in endothelial cells lead to reduced survival and senescence phenotype of endothelial cells. Our observation is in line with other reports on the role of exogenous NTN4 in promoting endothelial cell survival via kinase activation or activation of integrins [7]. In ApoE knockout mouse, increased endothelial cell proliferation and turnover was observed in the aorta surface, especially in atheroprone regions [8]. The increased turnover could be viewed as a repair response to damage of endothelium. As reviewed in **Chapter 2**, proliferation of endothelial cells requires the cells to deviate from the quiescent state, one the consequences of which is impaired endothelial barrier function. It has long been known that leukocyte infiltration and endothelial cell proliferation occurs concurrently in early atherosclerosis [9]. Together, these observations provide theoretical possibility that factors, like NTN4, that promote endothelial cell survival could counteract damage to the endothelium. However, the essence of NTN4 in such role in vivo is still yet to be established. In summary, NGCs are among the mediators of functional adaption to vessel wall shear stress of endothelial cells. Insights in functional importance of NGCs are accumulating on cell level, but investigations of the in vivo functions of NGCs in relation to atherosclerosis are largely lacking, except for well-studies ones like NTN1.

7.3 In search for potential therapeutic targets in atherosclerosis: where do NGCs fit in?

Different methodological approaches have been applied to discover new therapeutic targets of atherosclerosis. Mechanisms involved in pathogenesis of atherosclerosis have been extensively studied with various therapeutic targets unraveled. One of the earliest studies in atherosclerosis established the importance of blood cholesterol in development of atherosclerosis with high cholesterol diet fed rabbit being the first experimental animal models of atherosclerosis [10, 11]. From that time onward, numerous efforts have been made to tackle hypercholesterolemia, which is to date most effective strategy of atherosclerosis intervention (reviewed in [12]). There were also early efforts made in epidemiological research to access the risk factors for atherosclerosis, including alcohol consumption [13], diabetes [14], blood pressure, body mass [15] and later also smoking [16]. These traditional risk factors were later confirmed in different situations and are still primary targets of intervention. It was later found that atherosclerosis is an inflammatory condition, caused by factors including vessel wall shear stress, dyslipidemia and infection [17, 18]. In early stage of atherosclerosis, these factors cause endothelial dysfunction. In **Chapter 3 and 4** of the thesis, we discussed the role of NTN4 and SEMA3F in endothelial cell function in the context of shear stress and inflammation. In **Chapter 5**, we discussed the expression, regulation, and functional relevance of NGCs in monocyte to macrophage differentiation. Our studies are part of continuing efforts to explore mechanisms involved in pathogenesis of atherosclerosis. In modern times, advances in molecular biology, genetics, high-throughput nucleotide assays, establishment of experimental atherosclerosis animal models and development of genetic engineering tools have boosted the discoveries of new therapeutic targets. Targets are discovered both by screening in population or high-risk families and by mining in the genes (or non-coding elements) that can be possibly involved in pathogenesis of atherosclerosis. As a population screening method, genome wide association studies (GWAS, GWA studies) are normally done to screen the genomic regions that are relevant to cardiovascular disease traits [19]. Regions with best association strength are picked to study further to narrow down to a causal gene or regulatory segment. GWAS led to discoveries of genomic hot spots like chromosome 1p13 near CELSR2-PSRC1-SORT1 genes [19]. GWA studies have several advantages: discoveries are directly relevance in human situation; associations can be made regarding different outcomes; findings are not limited to coding regions; results can be interpreted with future

knowledge. The principle of GWAS dictates that genotype polymorphisms with reasonably prevalence in the studied population can be found. On the other hand, rare variants with high genetic penetrance have been found in patients with familial atherosclerosis. Early studies in familial hypercholesterolemia identified causal mutations in LDLR and ApoB100 genes [20]. With the development next generation sequencing technology, whole exome sequencing can be performed now in familial premature atherosclerosis patients to reveal the causal gene targets in a high-throughput manner [21]. An on-going research in our group makes use of exome sequencing data from familial pre-mature atherosclerosis families with normal blood cholesterol level (data not shown here because it is out of the scope of this thesis). The sequencing identified several mutations in NGCs, which could potentially explain the phenotypes in these patients [22]. Such experimental setup is also beneficial in discovering gene targets that are functioning independent of hyperlipidemia if the affected individuals suffer from atherosclerosis despite having normal lipid profiles.

7.4 How can machine learning tools aid biomedical research and its applications?

Modern omics technologies like microarrays and next-generation sequencing have made it possible to generate enormous number of features from biological samples. A traditional way to combine information from different clinical features is to have an accumulative scoring system based on the value of each measurements that can be calculated manually. However, with the dimensions given by omics data, it is no longer possible to do it. Such situation prompted the need for better tools to deal with huge and complex biological features, which in our and others' opinion can be met with machine learning methods (or predictive modeling). In **Chapter 6**, we gave the proof of concept that by using NGC expression in circulating CD14-positive monocytes, one can distinguish between healthy individuals and CVD patients. Biological omics data are by nature not necessarily independent (between features) nor linear (the features themselves). Various predictive modeling methods were developed to accommodate the complexity of data in these aspects (discussed in the book by Max Kuhn [23]). By modeling the biological data to a certain disease outcome, associations of the biological data and the disease outcome can be made, giving directions for further causality studies. Machine learning methods can iterate in ranges of different parameters, the optimal models chosen from the iterations have the possibility to come close to the maximum prediction power of a certain dataset. Such ability makes decision making easier regarding

whether the pool of the observations is relevant for the purpose of the study. Furthermore, machine learning methods can build the link between functional genes/transcripts/proteins and disease phenotypes prior to full elucidation, thus accelerating the translation of knowledge to clinical situations.

7.5 NGCs as targets of atherosclerosis intervention: the challenges and future perspectives

Despite a much better understandings of the functions of NGCs in cardiovascular system, several challenges remain before successful interventions can be developed targeting NGCs. The broad spectrum of functions of NGCs means targeting NGCs could lead to many undesirable or unexpected effect. The problem is further complicated by the multi-to-multi binding patterns of NGC ligands and receptors. Despite the descent amount of knowledge on the functional importance of netrins and semaphorins in endothelial cell and monocyte biology, insights in the downstream signaling pathways are relative scarce. Future work should aim at comprehensive mapping of the downstream signaling pathways to pinpoint more specific druggable targets. Moreover, it is sometimes clear that a simple agonist/antagonist approach is not feasible. For example, endothelial derived NTN1 is atheroprotective owning to its ability to work as repellent for monocytes, whereas macrophage derived NTN1 decrease inhibits macrophage emigration from atherosclerotic lesions and is therefore atherogenic [4, 24]. Tissue specific drug delivery strategy is necessary in such situation. The effects of NGCs are often dose dependent. There are sometimes optimal concentrations for benefit effect of NGCs. For example, repellent effect of NTN1 and SEMA3A on monocyte migration has optimal concentration [2]. High concentration of exogenous SEMA3F was shown to cause collapse of endothelial cytoskeleton, whereas we showed in **Chapter 3** SEMA3F deficiency in endothelial cells impaired stability of adherens junction via excessive activation of F-actin [25]. If NGCs were developed as drug targets, it is important to know the optimal dose of NGCs for the beneficial effect. It is, however, promising for NGCs to be biomarkers for CVD patient stratification. Based on functional importance of NGCs in monocytes as described in **Chapter 5**, we speculated that peripheral blood monocytes could carry information of patients' disease status. We confirmed the speculation by modeling the predictive power of monocytic expression of NGCs in **Chapter 6** in a preliminary setting. To further establish NGC expression as features for patient stratification, a larger prospective cohort would be needed. In addition, a better choice of the cell type to be profiled could theoretically im-

prove the prediction power further. In summary, to prove therapeutic value of NGCs, deeper understanding of the signaling pathways and the dosing is needed, among other challenges.

7.6 Conclusion

In the first half of my thesis, I started with reviewing the recent research regarding functions of semaphrorins and netrins in mature endothelial cell biology. In the review, I identified SEMA3F and NTN4 as two highly expressed NGCs, for which there was a lack of knowledge of their function in mature endothelial cells. In the following chapters, their roles in maintaining endothelial barrier function, inhibition of monocyte migration, prevention of endothelial cell senescence and promotion of endothelial cell survival were revealed. In the second half of my thesis, I focused on comprehensive analysis of regulation of NGC expression in monocytes and macrophages. I then took a step forward found that regulation of NGC expression in monocytes could be informative for prediction whether patients were currently affected by CVD. Findings in the thesis add to the growing knowledge that NGCs are widely involved in pathological processes underlying atherosclerosis.

References

1. *Baeyens, N., C. Bandyopadhyay, B.G. Coon, et al., Endothelial fluid shear stress sensing in vascular health and disease. J Clin Invest, 2016. 126(3): p. 821-8.*

2. *van Gils, J.M., B. Ramkhelawon, L. Fernandes, et al., Endothelial expression of guidance cues in vessel wall homeostasis dysregulation under proatherosclerotic conditions. Arterioscler Thromb Vasc Biol, 2013. 33(5): p. 911-9.*

3. *Zhang, H., D. Vreeken, C.S. Bruikman, et al., Understanding netrins and semaphorins in mature endothelial cell biology. Pharmacol Res, 2018. 137: p. 1-10.*

4. *Passacquale, G., A. Phinikaridou, C. Warboys, et al., Aspirin-induced histone acetylation in endothelial cells enhances synthesis of the secreted isoform of netrin-1 thus inhibiting monocyte vascular infiltration. Br J Pharmacol, 2015. 172(14): p. 3548-64.*

5. *Matsuda, I., H. Shoji, N. Yamasaki, et al., Comprehensive behavioral phenotyping of a new Semaphorin 3 F mutant mouse. Mol Brain, 2016. 9: p. 15.*

6. *Rattanasopa, C.P., C.K.Y; Liehn, E.; Castano, D.; Singaraja, R.R.; Ghosh, S., Semaphorin 3F Inhibits Transendothelial Monocyte Migration and Protects Against Atherosclerosis. Circulation, 2019. 140:A11736.*

7. *Larrieu-Lahargue, F., A.L. Welm, K.R. Thomas, et al., Netrin-4 activates endothelial integrin alpha6beta1. Circ Res, 2011. 109(7): p. 770-4.*

8. *Foteinos, G., Y. Hu, Q. Xiao, et al., Rapid endothelial turnover in atherosclerosis-prone areas coincides with stem cell repair in apolipoprotein E-deficient mice. Circulation, 2008. 117(14): p. 1856-63.*

9. *Jerome, W.G., J.C. Lewis, R.G. Taylor, et al., Concurrent endothelial cell turnover and leukocyte margination in early atherosclerosis. Scan Electron Microsc, 1983(Pt 3): p. 1453-9.*

10. *Clarkson, S. and L.H. Newburgh, THE RELATION BETWEEN ATHEROSCLEROSIS AND INGESTED CHOLESTEROL IN THE RABBIT. J Exp Med, 1926. 43(5): p. 595-612.*

11. *Morrison, L.M., L. Hall, and A.L. Chaney, Cholesterol metabolism and its relationship to atherosclerosis, coronary artery disease, and arteriosclerosis. Am J Med, 1948. 4(4): p. 616.*

12. *Hartz, J. and S. Clauss, Treatment Strategies for Hypercholesterolemia. Curr Pediatr Rev, 2017. 13(4): p. 243-254.*

13. *Wilens, S.L., The relationship of chronic alcoholism to atherosclerosis. J Am Med Assoc, 1947. 135(17): p. 1136-9.*

14. *Goodman, J.I., S. Wasserman, L.J. Marcus, et al., A study of atherosclerosis in a group of diabetic patients. Am J Med Sci, 1950. 220(1): p. 30-45.*

15. *Lund, F. and M. Faber, The influence of blood pressure and body weight on the atherosclerosis of aorta. Acta Med Scand Suppl, 1950. 239: p. 401-4.*

16. *Auerbach, O., E.C. Hammond, and L. Garfinkel, Smoking in relation to atherosclerosis of the coronary arteries. N Engl J Med, 1965. 273(15): p. 775-9.*

17. *Hemmat, N., A. Ebadi, R. Badalzadeh, et al., Viral infection and atherosclerosis. Eur J Clin Microbiol Infect Dis, 2018. 37(12): p. 2225-2233.*

18. *Taleb, S., Inflammation in atherosclerosis. Arch Cardiovasc Dis, 2016. 109(12): p. 708-715.*

19. *Manolio, T.A., Genomewide association studies and assessment of the risk of disease. N Engl J Med, 2010. 363(2): p. 166-76.*

20. *Hobbs, H.H., M.S. Brown, and J.L. Goldstein, Molecular genetics of the LDL receptor gene in familial hypercholesterolemia. Hum Mutat, 1992. 1(6): p. 445-66.*

21. *Braenne, I., B. Reiz, A. Medack, et al., Whole-exome sequencing in an extended family with myocardial infarction unmasks familial hypercholesterolemia. BMC Cardiovasc Disord, 2014. 14: p. 108.*

22. *Bruikman, C.S., D. Vreeken, H. Zhang, et al., The identification and function of a Netrin-1 mutation in a pedigree with premature atherosclerosis. Atherosclerosis, 2020. 301: p. 84-92.*

23. *Kuhn, M. and K. Johnson, Applied Predictive Modeling. 2013: Springer.*

24. *van Gils, J.M., M.C. Derby, L.R. Fernandes, et al., The neuroimmune guidance cue netrin-1 promotes atherosclerosis by inhibiting the emigration of macrophages from plaques. Nat Immunol, 2012. 13(2): p. 136-43.*

25. *Bielenberg, D.R., A. Shimizu, and M. Klagsbrun, Semaphorin-induced cytoskeletal collapse and repulsion of endothelial cells. Methods Enzymol, 2008. 443: p. 299-314.*

Chapter 8

Nederlandse Samenvatting

Nederlandse Samenvatting

Ondanks aanzienlijke vooruitgang in de behandeling, blijven hart- en vaatziekten een van de meest voorkomende doodsoorzaken. Atherosclerose, ook wel bekend als aderverkalking, is een proces dat centraal staat binnen de cardiovasculaire ziekten en is gekenmerkt door excessieve ophoping van vetten en immuun cellen in de vaatwand (plaques). De belangrijkste strategie om mortaliteit door atherosclerose te verminderen is het corrigeren van dyslipidemie (afwijkingen in de samenstelling van vetten, waaronder triglyceriden en cholesterol, in het bloed). De meest succesvolle en meest gebruikte interventie is de remming van de aanmaak van cholesterol door statines. Additionele behandeling met een antilichaam tegen PCSK9 kan de cholesterol niveaus nog verder verlagen. Ondanks de mogelijkheid tot het corrigeren van cholesterol levels, is er echter nog steeds een aanzienlijk risico op cardiovasculaire ziekten.

Naast de cholesterolverlagende strategie, is er steeds meer onderzoek naar strategieën die ingrijpen op de immunologische reacties, ontstekingsreacties, die plaatsvinden bij atherosclerose. Behandeling met Canakinumab (een antilichaam tegen IL-1β) bleek hart- en vaatziekten met 16% te verlagen. Ondanks een toename in het aantal (dodelijke) infecties als gevolg van een verminderde afweer van de patiënt, toont deze studie het belang van ontstekingsreacties bij atherosclerose. Verder is het bekend dat atherosclerotische plaques zich vaak ontwikkelen in gebieden met onregelmatige bloedstroming, zoals bloedvat vertakkingen, terwijl het overige vatenstelsel relatief onaangedaan is. Dit duidt op een rol voor endotheelcellen, cellen die de binnenwand van de bloedvaten bekleden, bij het ontstaan van atherosclerose. Bovenstaande ontwikkelingen stimuleren onderzoeksinspanningen om diepere inzichten te verkrijgen in de bijdrage van endotheelcellen en ontstekingsreacties in de pathogenese van atherosclerose om het resterende risico op hart- en vaatziekten verder aan te pakken.

Neuronal guidance cues (NGC's) zijn een verzameling van receptoren en liganden die een belangrijke rol hebben bij de embryonale ontwikkeling van zowel het zenuw- als bloedvatenstelsel. Door een samenspel van aantrekkende en afstotende signalen naar cellen, regisseren NGC's de patroonvorming van deze stelsels. Afhankelijk van de context worden NGC's ook wel neuronal guidance eiwitten (naar hun moleculaire eigenschap), axonal guidance cues (naar hun oorspronkelijke functie) of zelfs neuro-immune guidance cues (naar hun later gevonden rol in de immunologie) genoemd. De NGC's bestaan uit 4 families van liganden,

namelijk netrin, semaphorin, slit en ephrin. Binding van deze liganden aan hun diverse receptoren, met verschillende specificiteit en affiniteit, leidt tot een complexe stroom aan signalen in de betrokken cellen. Een groot deel van deze signalen resulteert in veranderde activiteit van GTPase enzymen, welke de organisatie van het cytoskelet van de cel reguleren waarmee NGC's hun aantrekkende en afstotende effect kunnen realiseren. Naast de rol van NGC's tijdens de ontwikkeling, zijn ook functies van NGC's beschreven in zowel volwassen endotheel- als immuun cellen, wat ook de focus van dit proefschrift is. Met de kennis in dit proefschrift demonstreer ik de relevantie van NGC's in de vasculaire biologie vanuit fundamentele celbiologie tot aan hart- en vaatziekten patiënten.

In **Hoofdstuk 2** wordt een gedetailleerd literatuuroverzicht gegeven van de functies van semaphorin en netrin NGC's in volwassen endotheelcellen. Op basis van transcriptomic gegevens verkregen op het GPL570-platform, is de gemiddelde expressie van semaphorins en netrins vermeld. Verder wordt in dit hoofdstuk de rol van semaphorin en netrin NGC's in verschillende functies van endotheelcellen, zoals barrièrefunctie en de controle van bloeddruk, samengevat. Uit zowel het literatuuronderzoek als eigen experimenten viel op dat op bijna alle verschillende soorten endotheelcellen een hoge expressie van SEMA3F en NTN4 hebben. Er was echter minder bekend over de functie van deze twee specifieke NGC's in volwassen en gezonde endotheelcellen.

In **Hoofdstuk 3 en 4** is dan ook de regulatie en functie van SEMA3F en NTN4 in endotheelcellen onderzocht. De expressie niveaus van zowel SEMA3F als NTN4 worden gereguleerd door ontstekingsfactoren en hemodynamische factoren. In **Hoofdstuk 3** wordt beschreven hoe vermindering van SEMA3F, door een verandering in het cytoskelet, de endotheel barrièrefunctie verminderd. Verder is aangetoond dat monocyten de SEMA3F receptoren NRP2, PLXNA1 en PLXNA3 tot expressie brengen en dat aanwezigheid van SEMA3F de migratie van monocyten remt. In **Hoofdstuk 4** is beschreven dat dat verlaagde expressie van NTN4 leidt tot een verouderd fenotype van endotheelcellen. Aanwezigheid van NTN4 in de extracellulaire matrix verhoogt het vermogen van endotheelcellen om aan de matrix te hechten en bevordert de overleving van endotheelcellen. Beide studies tonen het belang van de twee NGC's in de endotheelcelbiologie aan.

NGC's blijken ook een rol te spelen in de biologie van monocyten. Differentiatie van monocyten naar macrofagen is een kritisch proces tijdens de ontwikkeling van atherosclerose. **Hoofdstuk 5** beschrijft dan ook een uitgebreide meta-analyse van NGC-genexpressie tijdens

deze differentiatie. Onze analyse bevestigt de betrokkenheid van NGC's in het differentiatie-proces van monocyten tot macrofagen. De verandering van het NGC-expressieprofiel komt overeen met de noodzakelijke functieaanpassingen voor klassiek geactiveerde macrofagen. Onstekingsstimulerende NGC's, zoals SEMA7A, worden verhoogd in macrofagen, terwijl ontstekingsremmende NGC's, zoals SEMA4D, worden verminderd. Daarnaast hebben we geconstateerd dat de NGC-receptoren die verantwoordelijk zijn voor cel migratie meer tot expressie worden gebracht door het differentiatie proces. Vervolgens hebben we de regulatie van NGC expressie niveaus door het RNA bindende eiwit quaking (QKI) onderzocht en hebben we een regulerende hotspot in het 3'UTR van het SEMA7A-transcript gevonden. Competitieve binding van een cluster van microRNA's en QKI op deze hotspot reguleren mogelijk de expressie van SEMA7A. De in silico-voorspelling dat SEMA7A wordt gereguleerd door QKI wordt bevestigd met laboratoriumwaarnemingen.

Gezien de implicaties van NGC's in monocyt functie, hebben we vervolgens de relevantie van NGC expressie door monocyten gevalideerd met behulp van een cohort van patiënten met coronaire vaatziekte. In **Hoofdstuk 6** wordt de voorspellende kracht van NGC-expressie van monocyten in het bloed bepaald. Met behulp van voorspellende modelleringsmethoden waren we in staat om modellen te vinden die patiënten met hart- en vaatziekten correct kunnen onderscheiden van gezonde individuen. Dit laat zien dat de NGC expressie van monocyten voldoende informatie bevat voor de ziektestatus van de patiënten in dit cohort. Dit geeft een duidelijke link tussen NGC expressie van monocyten en een klinisch fenotype bij hart- en vaatziekten patiënten.

De resultaten beschreven in dit proefschrift over de expressie, regulatie en functie van NGC's in endotheelcellen en monocyten (de twee celtypen die een hoofdrol spelen bij de ontwikkeling van atherosclerose) leveren bewijs voor een centrale rol voor NGC's in vasculaire biologie en daarmee ook hart- en vaatziekten. Deze bevindingen vormen een basis voor toekomstig onderzoek naar NGC's als nieuwe mogelijkheid bij behandeling van atherosclerose.

Chapter 9

Appendices

9.1 Curriculum Vitae

Huayu Zhang was born in Qiqihar, Heilongjiang Province, China in 1989. In 2007, he started his undergraduate study in Peking University Health Science Center majoring in basic medicine. From 2010, he joined the research group led by Prof. Liu Guoqing and Dr. Qi Rong investigating the anti-inflammatory effect of dendrimers. He obtained Bachelor of Science degree in 2012 and was awarded the Leiden University Excellent Scholarship for his master of science study in Leiden University Medical Center majoring biomedical sciences. He did a 6-month internship in Endocrinology department, Leiden University Medical Center, on the subject of effect of exendin-4 in atherosclerosis and liver inflammation, supervised by Prof. Patrick Rensen, Prof. Yanan Wang and Dr. Edwin Parlevliet. With a sponsorship from Eurolife foundation, he did a 9-month exchange studentship in Roslin insitute, University of Edinburgh, on the subject of influence of CpG dinucleotide frequencies on flu infectivity, supervised by Prof. Peter Simmonds and Dr. Nicky Atkinson.

After obtaining his Master of Science degree in 2014, he joined the group led by Prof. Anton Jan van Zonneveld and Dr. Janine van Gils for his PhD training. His research focused on the function of neuronal guidance cues in endothelial cell and monocyte biology and the implication of monocytic expression of neuronal guidance cues in coronary heart disease patients.

From 2019, he has been working as a research fellow in Centre for Medical Informatics and Advanced Care Research Centre, University of Edinburgh focusing on the application of natural language processing tools, knowledge graph and machine learning tools in improving patient care.

9.2 List of Publications

1. **Zhang, H.**, Ferguson, A., Robertson, G., Jiang, M., Zhang, T., Sudlow, C., Smith, K., Rannikmae, K. & Wu, H. Benchmarking network-based gene prioritization methods for cerebral small vessel disease. *Brief Bioinform* (2021).

2. **Zhang, H.**, Vreeken, D., Leuning, D. G., Bruikman, C. S., Junaid, A., Stam, W., de Bruin, R. G., Sol, W., Rabelink, T. J., van den Berg, B. M., van Zonneveld, A. J. & van Gils, J. M. Netrin-4 expression by human endothelial cells inhibits endothelial inflammation and senescence. *Int J Biochem Cell Biol* **134,** 105960 (2021).

3. Bruikman, C. S., Vreeken, D., **Zhang, H.**, van Gils, M. J., Peter, J., van Zonneveld, A. J., Hovingh, G. K. & van Gils, J. M. The identification and function of a Netrin-1 mutation in a pedigree with premature atherosclerosis. *Atherosclerosis* **301,** 84–92 (2020).

4. Vreeken, D., Bruikman, C. S., Cox, S. M. L., **Zhang, H.**, Lalai, R., Koudijs, A., van Zonneveld, A. J., Hovingh, G. K. & van Gils, J. M. EPH receptor B2 stimulates human monocyte adhesion and migration independently of its EphrinB ligands. *J Leukoc Biol* **108,** 999–1011 (2020).

5. Vreeken, D., **Zhang, H.**, van Zonneveld, A. J. & van Gils, J. M. Ephs and Ephrins in Adult Endothelial Biology. *Int J Mol Sci* **21** (2020).

6. Wang, K., Zhang, X., Sun, J., Ye, J., Wang, F., Hua, J., **Zhang, H.**, Shi, T., Li, Q. & Wu, X. Differences of Severe Acute Respiratory Syndrome Coronavirus 2 Shedding Duration in Sputum and Nasopharyngeal Swab Specimens Among Adult Inpatients With Coronavirus Disease 2019. *Chest* **158,** 1876–1884 (2020).

7. Wu, H., **Zhang, H.**, Karwath, A., Ibrahim, Z., Shi, T., Zhang, X., Wang, K., Sun, J., Dhaliwal, K., Bean, D., Cardoso, V. R., Li, K., Teo, J. T., Banerjee, A., Gao-Smith, F., Whitehouse, T., Veenith, T., Gkoutos, G. V., Wu, X., Dobson, R. & Guthrie, B. Ensemble learning for poor prognosis predictions: a case study on SARS-CoV2. *J Am Med Inform Assoc* (2020).

8. **Zhang, H.**, Bredewold, E. O. W., Vreeken, D., Duijs, J., de Boer, H. C., Kraaijeveld, A. O., Jukema, J. W., Pijls, N. H., Waltenberger, J., Biessen, E. A. L., van der Veer, E. P., van Zonneveld, A. J. & van Gils, J. M. Prediction Power on Cardiovascular

Disease of Neuroimmune Guidance Cues Expression by Peripheral Blood Monocytes Determined by Machine-Learning Methods. *Int J Mol Sci* **21** (2020).

9. **Zhang, H.**, Prins, J., Vreeken, D., Florijn, B. W., de Bruin, R. G., van Hengel, O. R., van Essen, M. F., Duijs, J. M., Van Esch, H., van der Veer, E. P., van Zonneveld, A. J. & Gils, J. M. V. Comprehensive analysis of neuronal guidance cue expression regulation during monocyte-to-macrophage differentiation reveals post-transcriptional regulation of semaphorin7A by the RNA-binding protein quaking. *Innate Immun* **27** (2020).

10. **Zhang, H.**, Shi, T., Wu, X., Zhang, X., Wang, K., Bean, D., Dobson, R., Teo, J., Sun, J., Zhao, P., Li, C., Dhaliwal, K., Wu, H., Li, Q. & Guthrie, B. Risk prediction for poor outcome and death in hospital in-patients with COVID-19: derivation in Wuhan, China and external validation in London, UK. *medRxiv,* 2020.04.28.20082222 (2020).

11. **Zhang, H.**, Vreeken, D., Junaid, A., Wang, G., Sol, W., de Bruin, R. G., van Zonneveld, A. J. & van Gils, J. M. Endothelial Semaphorin 3F Maintains Endothelial Barrier Function and Inhibits Monocyte Migration. *Int J Mol Sci* **21** (2020).

12. Bruikman, C. S., **Zhang, H.**, Kemper, A. M. & van Gils, J. M. Netrin Family: Role for Protein Isoforms in Cancer. *J Nucleic Acids* **2019,** 3947123 (2019).

13. Hu, S., Liu, Y., You, T., Heath, J., Xu, L., Zheng, X., Wang, A., Wang, Y., Li, F., Yang, F., Cao, Y., **Zhang, H.**, van Gils, J. M., van Zonneveld, A. J., Jo, H., Wu, Q., Zhang, Y., Tang, C. & Zhu, L. Vascular Semaphorin 7A Upregulation by Disturbed Flow Promotes Atherosclerosis Through Endothelial beta1 Integrin. *Arterioscler Thromb Vasc Biol* **38,** 335–343 (2018).

14. **Zhang, H.**, Vreeken, D., Bruikman, C. S., van Zonneveld, A. J. & van Gils, J. M. Understanding netrins and semaphorins in mature endothelial cell biology. *Pharmacol Res* **137,** 1–10 (2018).

15. De Bruin, R. G., van der Veer, E. P., Prins, J., Lee, D. H., Dane, M. J., **Zhang, H.**, Roeten, M. K., Bijkerk, R., de Boer, H. C., Rabelink, T. J., van Zonneveld, A. J. & van Gils, J. M. The RNA-binding protein quaking maintains endothelial barrier function and affects VE-cadherin and beta-catenin protein expression. *Sci Rep* **6,** 21643 (2016).

16. Gaunt, E., Wise, H. M., **Zhang, H.**, Lee, L. N., Atkinson, N. J., Nicol, M. Q., Highton, A. J., Klenerman, P., Beard, P. M., Dutia, B. M., Digard, P. & Simmonds, P. Elevation

of CpG frequencies in influenza A genome attenuates pathogenicity but enhances host response to infection. *Elife* **5,** e12735 (2016).

17. Ma, Q., Han, Y., Chen, C., Cao, Y., Wang, S., Shen, W., **Zhang, H.**, Li, Y., van Dongen, M. A., He, B., Yu, M., Xu, L., Banaszak Holl, M. M., Liu, G., Zhang, Q. & Qi, R. Oral absorption enhancement of probucol by PEGylated G5 PAMAM dendrimer modified nanoliposomes. *Mol Pharm* **12,** 665–74 (2015).

18. Tang, Y., Han, Y., Liu, L., Shen, W., **Zhang, H.**, Wang, Y., Cui, X., Wang, Y., Liu, G. & Qi, R. Protective effects and mechanisms of G5 PAMAM dendrimers against acute pancreatitis induced by caerulein in mice. *Biomacromolecules* **16,** 174–82 (2015).

9.3 Acknowledgement

The work in this thesis could not have been done without the generous support from colleagues and families and the infrastructure of Leiden University Medical Center.

Dear **Anton Jan** thank you for always being insightful and supportive. Your enthusiasm is inspiring for junior researchers like me. It was great pleasure attending the European Atherosclerosis Society meeting in Innsbruck with you and discussing about life and career over a drink on the outside table of a wine bar. I also want to thank you for supporting my family by giving my wife an orientation of potential job opportunities in the institute.

Dear **Janine** thank you for being a thoughtful, open-minded and knowledgeable supervisor. You took care of me in all aspects and gave me opportunities to develop myself. I would have gained far less diverse skill set without the freedom you gave me and your kindness. You have been helping with finishing the research projects and the revisions of research articles. I just cannot ask any more from you.

Dianne I have lost count of how much you helped with experiments, article writing and revisions. You are also so kind-hearted to organize many social events to make the workplace a place with warmth for all of us. Thank you **Caroline** for bringing in clinical perspectives and your sharpness to the group. It was nice to work with you.

I have been fortunate to receive great advice, suggestion and criticism from the PIs in vascular nephrology group and nephrology department, **Eric**, **Hetty**, **Bernard** and **Roel**. The project using patient monocytic transcript profiling received help from **Edwin**. I want to thank **Prof. Ton Rabelink** for the advice to my research at various symposia. I also received great help from fellow postgraduates in K5 **Jurriën**, **Carla**, **Barend**, **Taya**, **Gangqi**, **Abidemi**, **Sophie**, **Wouter** and **Vincent**, from more senior colleagues **Ruben**, **Daniëlle** and **Margien**. I could not have functioned well in the laboratory without the help of technicians, **Wendy MPJS**, **Wendy S**, **Angela**, **Richard**, **Annemarie vOR**, **Jacques**, **Reshma**, **Kelly**, **Ellen** and **Annemarie dG** and of colleagues from Thrombosis and Hemostasis department, **Annika**, **Julia**, **Suzan**, **Marco**, **Chantal**, **Mettine** and **Bart**. I want to thank other colleagues including other PIs, staffs and fellow postgraduate working at D3, who attended nephrology project meetings for their fruitful discussions and helpful advice. Many excellent students and exchange staffs contributed to the research project in this thesis, especially **Oscar** and **Mehdi**.

I want to thank all the colleagues who arranged and joined various social events like Lab weekends, Einthoven lab day outs, lab skis and 12 pub crawls to keep me socially connected with the groups. You are all just cool people!

I feel grateful for all my previous supervisors for preparing me for a PhD study. It was a very special occasion in my career when I met **Prof. Patrick Rensen** and **Prof. Yanan Wang** during a conference in Beijing and Inner Mongolia, introduced by my supervisor of undergraduate study **Prof. Guoqing Liu**. The meeting led to a master program in LUMC with an internship in Patrick's group. I also did a memorable exchange in University of Edinburgh under the supervision of **Prof. Peter Simmonds**.

Many of my friends gave me priceless support during my time in Leiden, including but not limited to my wine bar companions (**Lin Yazhi** and **Yang Xue**), my tennis opponents (**Chen Zhen and Shen Qing**), my pool opponents (**Wang Xiyu** and **Zhang Yunpeng**) and the Peking University alumni with plus-ones (**Wang Qing**, **Vincent**, **Guan Zexu**, **Yang Bingying** and **Thomas**). I also thank **Feng Liu** for giving me precious career insights.

Last but not least, my families have been giving me the best support I can ever imagine. I want to thank my wife **Ting** for holding me together during my down times. Thank you for always staying organized and keeping our small family going. Thank you for the love. **Esmée**, my little angel, to me you are the most beautiful thing on the earth and you have encouraged me more than you would know. **Mom** and **Dad**, thank you for giving me the best regardless of the circumstances. Thank you for putting faith in me when the thesis was taking quite some time to finish. It is either because I am not smart enough or because I did some hard core science. I believe you can find the answer in this book.

The years in the Netherlands are some of the most amazing years in my life. Here, I started to have the sense of independence and dignity. I love how the Dutch system could bring some social and economic practice to a next level to avoid common coordinating failures. Ik ga alle mensen, de grachten, de dammen, de windmolens, de taal en de (vaak vertraagde) treinen heel erg missen.

Huayu Zhang

Edinburgh 2021